Power Transformer Transient Modeling Using Frequency Response Analysis

by

Hosam Salem Alharbi

A thesis submitted to the Faculty of Graduate Studies of

The University of Manitoba

in partial fulfilment of the requirements for the degree of

MASTER OF SCIENCE

Department of Electrical and Computer Engineering

University of Manitoba

Winnipeg

Acknowledgment

I would like to thank my advisor Dr. Behzad Kordi for his motivation and guidance and the examining committee, Dr. Athula Rajapakse and Dr. Fariborz Hashemian. I would like to thank Manitoba Hydro High Voltage Test Facility for providing us with data and Manitoba HVDC Research Center for providing an actual model for a network to test the transformer transient response and its effects on the network. I am also grateful to Dr. Athula Rajapakse (University of Manitoba), Reg Gamblin (Manitoba Hydro High Voltage Test Facility), and Dharshana Muthumuni(Manitoba HVDC Research Center).

Finally, I would like to express my sincere gratitude to the Saudi Cultural Bureau and the Saudi Government for their financial support throughout my studies at the University of Manitoba.

Abstract

Vector Fitting is employed to approximate the Frequency Response Analysis (FRA) measurement data of a 13.8 kV/136.8 kV, 50-MVA single phase transformer. The frequency response of the primary and secondary coils as well the coupling between the coils have been measured in the frequency range of up to 2 MHz. The measured data includes the stray capacitances that exist between the coils. A circuit synthesis model is used to represent the measured data in the form of a two-port passive RLC network. The derived network is implemented in a commonly used power system transient simulator (PSCAD/EMTDC). The proposed RLC model is passive to ensure the stability of the network. The model can be used to investigate transient response of the transformer including the simulation of switching and lightning overvoltage transients. The results are compared with those derived from existing simple models.

Table of Contents

List of Figures

List of Tables

Chapter 1

Introduction

1.1 Background

Since transformers deal with many transient behaviours such as lightning and switching, an accurate modeling of the transformer is required to study the transient response of a transformer. Further an accurate modeling of a transformer is required to deal with non linear parameters of a transformer. In designing a substation or providing a suitable protection for an electric equipment, the transient response should be modeled and studied to know the maximum peak and the duration time for the transient response. The modeling of transient response of a transformer can be carried either by measuring some data from the transformer or by obtaining a design data from the manufacturers [1] [2]. A three phase transformer is modeled using transfer voltage ratio measurements and input admittance measurements, in [3]. By identifying the resonance frequencies of the measured data and calculating the circuit element associated to these resonances, a transient model was presented. Since this model is based on estimation of some parameters of transformer from measured data, this model will not provide a perfect match between the measured data and the simulation as shown in the paper. Unlike [3], the model used in [4] is based on data provided by the manufacturer. The model is tested and compared with measured data and simulation results. The model used in [4] is known as a first order model and it is shown in 1.1. The first order model is used in both lightning and switching simulation and

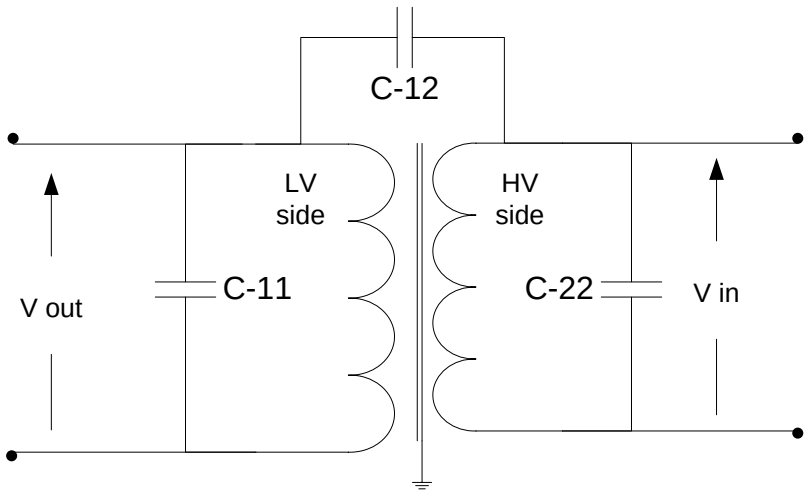

Figure 1.1: Commonly-used capacitive model for transient analysis of transformers [2]
.

the obtained results have been compared with measured data [4]. This model has a wide range of capacitance values and to identify the maximum peak of the transient response and the duration, the simulation has to be carried for many capacitance values within the provided range. Also in [2], the same model (that is referred to a capacitive model in this thesis) is used to test the transient recovery voltage of transformers. In [5], another model is obtained by calculating some of the transformer parameters. A three serially connected LC parallel circuit is developed and tested as a high frequency (around 1 MHz) circuit model for an oil-immersed transformer. The model is verified by comparison the simulation with the measured data. The frequency response of the transformer and the simulated circuit is measured and calculated respectively and found to be in a good agreement [5]. A simplified model is proposed in [6] to simulate the transient response of a transformer. The proposed model is similar to the capacitive model with regards to the capacitance values between the windings. In this model, the capacitance between the winding and the ground is added. Through an estimation method the capacitance values were calculated [6].

In this thesis a model is presented to overcome the problem of estimation or approximation of the transient response through measurement data. The transient response of the model will be compared with the transient response of the transformer to ensure that both of the model and the measured response have the same transient response.

1.2 Problem Definition

The commonly used model by the industry is a capacitive model as show in Figure 1.1. The capacitive values of this model are provided by transformer manufactures. The capacitive model currently used is incapable of simulating fast transients accurately. This is due to the fact that capacitive models are valid only for switching, up to 10 kHz [2]. The capacitive values given by manufacturers are in a wide range, thus to study the effects of lightning, from 10 kHz to 1 MHz [2], all capacitive values should be consider and simulated. In addition, when the transformer ages or faces a catastrophic failure, then these capacitive values will not give an accurate representation of the transformer transient behaviour. Some of the proposed models for transient simulation beside the capacitive model are based on estimation of some of the transformer parameters,e.g. the capacitances between each turn. The estimations of theses values could change the transient response of the transformer, e.g. winding movement due to mechanical or electrical forces.

To overcome all these problems, e.g. the wide range of capacitive values, an accurate transformer transient model based on measured data is proposed in Figure 1.2. The research carried out in this thesis will demonstrate that the simple capacitive model is not very accurate for fast transients. A flow chart that summarizes the procedure of the determination of the proposed model is shown in Figure 1.3

1.3 Objective

The goal of this thesis is to obtain passive circuit model for transformers that can be employed to simulate the behaviour of transformer in case of transient excitations such as switching or lightning.

1.4 Contribution

A passive model for transient response simulation from measured data is presented in this thesis. This model used Vector Fitting to fit the admittance curve and obtain a state-space

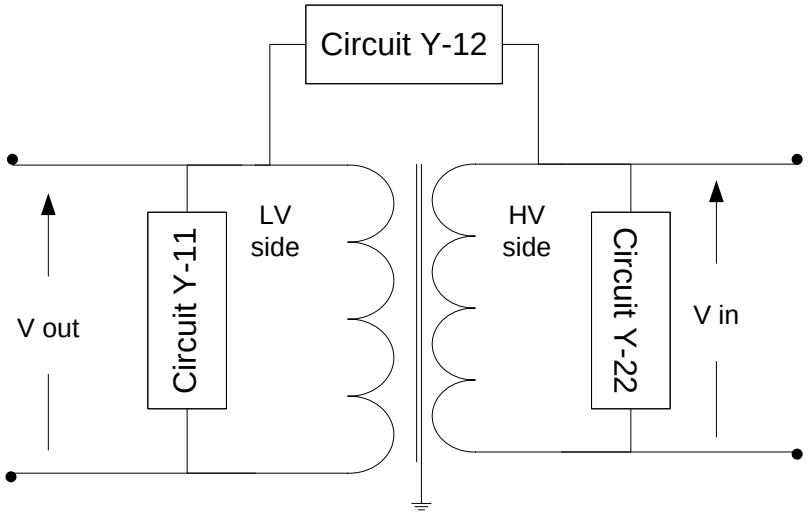

Figure 1.2: Proposed model for transient analysis of transformers. The objective of this thesis is to determine Y_{ij} circuits accurately based on FRA measurements.

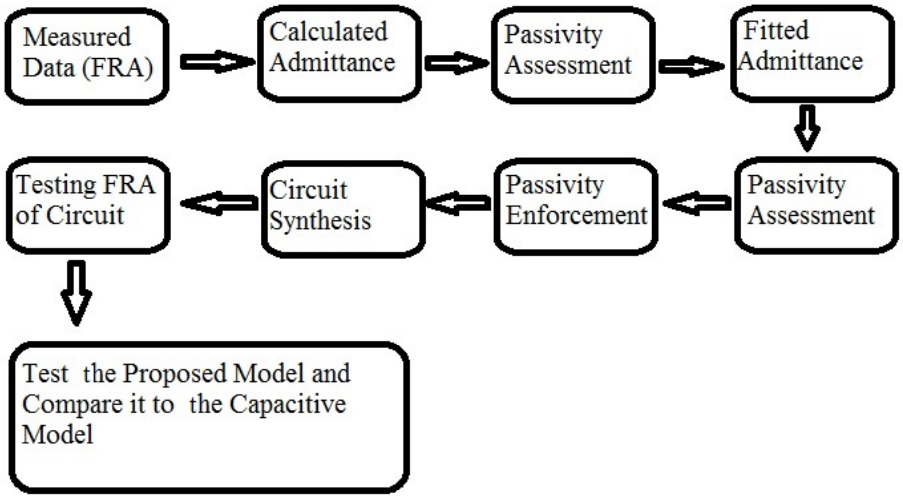

Figure 1.3: Steps to synthesize the proposed model.

model. From the state-space model an equivalent circuit is synthesized and tested for the transient response. The presented model is found to have the same transient response as the measured response of the transformer. The difference between this model and the used models is this model is obtained from a measured frequency response of the transformer directly each time the model is simulated. Thus, the model will change if the transformer faced a mechanical force such as transportation or an electromagnetic force such as fault electrical current. While the others model are based on one set of measurement and the model is fixed. In addition, if the transformer age, the transient response of the transformer will change because the transformer parameters will change as well and the model will change as well. So, this model even though it required measurement each time the model is simulated, it will give an accurate transient response, since both the model and the transformer transient response are the same.

1.5 Thesis Outline

To model the proposed circuit for transient simulation of a transformer using frequency response analysis, tests should be conducted first, and they are discussed in Chapter 2. Evaluation of the passivity of the measured data is to ensure the stability of the proposed model. If the model is not passive (not stable in the time domain) then an enforced passivity should be conducted before synthesizing a circuit model as discussed in Chapter 3. After that, synthesizing a circuit model from the frequency response and ensuring that the model and the transformer behaviour are the same in the frequency range of interest, will be presented in Chapter 4. A frequency response of the proposed model is conducted and matched the transformer frequency response. A comparison of the models (capacitive and the proposed model) will be discussed in Chapter 5.Finally, chapter 6 suggests the future work on this thesis and gives a conclusion of the work done in the thesis.

Chapter 2

Frequency Response Analysis Measurements

2.1 Frequency Response Analysis (FRA)

Frequency response analysis is a useful tool which helps in understanding the transient response of electric equipment or networks. It has been used in detecting any problems in a network or electric equipment. Since transformer failures have significant impact on safety, environment, and economy, frequency response analysis of transformer has received much attention and provide a non-destructive test to identify mechanical or electrical problems in a transformer at an early stage [7]. In this thesis, a distribution transformer is our main focus.

2.2 Applications of FRA Measurement and Literature Review in Transformer Modeling

Frequency response analysis of transformers has originally been developed to mitigate transformer failure by detecting any changes in transformer. After designing and building a transformer, different frequency response analysis tests are carried out to obtain a finger-

print response. The fingerprint response is the frequency response of transformer after it has been manufactured and before and after installation. Since the power frequency equivalent circuit of a transformer in Figure 2.1 is not valid for transient analysis and simulation, a more complex equivalent circuit such as combination of R, L, and C as shown in Figure 2.2 [8] is needed to represent a transformer in transient response analysis. Since most the circuit elements in the Figure 2.2 are not known, a FRA measurements is suggested. Any change in any of these elements will affect the frequency response of transformer. This main frequency response analysis (fingerprint) will be a framework with which any future frequency response analysis tests will be compared. Since the development of frequency response analysis has been based on practical experience, therefore, interpretation of the result will be based on the practical experience as well. The usage of frequency response analysis for transformer can be summarized as [7]:

- Core movements
- Winding deformations and axial or radial displacements
- Faulty core grounds
- Partial winding collapse
- Detecting winding movement (axial movement, or radial movement)
- Detecting an internal fault between turns, and
- Detecting an axial conductor bending

The origin of winding movement or deformation is either electromagnetic forces or mechanical forces. Since the transformer is continually subject to electrical current, the electromagnetic forces will keep affecting the transformer winding especially when fault currents pass through the transformer winding. Also, the mechanical forces affect the transformer winding, for instance during the transportation of the transformer. Thus the fingerprint of the transformer is to be measured again once the transformer is installed [9].

An interpretation of frequency response analysis of transformers has been studied in [11]. By using rational functions, one coil of a transformer has been modeled as a one-port circuit. The main focus of modeling a transformer coil is to interpret the frequency

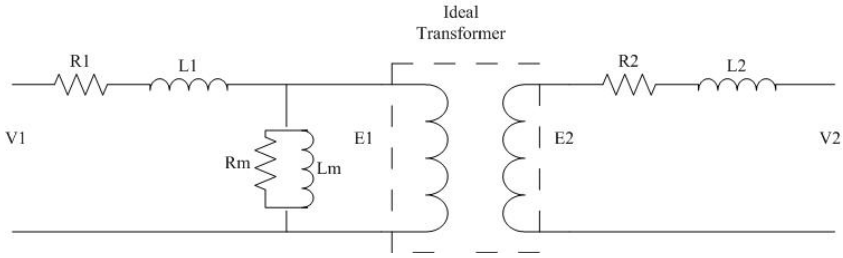

R1 = Resistance of the first winding.

R2= Resistance of the second Winding.

L1=: Inductance of the first Winding.

L2=inductance of the second winding.

Rm=resistance Represents Core loss in Eddy current.

Lm=mutual inductance of the Coil.

Figure 2.1: Power frequency transformer equivalent circuit [10].

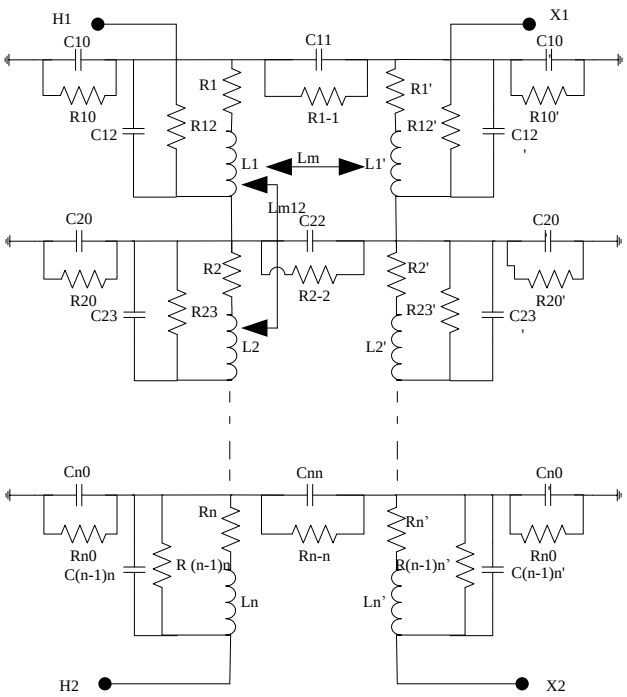

H1_H2: the High Voltage winding.

X1_X2: the Low Voltage winding.

R1: resistance of the first turn of high voltage winding.

R1': resistance of the first turn of low voltage winding.

R1: resistance represents the core loss in eddy current.

Lm: mutual inductance between L1 and L1' coils.

L1: inductance of the first turn of HV winding.

L1': inductance of the first turn of LV winding.

C11: the capacitance between the first turn in HV winding and the first turn in the LV winding.

Lm12: the mutual inductance between the fist and the second turn in the HV winding.

C12: the capacitance between the first and the second turn in HV winding.

R12: the resistance between the first turn and the second turn.

C10: The capacitance from the first turn to the ground.

R10: The resistance between the first turn to the ground.

Figure 2.2: Detailed transformer equivalent circuit [8].

response analysis using impedance equivalent circuits, by comparing both of the obtained frequency response results from the same transformer. The results presented in this paper [11] are related to the transformer in original condition and after axial displacement of a coil. In [12], a frequency range up to 10 MHz is investigated in the frequency response analysis test. The frequency response analysis shows more details and therefore, the test is more sensitive at higher frequencies. Thus, its easier to detect any winding movement or deformation at high frequency. This proposed method is called High Frequency Internal Response Analysis (HIFRA). Also, shunt resistance which is used in the measurement of the frequency response analysis has been investigated and it is shown that as shunt resistance increases the sensitivity of the measurements decreases. A number of frequency response analysis tests have been discussed in [7] and their different schematic connections are shown. In addition, this paper investigates their advantages and disadvantages. In [13], A model has been developed to determine the magnetic permeability and electric conductivity of the power transformer core. It focuses on the core identification than the winding displacement or movement. This paper [13] presents another usage of frequency response analysis. The frequency response analysis test is used in [14] as a diagnosing tool for power transformers. The paper discusses the difficulty of frequency response analysis tests which is the interpretation of the results to identify what the problem is and where it is, either in transformer core or in its windings. In [9], [15], an interpretation of transformer frequency response analysis has been investigated from theoretical point of view. An investigation of the resonance and antiresonance response in the frequency response analysis test along with the meaning of these resonance responses from the circuit point of view are presented. Many different types of transformers were investigated and simulated. In [16], diagnosis of a power transformer has been conducted using frequency response analysis in the range of 10 Hz to 10 MHz, and by comparing results of normal condition and faulty condition, where changes in transformer winding or coil are detected. Thus, an interpretation of the frequency response analysis tests based on the experimental results with the associated fault type were developed.

2.3 FRA Measurement Methods

There are different methods to measure the frequency response analysis of transformer windings, each of which describe different characteristics of transformers windings and/or the core. Each of these methods has its own connection scheme and how its response has been calculated from the measurements. The three most common methods have been used by the industries are [7], [16]:

2.3.1 End-to-end Voltage Ratio Measurement (FRAee)

In end-to-end voltage ratio test, a voltage source is applied to one of the coils and the voltages of the terminals of the same coil are measured while the second coil either open or shorted as shown in Figures 2.3 and 2.4. In these figures, the 50 Ω load represent the input impedance of the measurement device.

$$|FRA_{ee}|_{dB} = 20log\left|\frac{V_{out}}{V_{in}}\right| \tag{2.1}$$

$$\angle FRA_{ee} = \angle\frac{V_{out}}{V_{in}} \tag{2.2}$$

2.3.2 Input Admittance Measurement (FRAad)

In this method, a voltage source is applied to one of the coils and the voltage and the current at the terminal of the same coil is measured while the second coil is open (Figure 2.5).

$$|FRA_{ad}|_{dB} = 20log\left|\frac{I}{V}\right| \tag{2.3}$$

$$\angle FRA_{ad} = \angle\frac{I}{V} \tag{2.4}$$

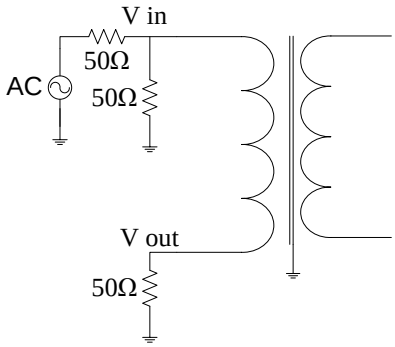

Figure 2.3: End-to-end voltage ratio test schematic connection with the other winding left open.

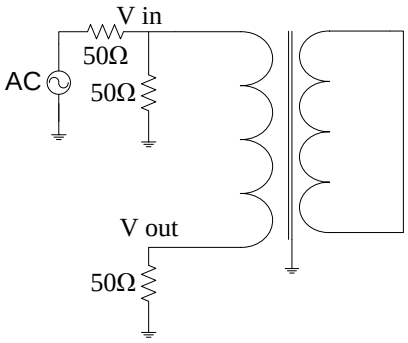

Figure 2.4: End-to-End voltage ratio test schematic connection with other winding shorted.

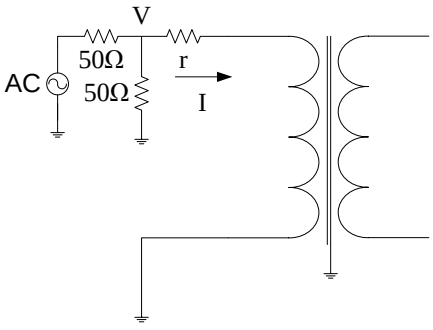

Figure 2.5: Input admittance test schematic connection, where r is the ammeter resistance.

2.3.3 Transfer Voltage Ratio Measurement (FRAtr)

In this method, a voltage source is applied to the terminal of one of the coils and the voltage at the terminals of the primary and the secondary coil are measured, while both of the transformer coils are disconnected from the ground. This essentially is used to measure the coupling between the windings and between the winding and the transformer core, (Figure 2.6).

$$|FRA_{tr}|_{dB} = 20log\left|\frac{V_{out}}{V_{in}}\right| \tag{2.5}$$

$$\angle FRA_{tr} = \angle\frac{V_{out}}{V_{in}} \tag{2.6}$$

2.4 FRA Measurements and Their Interpretations

Since the frequency response analysis method has been developed based on practical experience, the interpretation of the result is based on the experience. It has been found that the frequency response of transformer can be divided in to three regions [7], [9]. The first region is the low frequency region (10 Hz - 500 kHz), which shows the effect of the core of the transformer on the frequency response analysis test. The second region is the mid frequency range (500 kHz - 800 kHz). This region shows the problem associated with the winding movement and/or deformation especially in the radial direction. The third region is the high frequency region(800 kHz - 2000 kHz). This region shows the associated problem with axial movement and/or deformation [7], [9].

2.4.1 Advantages of FRA Method

Frequency response analysis test has many advantages [7], [9]:

- Non-destructive test: frequency response analysis test detects an internal fault of transformer without applying a huge electric current in which it may causes more damages than detect a problem.

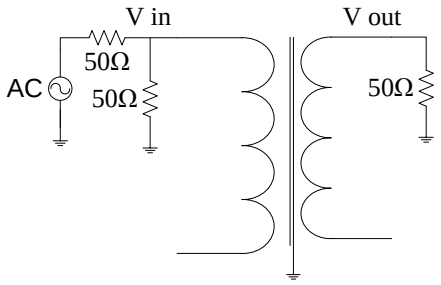

Figure 2.6: Transfer voltage ratio test schematic connection.

- Ability to detect any problem before catastrophic failure: Frequency response analysis test can detect an internal insulation problem before it takes place.
- Ability to detect winding movement and deformation.
- Ability to detect in which component the problem is located, e.g. core, windings.

2.4.2 A Comparison Between FRA Methods

The three different tests of frequency response analysis discussed in previous section have different advantages and disadvantages. From experience in using these tests, they are employed for the diagnosis of different problem in transformers.

It has been found that the least sensitive test in detecting any problem is the input admittance test. For transfer voltage ratio measurement, it has been found that it is more sensitive in detecting radial deformation of transformer winding, and axial displacement between windings. For end-to-end voltage ratio measurement, it has been found that it is the most sensitive for conductor axial bending [7].

2.5 FRA Measurements Employed in This Thesis

The FRA measurements employed in this thesis are provided by Manitoba Hydro. They consist of two sets of frequency response analysis that are similar to those obtained from schematics of Figures 2.3 and 2.6. Since the main focus of this thesis is to provide a model for a transformer which is suitable for a transient response, the data must be converted to

admittance response, and then obtain the suitable equivalent circuit from the frequency response.

Since the provided data is in the form of

$$|FRA_{ee}|_{dB} = 20log\left|\frac{V_{out}}{V_{in}}\right| \tag{2.7}$$

$$\angle FRA_{ee} = \angle\frac{V_{out}}{V_{in}} \tag{2.8}$$

Thus,

$$\frac{V_{out}}{V_{in}} = 10^{\frac{|FRA_{ee}|_{dB}}{20}}.e^{j\angle FRA_{ee}}$$

From Figure 2.3, the coil impedance:

$$\frac{V_{out}}{V_{in}} = \frac{50}{50 + Z_{Tx}}$$

Z_{Tx} is the transformer coil impedance, thus

$$\frac{V_{in}}{V_{out}} = \frac{50 + Z_{Tx}}{50}$$

$$\frac{V_{in}}{V_{out}}.50 = 50 + Z_{Tx}$$

$$Z_{Tx} = \frac{V_{in}}{V_{out}}.50 - 50$$

Let

$$|H| = \left| \frac{V_{out}}{V_{in}} \right|$$

$$\angle H = \angle \frac{V_{out}}{V_{in}} \tag{2.9}$$

Then,

$$Z_{Tx} = 50(\frac{1}{|H|\, e^{\angle \frac{V_{out}}{V_{in}}}} - 1)$$

$$Z_{Tx} = 50(\frac{1 - |H|\, e^{\angle \frac{V_{out}}{V_{in}}}}{|H|\, e^{\angle \frac{V_{out}}{V_{in}}}})$$

To calculate the admittance, we use

$$Y_{Tx} = \frac{1}{50}(\frac{|H|\, e^{\angle \frac{V_{out}}{V_{in}}}}{1 - |H|\, e^{\angle \frac{V_{out}}{V_{in}}}}) \tag{2.10}$$

By taking a closer look at the admittance equation, one realizes that it will give an approximation value for the actual real admittance. As shown in Figure 2.7, the stray capacitances were ignored in the calculation of winding admittance using FRA_{ee} data. However, the admittance values are good approximations of the actual values at low frequencies, up to 500 kHz.

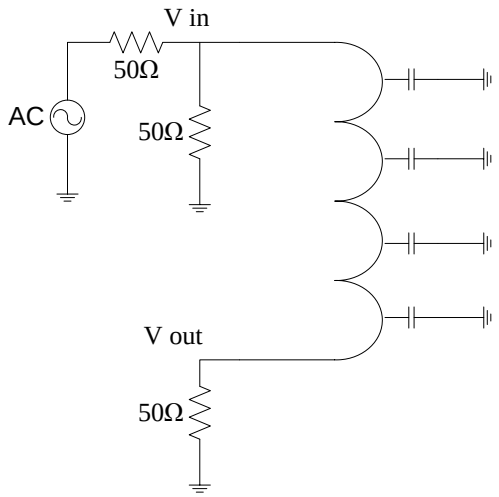

Figure 2.7: Winding stray capacitance.

Chapter 3

Rational Function Approximation of Measured Data and Passivity

3.1 Background

A rational function is a function where the numerator and the denominator are polynomials. Rational functions are used to approximate the the frequency response of the measured data. By fitting the frequency response of the measured data we obtain both of the polynomials of the numerator and the denominator. These two polynomials can be employed to derive a circuit with a similar frequency response. In this thesis the method used to find the rational function approximation is Vector Fitting [25].

Gustavsen and Semlyen [25] have described a methodology to fit measured or calculated data of frequency response by using rational function approximation method. One of the advantages of the described methodology is the ability to fit high number of resonance peaks of the measured or calculated transient response. Therefore, it will be very useful to represent a transformer or a network using this method as shown in the examples and the results.

In [26], Gustavsen has provided an example of modeling a three phase transformer. This paper shows the ability of the methodology which has been described by in [26] to

simulate and synthesize a multi-port system.

Gustavsen also provides a computer code to fit the frequency response of measured or calculated data [27]. This computer code calculates the state-space model of the frequency response. It can model different circuit models. For instance, it can represent a one port model or a multi-ports model. In addition, in this computer code, the passivity test for the system is embedded to ensure a passive system.

A genetic algorithm method was proposed to over come the passivity violations in [28] where the authors provide a stable model in the time domain. The paper shows how to obtain an all-positive circuit elements for the circuit model.

3.2 Vector Fitting

There are many approaches to the problem of fitting a rational function approximation to the main frequency response. One of these methods uses the inverse fast Fourier transform (IFFT) [18]. The main disadvantage associated with this method is the time consumed. Another method was presented to overcome some of the problems which have been encountered inverse fast Fourier transform (IFFT) [18]. This method is known as the rational function approximation. There are many different methods in applying the rational function approximation [18]. One of these methods is the Vector Fitting method [25]. The Vector Fitting is a robust method of the rational function approximation which has been developed by Gustavsen and Semlyen [18]. Vector Fitting is a general methodology to fit the measured or simulated frequency response data of an electric equipment or an n-port network [29]. The approximation of the calculated rational function response depends on many factors which will be discussed in this chapter.

Let us assume the rational function approximation

$$f(s) = \sum_{n=1}^{N} \frac{c_n}{s - a_n} + d + s.h \tag{3.1}$$

C_n: residues, could be real or complex number.

a_n: poles, could be real or complex number.

d,h : real values.

The model obtained by the rational function approximation can be converted to an equivalent circuit, which can be used in simulation software, such as PSpice, to perform electrical analysis.

Developing these methods to fit the frequency response of measured or simulated frequency response is mainly to overcome the complexity of the electric equipment or network in the transient response. As we know the response of some of the electric components are frequency dependent for example due to stray capacitances, that in normal operation at low frequency, do not have huge effects, i.e, we can ignore them. But in case of the transient, some of them show up and we cannot ignore their effects.

3.3 Passivity and Activity

3.3.1 Background

In understanding a network and its behaviour, it is necessary to understand many complementary qualitative properties which describe the network behaviour such as passivity, activity, and stability. In this chapter, the passivity will also be discussed in full detail. A two-port network is said to be passive if the initial energy stored in the system and the delivered energy to the system is greater than or equal to zero. In other words, the system cannot generate any energy [17].

The passivity issue in macromodeling an equivalent circuit of multi-port systems and its importance in the time domain simulation is discussed in [18]. The effect of passivity in time domain stability of the model is also shown. In [18], the author has mostly dealt with the scattering matrix instead of the admittance matrix or impedance matrix, but it is shown how to convert one into the other. Before checking the passivity of a system, the stability of the system must be tested. The authors have presented different methods to test the passivity of a system and discuss their advantages and disadvantages and which

method is the best to be used under different conditions. After detecting the passivity violation regions, the passivity enforcement methods have been discussed. Further methods of passivity enforcement to be considered in different conditions are discussed.

In [19], the author provided the mathematical theory and proof for passivity characterization of symmetric rational models. The paper mostly deals with the state space model in testing the stability and the passivity of the system. It also discusses some passivity tests using the Hamiltonian matrix in testing the stability of the model in the time domain.

One of the difficulties that has have been discussed in [20], is the passivity assessment and obtaining a passive model for the frequency response. There are a number of methods for testing the passivity that the authors of [20] have presented them as well as their advantages and disadvantages, such as the computational time and the numerical errors associated with the different methods. For instance, the computational time of the eigenvalues of Hamiltonian matrix have been discussed in the paper as well as different methods in achieving a better computational time.

The paper in [21], deals with the passivity problem from the point of view that the data could have some kind of measurement error. In this case, the system which has been measured by the frequency response could be stable and passive but because of the measurement error, the system is not stable or passive any more. To avoid errors the authors have taken the measurement of the admittance directly, instead of calculating the scattering matrix and then convert it to the admittance matrix, which helps in reducing the error in the measured data. Also, they have discussed the enhanced inverse Eigenvalue passivity enforcement to overcome the passivity problem.

An algorithm to overcome the passivity problem and the system stability caused by the non-passive circuit model which has been driven from the frequency response of a transformer or network is presented in [22]. The authors have presented two different examples (transformer and network) to show the effects of this algorithm. They have shown the violation region in the frequency domain and its effects on the model stability in the time domain simulation. In addition, they have shown how to implement this algorithm and how the time domain simulations are affected and stabilized.

In [23], the authors have presented a new technique for enforcing the passivity of a multi-port system. First, they tested the passivity of the system before applying the enforcement method they have presented. Once they identify the violation region in the frequency domain they use the presented algorithm to overcome the model instability in the time domain. Printed circuit boards are concerned in this work.

Gustavsen in [24], tests the passivity of a multi-port system and determines the passivity violation bands of the system before applying the passivity enforcement. The passivity enforcement method introduced in this paper requires less computational time. This method is known as the fast modal perturbation (FMP). In [24] a three phase distribution transformer and transmission line are given as an example and the computational time of the FMP method is compared with other methods.

In general, most of the papers that deal with the passivity, either present a new algorithm to enforce passivity or new methods for testing the passivity to insure stable model in the time domain, which will ensure a better representation of the system in the time domain, especially for transient studies.

3.3.2 Passivity

The passivity of a network can be described according to physical quantities such as time and energy. A network which cannot generate energy at any time is called passive. In another word, a network is passive if it is an absorber of energy. The definition of passivity could be helpful in understanding a network and its behaviour [17].

A passive n-port network can be defined by,

$$\int_{t_0}^{t} V^T(\tau) I(\tau) d\tau + \varepsilon(t_0) \geq 0 \quad \text{for any} \quad t > t_0 \tag{3.2}$$

where

$\varepsilon(t_0)$ is the initial energy stored in the network at t_0, $V(\tau)$ is the column vector of voltage values, $I(\tau)$ is the column vector of current values.

$\int_{t_0}^{t} V^T(\tau) i(\tau) d\tau$ is the delivered energy to the network from an external source during the

time [t_0,t].

As we can see in (3.2), the passivity does not depend only on the delivered energy from the external source but it also depends on the initial energy stored in the network. Therefore, the total energy delivered to the system at the time interval [t_0,t] should be greater than or equal to zero (see Figure 3.1). Figure 3.1 shows an example of time-energy curves for a passive, an active, and a generative network

Under the assumption that the initial stored energy in the network is zero, we can say

$$\lim_{t_0 \to -\infty} [\varepsilon(t_0)] = 0 \tag{3.3}$$

That leads to

$$\int_{-\infty}^{t} V^T(\tau) I(\tau) d\tau \geq 0 \tag{3.4}$$

Also, the system is said to be strictly passive if we take the equality sign out of (3.2), which means that the energy delivered to the system is always greater than zero for the entire time interval.

$$\int_{t_0}^{t} V^T(\tau) i(\tau) d\tau + \varepsilon(t_0) \ > 0 \tag{3.5}$$

Also we can assume that the network is initially relaxed which means the initial stored energy in the network is zero, which will give us

$$\int_{-\infty}^{t} V^T(\tau) i(\tau) d\tau \ > 0 \tag{3.6}$$

3.3.3 Activity

Similarly, an active n-port network can be defined by [17]

$$\int_{t_0}^{t} V^T(\tau) i(\tau) d\tau + \varepsilon(t_0) \ < 0 \quad \text{for any} \quad t > t_0 \tag{3.7}$$

We have to understand the fine line between activity and passivity, and the interrelation

among them. In case of passivity, the delivered energy should be greater than or equal to zero for all time interval, but in the case for active network, it should be less than zero for some of time interval and not all of it (see Figure 3.1).

Also we can assume that the network is initially relaxed which means the initial stored energy in the network is zero, which will give us

$$\int_{-\infty}^{t} V^T(\tau) i(\tau) d\tau < 0 \tag{3.8}$$

3.3.4 Generativity

A generative n-port network can be defined by [17]:

$$\int_{t_0}^{t} V^T(\tau) i(\tau) d\tau + \varepsilon(t_0) \ \leq 0 \quad \text{for any} \quad t > t_0 \tag{3.9}$$

In case of genrativity the energy should be less than or equal to zero for the whole time interval (see Figure 3.1)

Also we can assume that the network is initially relaxed which means the initial stored energy in the network is zero, which will give us:

$$\int_{-\infty}^{t} V^T(\tau) i(\tau) d\tau \leq 0 \tag{3.10}$$

A generative network can be either active or passive. It can be passive in case of lossless n-port network which means that the net energy absorbed and given by the network is zero, which satisfies both conditions of passivity and generativity. Also, in case of a generative n-port network it could be active in case that the net energy is less than zero. However, every active n-port network is not generative according to the condition of time interval.

The definition of a generative n-port network is a separate concept from activity and passivity. A passive n-port network is not an active n-port network and vice versa, but in case of generative this does not apply as explained above.

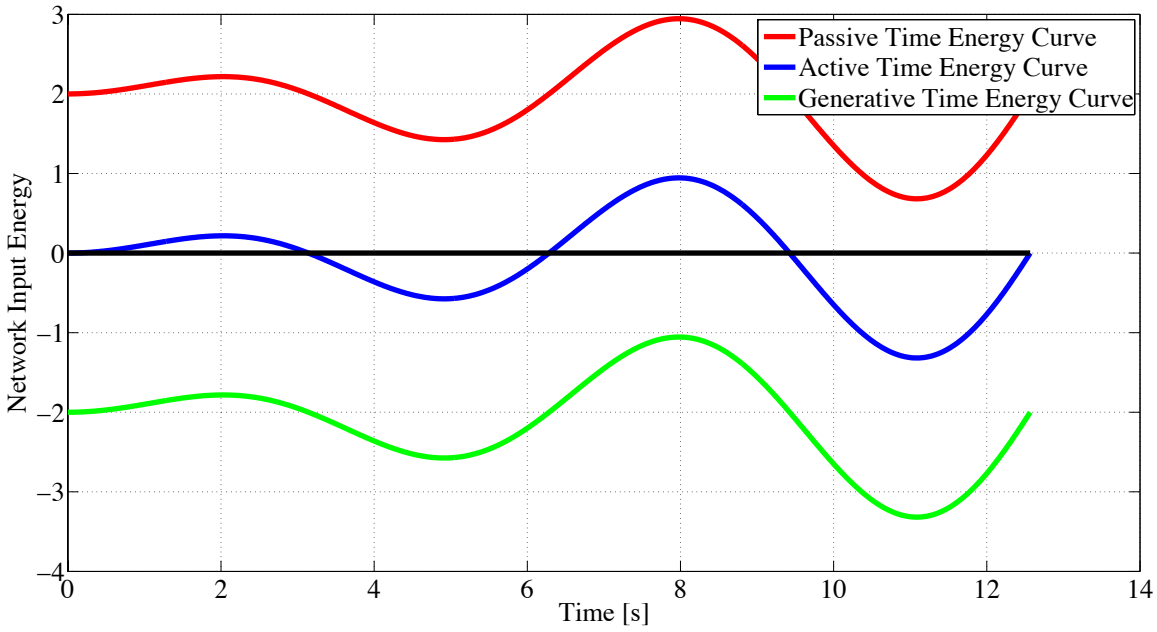

Figure 3.1: An example of time-energy curves for a passive, an active, and a generative network [17].

3.4 Passivity Test of an n-port Network

Without the loss of generality, consider the admittance of a two port network given by [17]

$$Y = \begin{bmatrix} Y_{11} & Y_{12} \\ Y_{21} & Y_{22} \end{bmatrix} = \begin{bmatrix} g_{11} + jb_{11} & g_{12} + jb_{12} \\ g_{21} + jb_{21} & g_{22} + jb_{22} \end{bmatrix} \tag{3.11}$$

The Hermitian matrix of the admittance matrix is defined as [17]

$$Y_h = \begin{bmatrix} g_{11} & \frac{Y_{12}+\overline{Y_{21}}}{2} \\ \frac{Y_{21}+\overline{Y_{12}}}{2} & g_{22} \end{bmatrix} = \begin{bmatrix} g_{11} & \frac{1}{2}(g_{12} + g_{21} + jb_{12} - jb_{21}) \\ \frac{1}{2}(g_{21} + g_{12} + jb_{21} - jb_{12}) & g_{22} \end{bmatrix} \tag{3.12}$$

The necessary and sufficient conditions to satisfy the passivity condition of an n-port network are [17]

First condition:

$$Real(Y_{11}) \geq 0 \quad \text{and} \quad Real(Y_{22}) \geq 0 \tag{3.13}$$

Second condition:

$$det(Y_h) \geq 0 \tag{3.14}$$

The second condition can be expressed in various forms [17]:

$$4\ g_{11}\ g_{22} - |Y_{12}|^2 - |Y_{21}|^2 - 2\ Re(Y_{12}\ Y_{21}) \geq 0 \tag{3.15}$$

$$4\ g_{11}\ g_{22} - (g_{12} + g_{21})^2 - (b_{12} - b_{21})^2 \geq 0 \tag{3.16}$$

$$g_{11}\ g_{22} - g_{21}\ g_{12} - \frac{|Y_{21} - Y_{12}|^2}{4} \geq 0 \tag{3.17}$$

$$4\ g_{11}\ g_{22} \geq \left|Y_{21} - \overline{Y_{21}}\right|^2 \tag{3.18}$$

A reciprocal n-port network is defined as a network in which all of its $n(n-1)/2$ pairs of port are reciprocal. This means that in case of impedance or admittance of a two port network, we have this

$$Z_{12} = Z_{21} \tag{3.19}$$

$$Y_{12} = Y_{21} \tag{3.20}$$

Thus, for reciprocal networks $Y_{12} = Y_{21}$, the second condition becomes

$$g_{11}\ g_{22} \geq g_{12}^2 \tag{3.21}$$

From (3.17) we get

$$g_{11}\ g_{22} - g_{21}\ g_{12} \geq \frac{|Y_{21} - Y_{12}|^2}{4} \tag{3.22}$$

By dividing both side by $g_{11}\ g_{22} - g_{21}\ g_{12}$

$$1 \geq \frac{|Y_{21} - Y_{12}|^2}{4\ (g_{11}\ g_{22} - g_{21}\ g_{12})} \tag{3.23}$$

Let us define the right hand side of equation (3.23) as U

$$U \triangleq \frac{|Y_{21} - Y_{12}|^2}{4\ (g_{11}\ g_{22} - g_{21}\ g_{12})} \tag{3.24}$$

Then, we can rewrite (3.24) for reciprocal network as

$$(g_{11}\ g_{22} - g_{21}\ g_{12})(1 - U) \geq 0 \tag{3.25}$$

or

$$U = \frac{Real(Y_{12}).Real(Y_{21})}{Real(Y_{11}).Real(Y_{22})} \tag{3.26}$$

To satisfy the passivity condition in the last equation, the value of U should be

$$0 \leq U \leq 1 \tag{3.27}$$

If $U < 0$, then the value of $(g_{11}\ g_{22} - g_{21}\ g_{12})$ in (3.25) is negative and as a result (3.27) can not be satisfied.

If $U > 1$, then (3.27) doesn't satisfy the condition of passivity.

3.5 Passivity Assessment

Before doing a transient simulation of a synthesized equivalent circuit, the stability of the circuit should be tested. For checking the stability of the fitted frequency response, the new calculated poles of the network should be tested. If the real part of the complex poles is positive then the synthesized equivalent circuit is unstable [18]. In some cases, the Vector Fitting [25], the algorithm that is employed in this research to approximate the frequency response, may produces some unstable poles. To overcome this problem [18], [30] we can either deleting the unstable poles, or flipping the unstable poles from the right side of the

complex plane to the left side, before calculating residues

Next, we have to test the passivity of the network. As presented before, the system admittance matrix of reciprocal network is said to be passive if [17] [31]:

1. $Real(Y_{11})$ and $Real(Y_{22}) \geq 0$
2. The detriment of (Y) ≥ 0

$$Y_h = \begin{bmatrix} g_{11} & \frac{Y_{12}+\overline{Y_{21}}}{2} \\ \frac{Y_{21}+\overline{Y_{12}}}{2} & g_{22} \end{bmatrix} = \begin{bmatrix} g_{11} & \frac{1}{2}(g_{12}+g_{21}+jb_{12}-jb_{21}) \\ \frac{1}{2}(g_{21}+g_{12}+jb_{21}-jb_{12}) & g_{22} \end{bmatrix} \tag{3.28}$$

$$U \triangleq \frac{|Y_{21}-Y_{12}|^2}{4\,(g_{11}\,g_{22}-g_{21}\,g_{12})}$$

To satisfy the passivity condition in the last equation, the value of U should be

$$0 \leq U \leq 1 \tag{3.29}$$

Since we are using Vector Fitting [25] in the modeling of the two port network model, it will be better if we test the passivity of the state space model instead of testing it as a Y-matrix [24]. Using Vector Fitting the Y-matrix of a network is approximated as

$$Y(s) = \sum_{m=1}^{n} \frac{R_m}{s-a_m} + D + sE \tag{3.30}$$

Whose state-space model representation is

$$Y(s) = C(sI-A)^{-1}B + D + sE \tag{3.31}$$

where C matrix is nxnN residues matrix, n is the number of ports and N is the order of approximation, (C matrix could be real or complex number), A matrix is nNxnN poles matrix (could be real or complex number), D and E are nxn real matrices, I matrix is the

identity matrix, B is a matrix of ones.

The Hamiltonian matrix of the state space model is given by [32], [20]:

$$M = \begin{bmatrix} A - B\,(D + D^T)^{-1}\,C & B\,(D + D^T)^{-1}\,B^T \\ -C^T\,(D + D^T)^{-1}\,C & -A + C^T\,(D + D^T)^{-1}\,B^T \end{bmatrix} \tag{3.32}$$

For testing the passivity of the state space model Hamiltonian matrix, we first calculates the eigenvalues of M, that will give us the crossover frequencies,CF (the crossover frequencies are the frequencies where a network will crossover to either a passive or non-passive frequency region) [20]:

$$CF = eig(M) \tag{3.33}$$

If the absolute value of the real part of crossover frequencies is greater than zero, then the system is passive, whereas if the absolute value of the real part of crossover frequencies is equal to zero then the system is not passive.

The disadvantages of Hamiltonian matrix for the of the passivity of a network are:

- The computational cost is high,
- The computational efficiency is not good, since the size of the Hamiltonian matrix is twice the size of the state space models,
- Only applicable to symmetrical model, and
- Do not give purely imaginary values of crossover frequencies (has numerical error).

To overcome these problems, the size of the Hamiltonian matrix should be reduced. Since the admittance matrix of the system is reciprocal, we could minimize the Hamiltonian matrix. Therefore, half-size Hamiltonian matrix approach has been proposed in [20] that is detailed in the following.

3.5.1 Singularity Test Matrix S and T

The following equations have been derived and presented by Semlyen and Gustavsen in [20] as the half-sized Hamiltonian matrix.

$$S = A\,(\,B\,D^{-1}\,C - A) \tag{3.34}$$

Or

$$T = (\,B\,D^{-1}\,C - A)\,A \tag{3.35}$$

Both S and T matrices provide the information on the passivity of the network. Since the half sized Hamiltonian matrix gives the same eigenvalues as the Hamiltonian matrix, we have

$$CF = eig(M) = \pm\sqrt{eig(S)} \tag{3.36}$$

This equation gives only one set of the complex numbers instead of showing the complex number and their conjugate pair. Thus, the computational cost is reduced.
Advantages of singularity matrix test include

- Increasing the computational speed by a factor of 8,
- Applicable to symmetrical and non symmetrical models, and
- Produce noiseless eigenvalues (less numerical error) [20].

3.6 Passivity Enforcement

After testing the passivity of a two port network and identifying the passivity violations, a passive enforcement method is used to compensate these violations to obtain a passive model. The passivity enforcement methods can be classified into two main group, a priori approach and a posteriori approach. The a priori approach is performed during the construction of state-space model. After obtaining the poles matrix of the state-space model, the poles matrix A of the model is retained and the residue matrix C, and the constant matrices, D and E are calculated to obtain a passive model. This method will required more computational time to recompute the residue and the constant matrices till obtaining a passive model. The a posteriori approach is achieved either by perturbing reside

matrices, pole matrices, eigenvalues of residues matrices, or eigenvalues of Hamiltonian matrices [18]. a Perturbation is mathematical methods to find an approximate solution for a problem. The method used in [27] which is implemented by Gustavsen in a computer code to enforce the passivity, is a posteriori approach. Since it requires less computational time than priori approach. Gustavsen, has used it in the computer code which is used in this thesis.

3.7 Case Studies

In this section, an example is studied to show the differences between each test method and their limitations. This example is divided into three different cases to present the advantages and disadvantages of each test methods. Besides, it will cover most of the scenarios for testing the passivity of a network. In the first case, a passive network with positive circuit elements is studied, which will show the numerical error for each test method if existed. In the second case, a passive network with a negative circuit element is tested. It is shown that even though the network has a negative element the network still passive. In the third case, a non-passive network with a negative circuit element is studied. This circuit will show the violation band of each test methods and which of them is the most accurate, has less numerical errors, and requires less computational time. Since the network tested, shown in the Figure 3.2, is a two port network, the method used to get the frequency response of the admittance is Matrix Fitting instead of Vector Fitting [25]. The order of approximation is set to 20, i.e. $n = 20$. The focus of this test is on the passivity more than fitting the admittance frequency response.

3.7.1 Case 1

In the first case, the circuit elements of the test circuit shown in Figure 3.2 are positive and hence the circuit is passive. Since this case deals with a passive network and positive circuit elements there should be no passivity violation regions and no crossover frequencies. The values of the circuit element for this case are shown in Table 3.1.

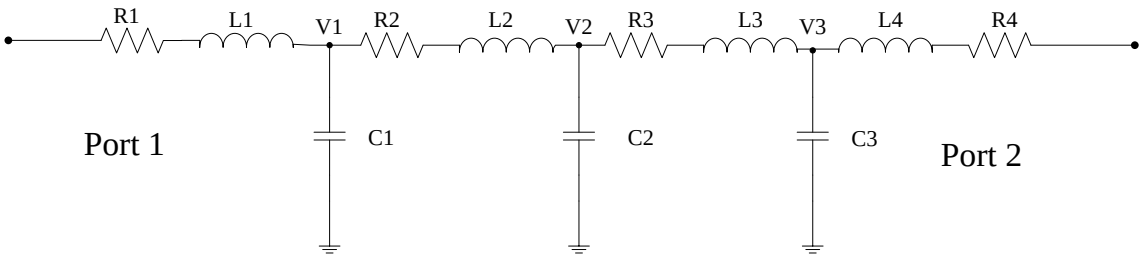

Figure 3.2: A test circuit used to study passivity assessment methods [31].

Table 3.1: The values of the network elements for case 1.

R1= 1 Ω	R2= 0.2 Ω	R3 = 0.1 Ω	R4 = 25 Ω
L1= 0.2 nH	L2= 0.8 nH	L3 = 3 nH	L4 = 4 nH
C1= 10 pF	C2= 2 pF	C3 = 1 pF	

3.7.2 Case 2

In this case, the elements values of the test circuit are the same as case 1 but one. R3 in this case has a negative value. However, the circuit is overall passive. Therefore, there should be no passivity violation regions and no crossover frequencies. The values of the circuit element for this case are shown in Table 3.2.

3.7.3 Case 3

In this case, the elements values of the equivalent circuit are positive and negative (see Table 3.3) and the overall circuit is not passive. Therefore, there will be passivity violation regions and crossover frequencies. The elements of the admittance matrices for cases 1 - 3 are plotted in Figure 3.3 to Figure 3.8. The real values of the admittance matrices have been plotted to show the first condition of the passivity assessment, where the angles of the admittance matrices have been plotted to show that the angle of circuit are between -180 to +180 [31].

Table 3.2: The values of the network elements of case 2.

R1= 1 Ω	R2 = 0.2 Ω	**R3= -0.1** Ω	R4 = 25 Ω
L1= 0.2 nH	L2= 0.8 nH	L3 = 3 nH	L4 = 4 nH
C1= 10 pF	C2= 2 pF	C3 = 1 pF	

Table 3.3: The values of the network elements of case 3.

R1= -1 Ω	R2= 0.2 Ω	R3 = 0.1 Ω	R4 = 25 Ω
L1= 0.2 nH	L2= 0.8 nH	L3 = 3 nH	L4 = 4 nH
C1= 10 pF	C2= 2 pF	C3 = 1 pF	

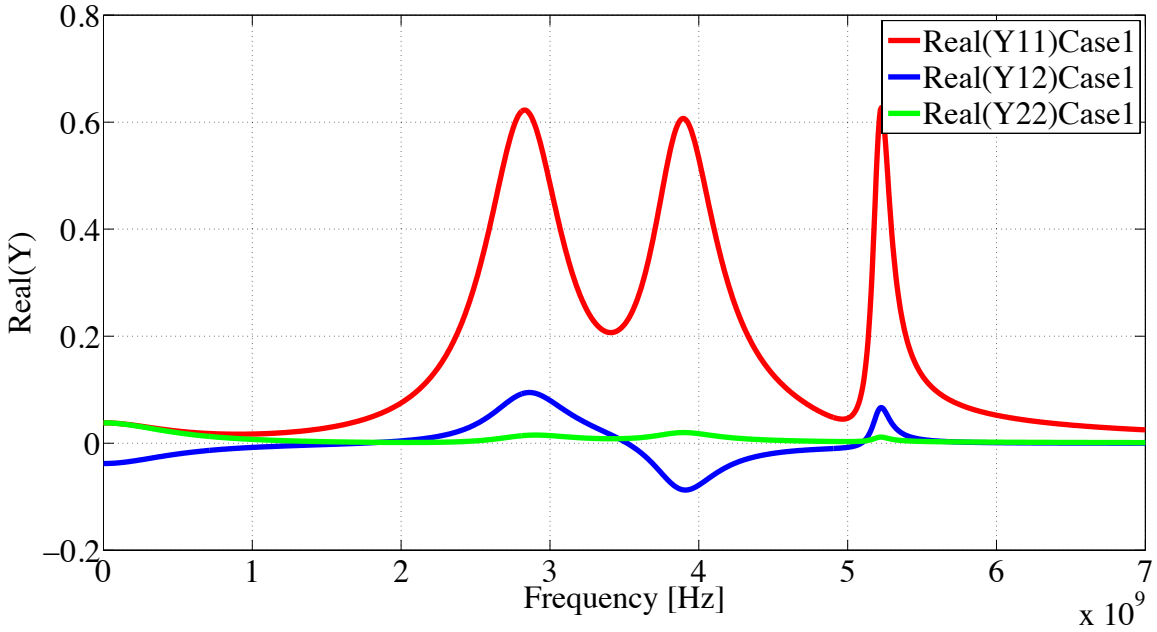

Figure 3.3: Real values of the calculated admittance of Case 1. [31].

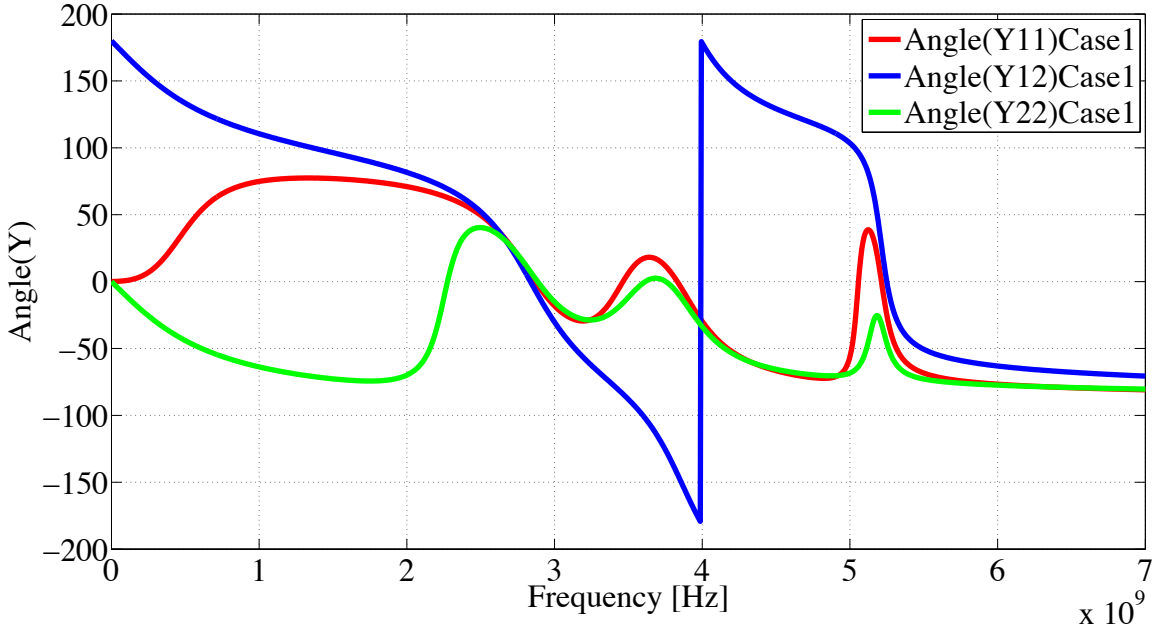

Figure 3.4: Angle of the calculated admittance of Case 1 [31].

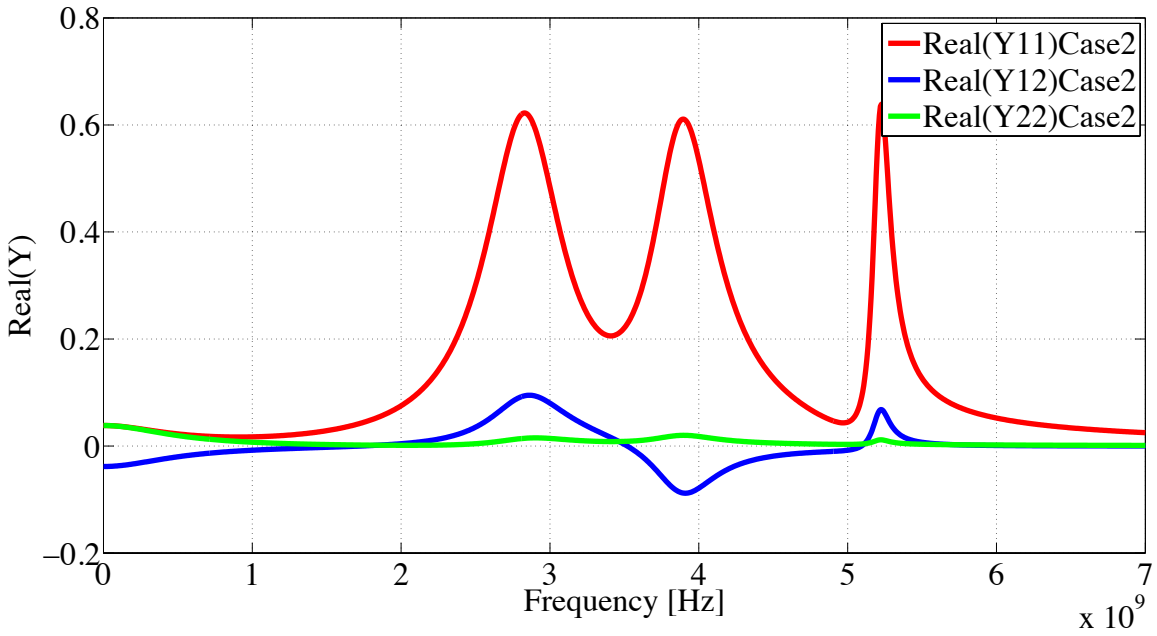

Figure 3.5: Real values of the calculated admittance of Case 2 [31].

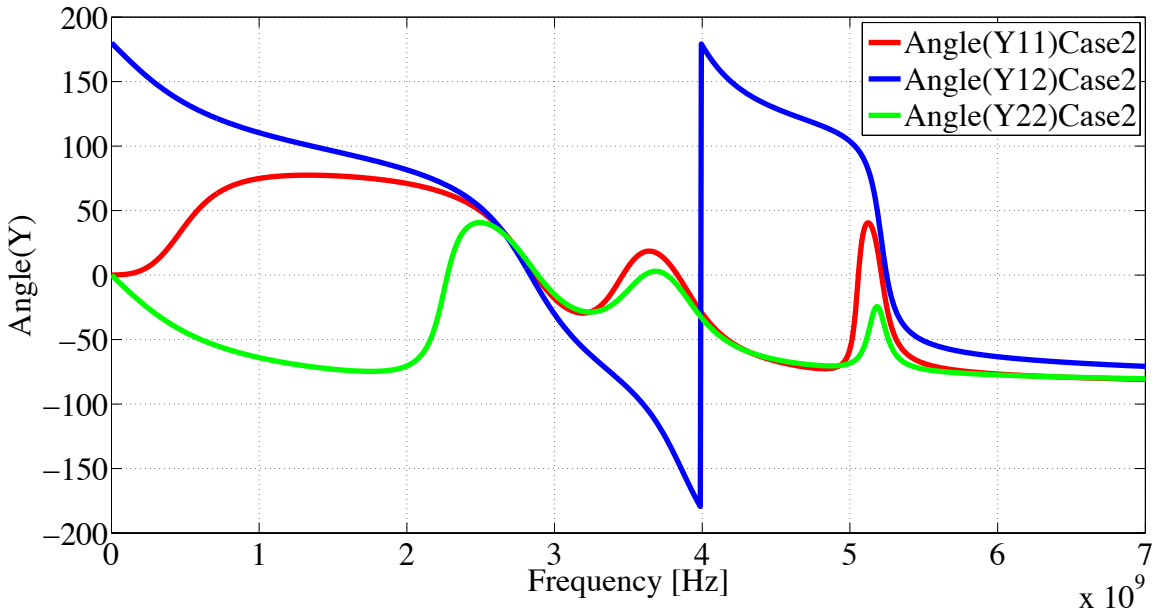

Figure 3.6: Angle of the calculated admittance of Case 2 [31].

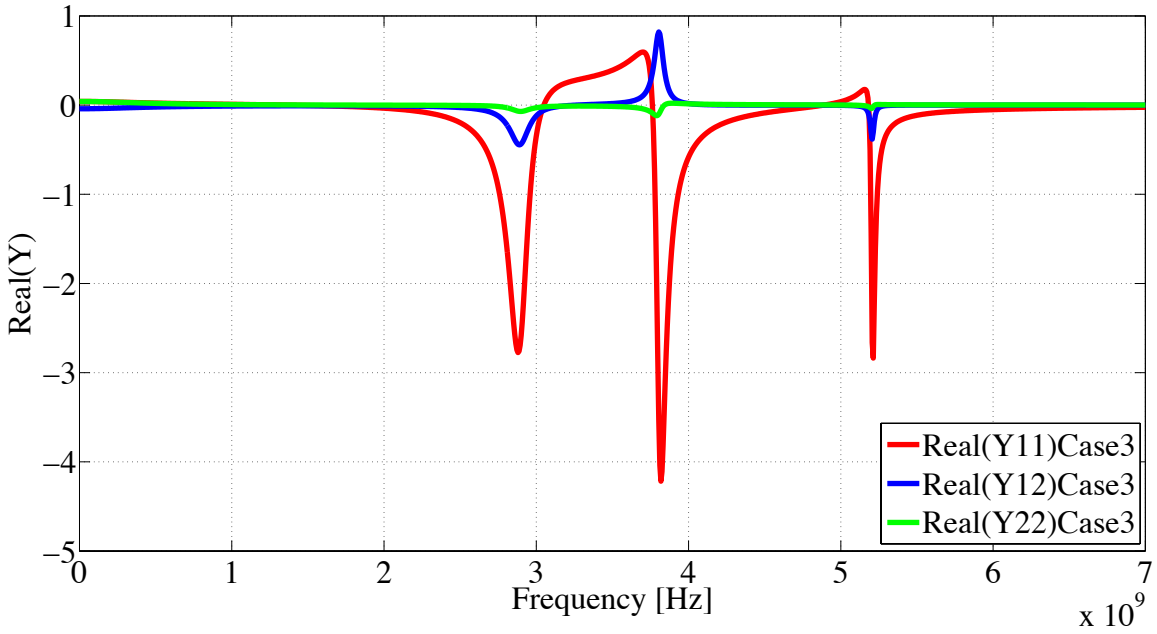

Figure 3.7: Real values of the calculated admittance of Case 3 [31].

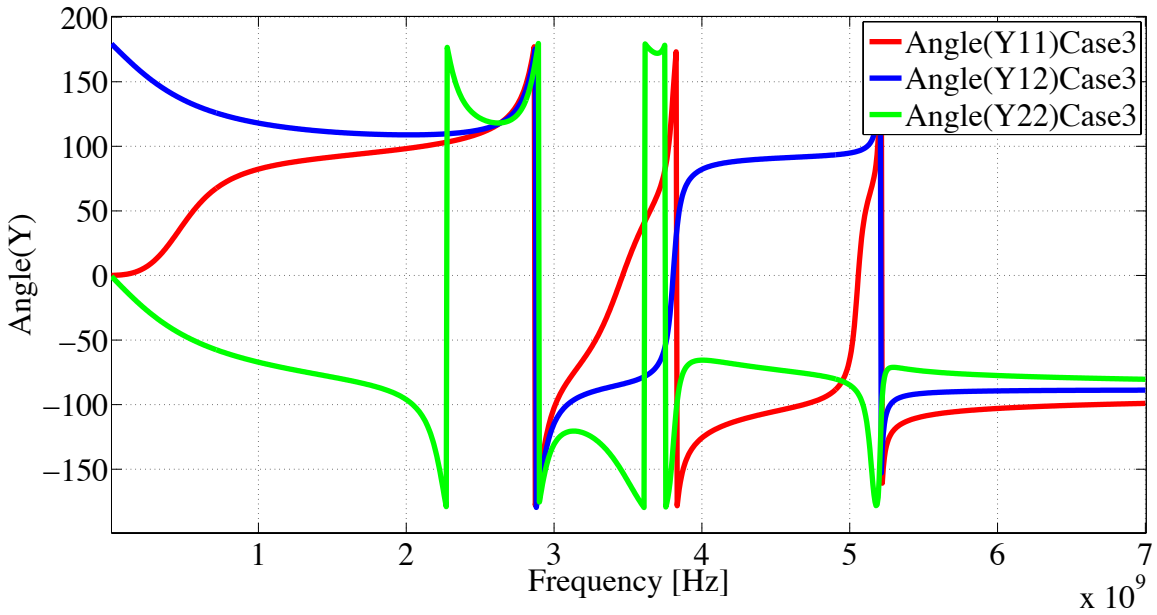

Figure 3.8: Angle of the calculated admittance of Case 3 [31].

3.8 Passivity Tests

3.8.1 Y-matrix Passivity Test

The Y-matrix in this example is nxn, where n is the number of ports, and since the sampling of Y-matrix in the frequency range from 0 Hz-7 GHz is 1000, then we have 1000 2x2 matrices. In the first and second cases, the real part of Y11 and Y22 are positive as shown in the Figure 3.3 and Figure 3.5. Therefore, the first condition of the passivity test of the network is satisfied. While in the third case the real part of Y11 and Y22 are changing between positive and negative values as shown in Figure 3.7. Therefore, the first condition of the admittance matrix passivity test of the network is not satisfied.
For the second condition of Y-matrix passivity test of a two port network we evaluate

$$U = \frac{Real(Y_{12}).Real(Y_{21})}{Real(Y_{11}).Real(Y_{22})} \tag{3.37}$$

To satisfy the passivity condition, the value of U should be (see Figure 3.9)

$$0 \leq U \leq 1 \tag{3.38}$$

Figure 3.10 shows that the first and the second cases are passive since the first and the second conditions of Y-matrix test are satisfied. Figure 3.9 shows the third case is not passive since the second condition of Y-matrix test is not satisfied.

3.8.2 Y-matrix Passivity Test of Fitted Admittance Matrix

Since the first and the second cases are passive, therefore the focus of violation regions or the crossover frequencies will be on the third case. In the third case, it seems like the violation region of passivity test of the fitted Y matrix should have the same violation regions as the calculated Y-matrix, but this is not the case. Since the fitted admittance is not a perfect fit and depends on many factors, for instant the order of approximation, therefore the crossover frequencies will not match the fitted admittance or the measured ones as shown in Figure 3.11. In this research, this is not an important issue because

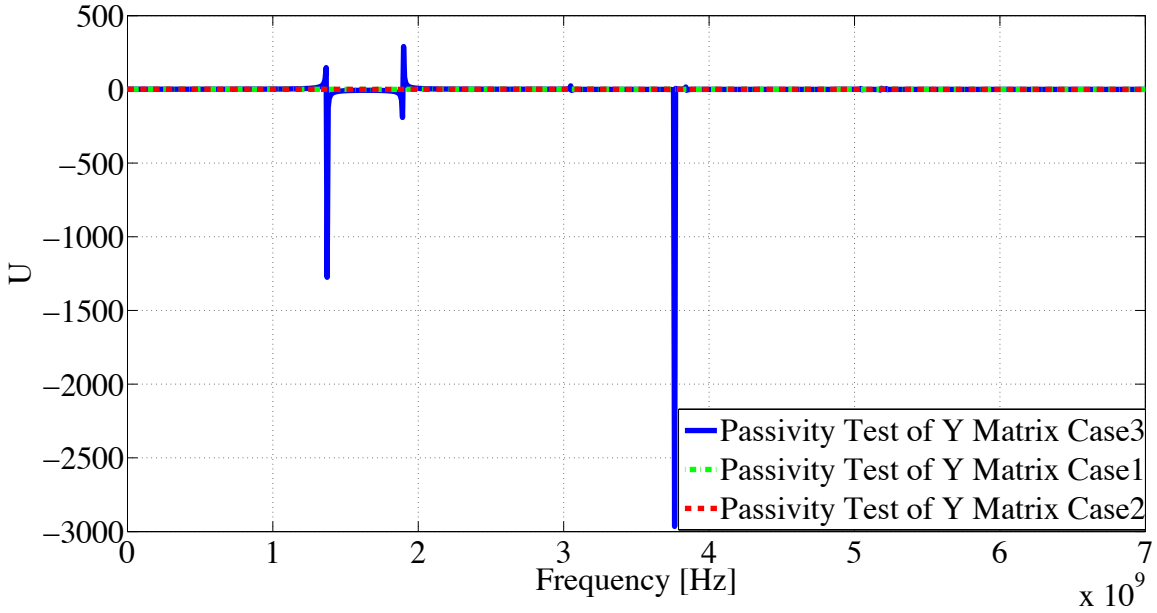

Figure 3.9: Y-matrix passivity tests of calculated admittance matrices for case 1, 2, and 3.

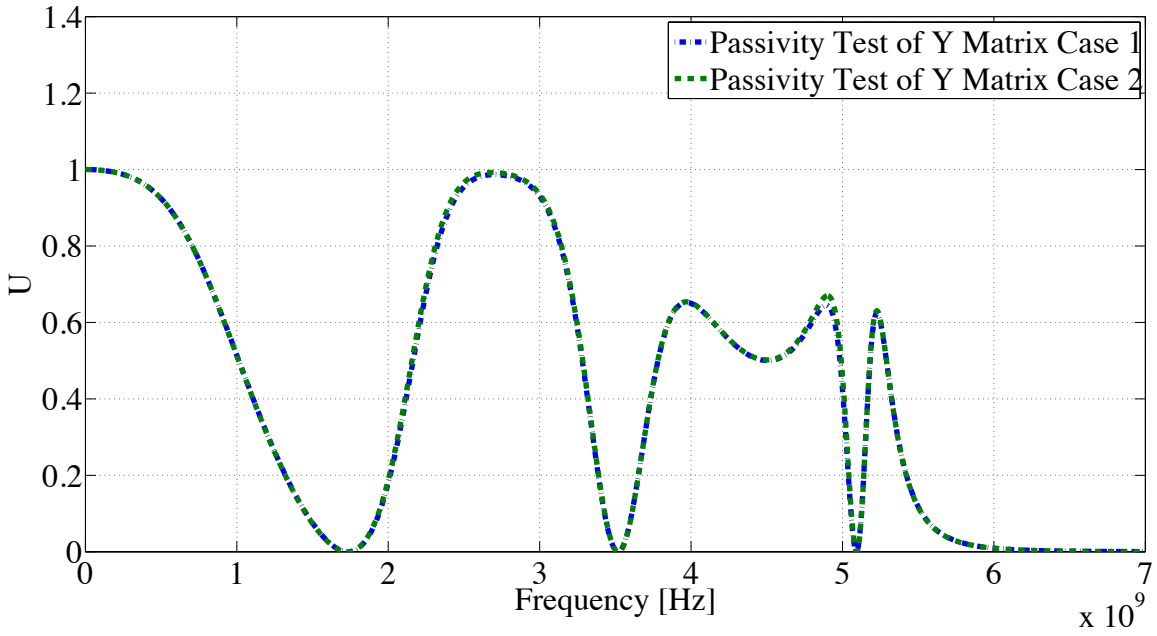

Figure 3.10: Y-matrix passivity tests of calculated admittance matrices for case1, and 2.

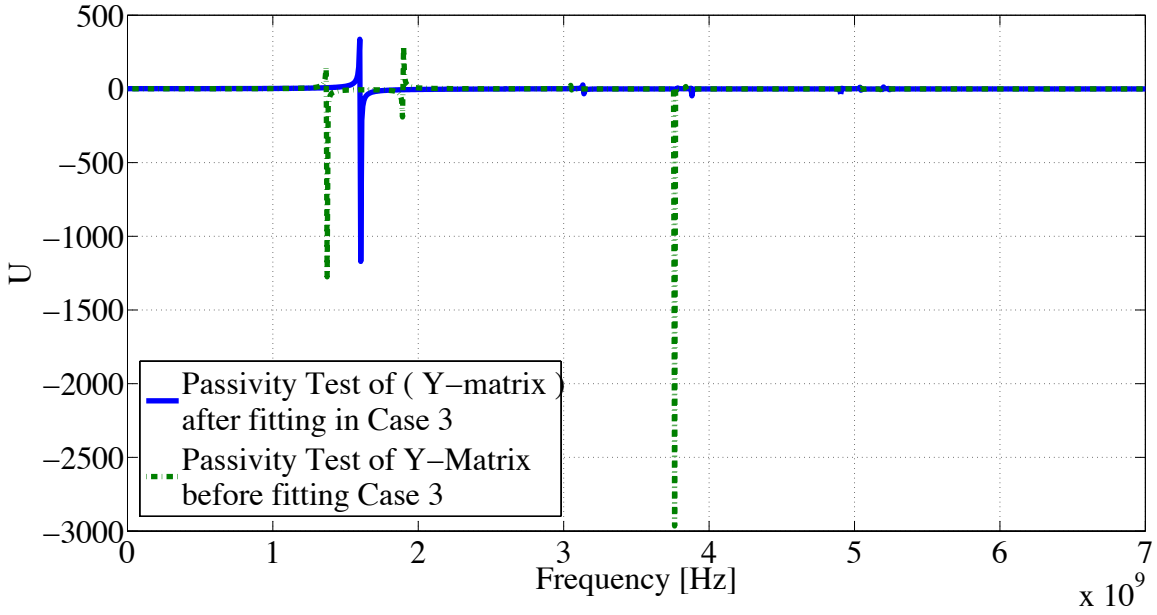

Figure 3.11: Hamilton matrix passivity test for the calculated admittance and the fitted one.

the focus of thesis is to find a passive equivalent circuit which could be used in transient analysis simulation.

3.8.3 Hamiltonian Matrix Test

The Hamiltonian matrix is a nnNxnnN matrix, where n is the number of ports and N is the order of approximation, so the Hamiltonian matrix in this example is 80x80 matrix. This test is carried out after fitting the admittance frequency response and obtaining the state-space model, described by A, B, C, and D matrices. Where A is a 40x40 poles matrix (this matrix is diagonal matrix, thus the poles values are the diagonal values), B is 40x2 matrix, C is a 2x40 residues matrix, and D is 2x2 constant matrix. The Hamiltonian matrix is given by [20]

$$M = \begin{bmatrix} A - B\,(D + D^T)^{-1}\,C & B\,(D + D^T)^{-1}\,B^T \\ -C^T\,(D + D^T)^{-1}\,C & -A + C^T\,(D + D^T)^{-1}\,B^T \end{bmatrix} \tag{3.39}$$

For testing the passivity of the state space model Hamiltonian matrix, the eigenvalues of M must be evaluated that include the crossover frequencies, CF.

$$CF = eig(M) \tag{3.40}$$

All the values from this equation (80 values) will not give the crossover frequencies, as discussed in passivity assessment section. To find the crossover frequencies from these values, the real part of each complex number identifies if this value is the crossover frequency or not. If the real part is zero or too small, then the imaginary part represents he crossover frequency, ω

$$\omega = 2\pi f \tag{3.41}$$

Therefore, by calculating the crossover frequencies and plotting them for the Y-fitted matrix we can identify the violation regions and compare both of the methods.

Hamiltonian Matrix Test has been developed to find the crossover frequencies with more accuracy with less number of frequency responses.

The disadvantages of Hamilton matrix test:

1. Numerical error: Since this network has only passive elements and there is no any internal source in the network and all the network elements have positive value, therefore this circuit should be passive at all frequency range. In the presented example there is a small numerical error for the first value of U, which has the value of 1.000000000000173.
2. Discreet points in frequency: This test method will not give the exact value of which the crossover frequency took place. Therefore, to find out the exact value where the crossover took place, the sampling number of the admittance calculation-in our case- or measurement should increase.
3. It requires more computing time.

3.8.4 State-space model half size Hamiltonian Matrix test (S-Matrix and T-Matrix)

The S or T matrices in this example are 40x40 matrices. This test is based on the sate-space model that has been developed to increase the accuracy of finding the crossover frequencies and less computational time compared to Hamiltonian matrix.

First, the S or T matrices are evaluated using

$$S \;=\; A\,(\,B\,D^{-1}\,C \;-\; A) \tag{3.42}$$

$$T \;=\; (\,B\,D^{-1}\,C \;-\; A)\,A \tag{3.43}$$

and, next, the crossover frequencies are calculated as

$$CF = eig(M) = \pm\sqrt{eig(S)} = \pm\sqrt{eig(T)} \tag{3.44}$$

All the values of this equation will not give the crossover frequencies. To find the crossover frequencies from all these values the real part of each complex number identifies if this value is the crossover frequency or not. If the real part is zero or too small then the imaginary part represents the crossover frequency $\omega = 2\pi f$

Therefore, we have to calculate the crossover frequencies and plot them for the Y-fitted matrix to identify the violation regions to compare it with other methods (see Figure. 3.12).

Since the first and the second cases are passive as shown in Figure 3.10, therefore the focus of violation regions or the crossover frequencies will be in the third case, as shown in Figures 3.13 - 3.16.

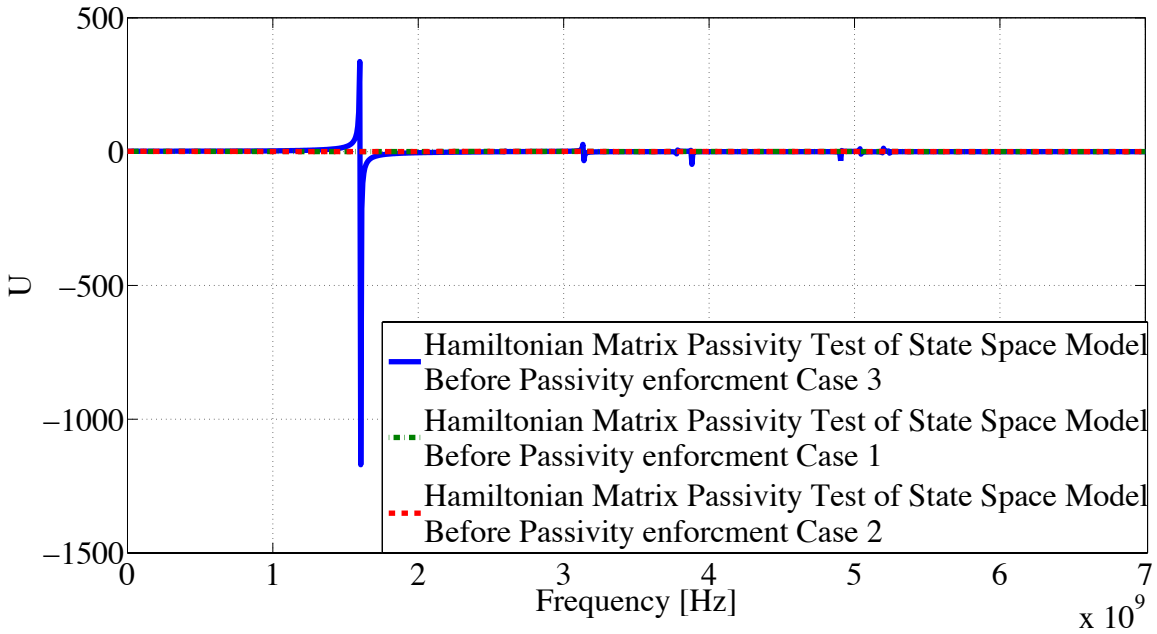

Figure 3.12: Hamiltonian Matrix Passivity test for all cases before applying the passivity enforcement.

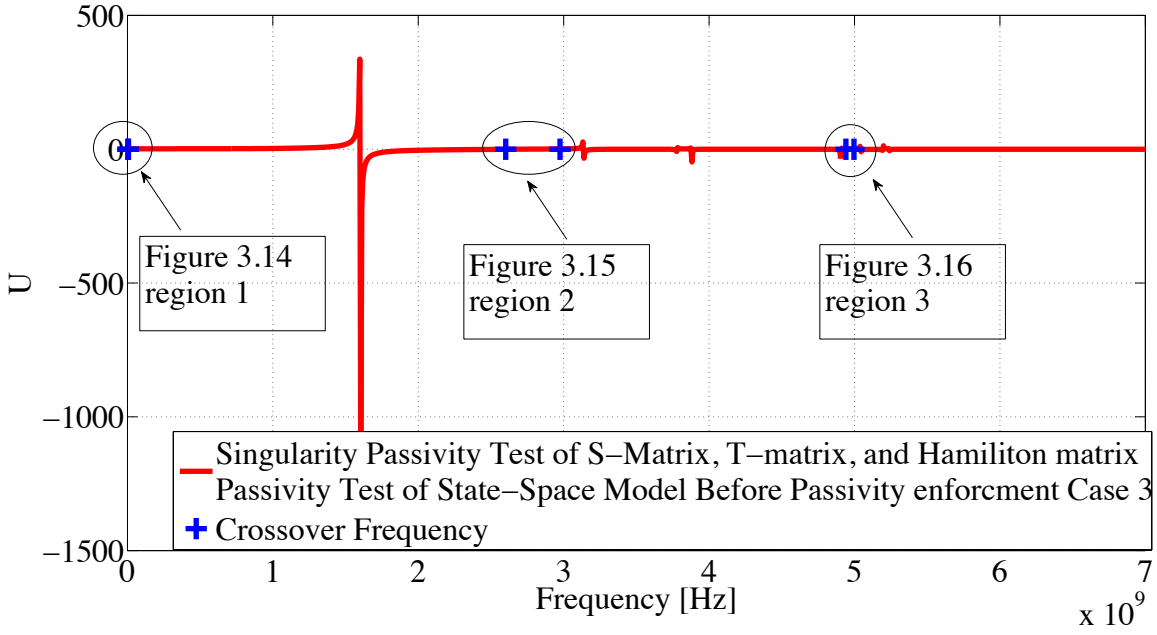

Figure 3.13: Crossover frequencies and passive region before passivity enforcement for case 3.

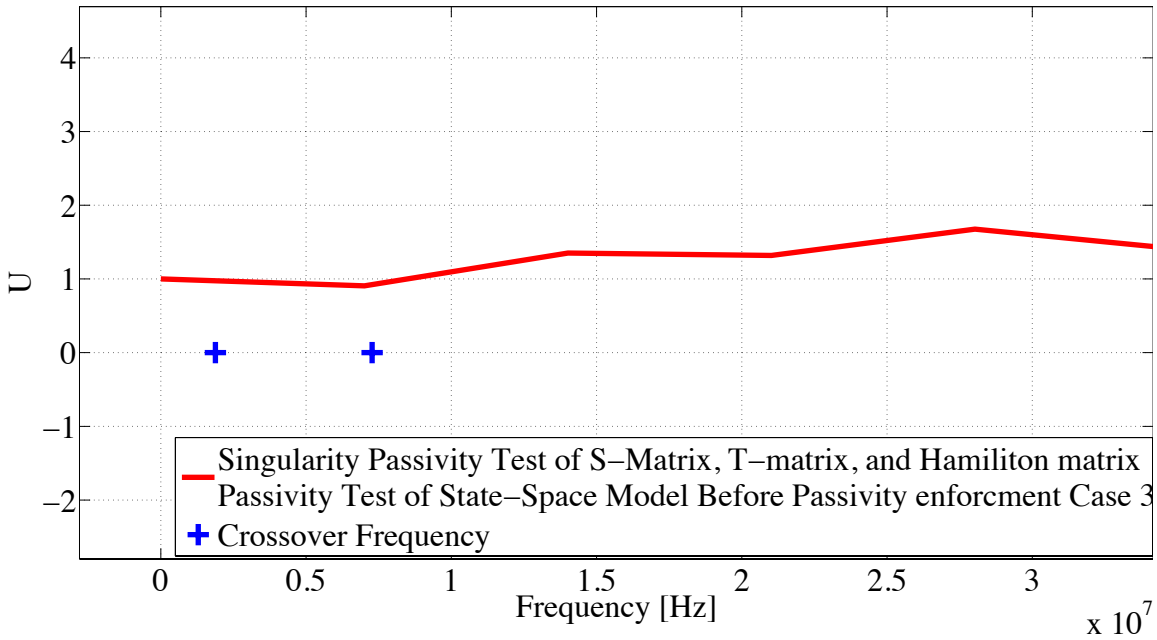

Figure 3.14: Crossover frequencies and passive region before passivity enforcement for case 3 for region 1.

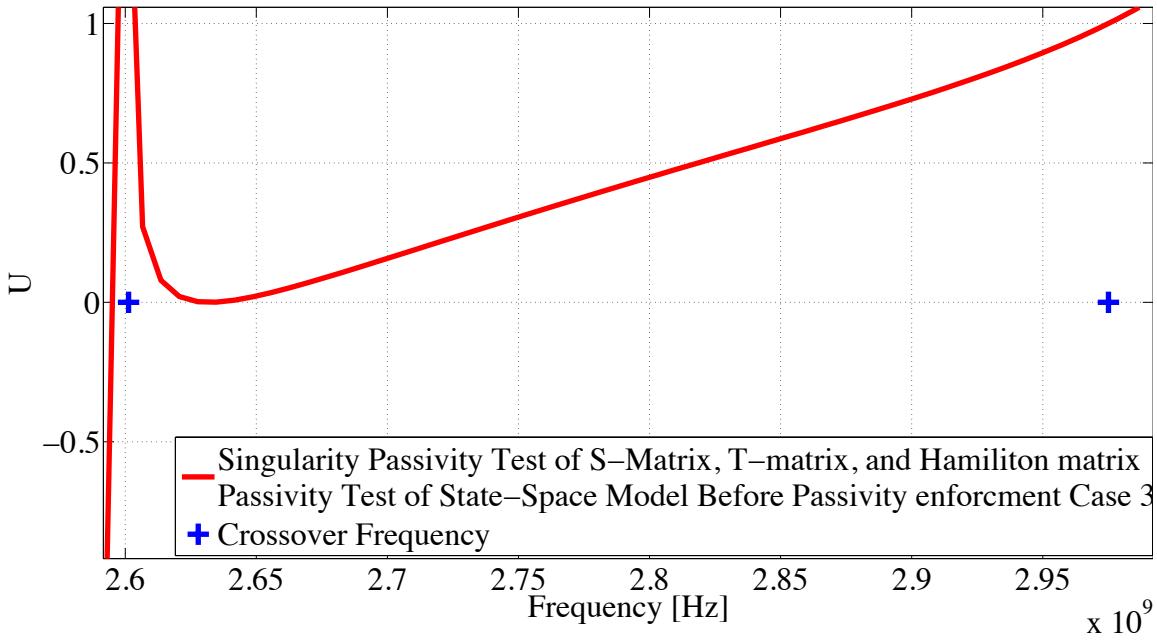

Figure 3.15: Crossover frequencies and passive region before passivity enforcement for case 3 for region 2.

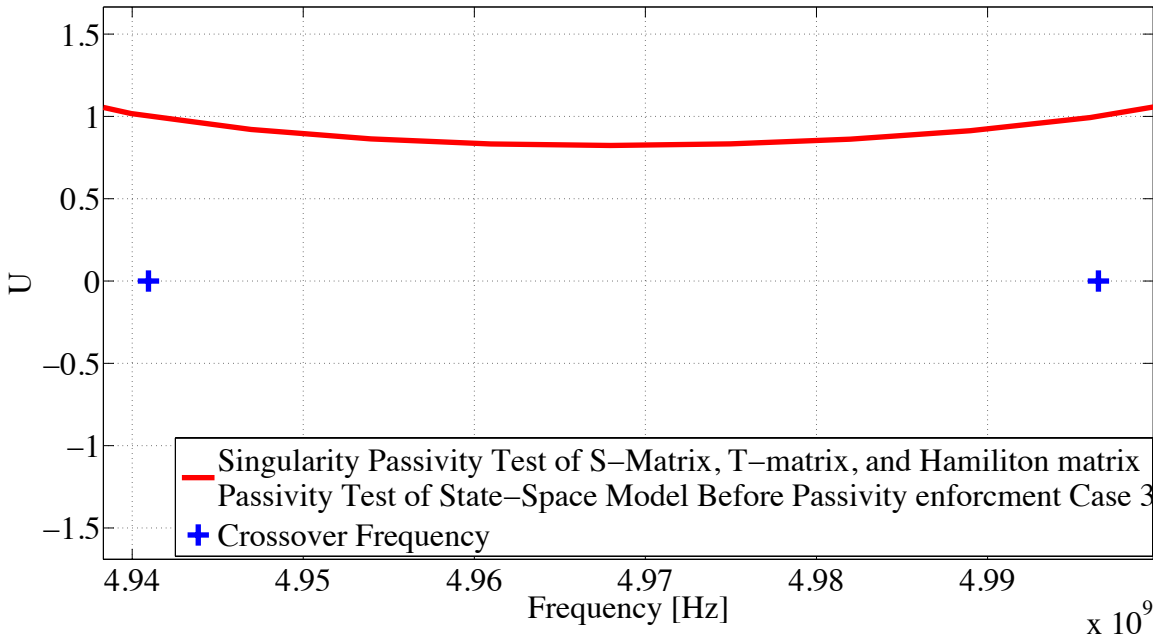

Figure 3.16: Crossover frequencies and passive region before passivity enforcement for case 3 for region 3.

3.9 Passivity Assessment of cases 1, 2, and 3

3.9.1 Cases 1 and 2

Since the values of the passivity assessment tests for S- matrices and T- matrices have no pure real values, the passivity assessment tests for M matrix has no imaginary values, and Y-matrix passivity assessment test satisfies both conditions of passivity assessment, so there are no any passivity violation regions or crossover frequencies for the first and the second cases. Thus, the two port network obtained from matrix fitting is passive.

3.9.2 Case 3

In Table 3.4, one can see that there are six crossover frequencies and three passivity violation regions for case 3. The Y-matrix passivity test obtained from the calculated admittance does not give exact values of crossover frequencies instead it estimated the crossover frequencies between two points. Thus, to get exact values of the crossover frequencies, the sampling number of the calculated admittance should increase significantly which will not

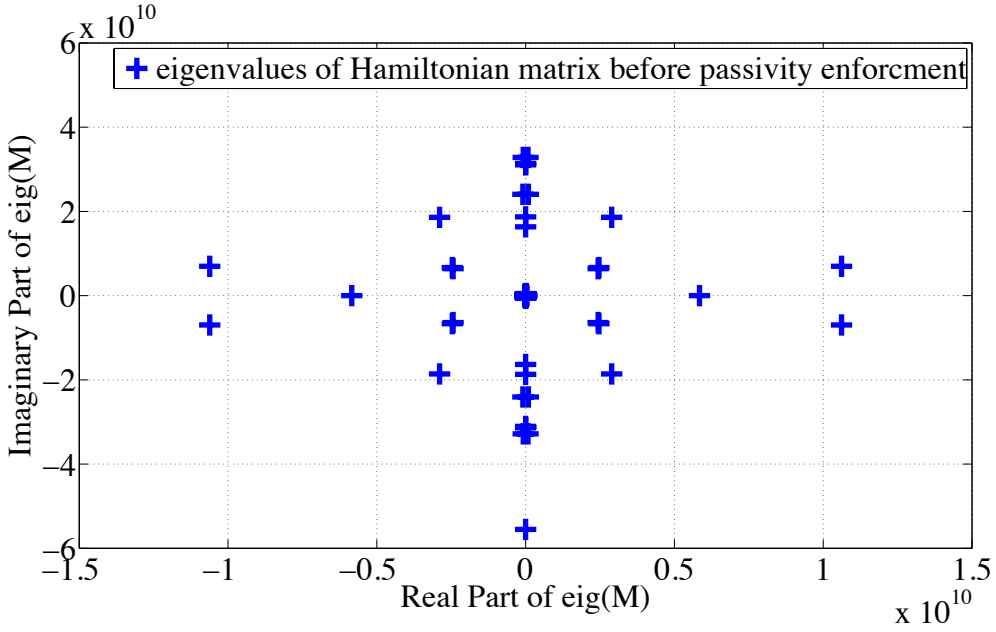

Figure 3.17: eEgenvalues of Hamiltonian matrix before passivity enforcement for case 3. The are many pure imaginary numbers of the eigenvalues of Hamiltonian matrix which identify passivity violation.

be practical. While the eigenvalues of Hamiltonian matrix, see Figure 3.17, of state-space model gives the exact values of the crossover frequencies, but in some cases gives inaccurate values as shown in Table 3.4. To overcome this problem the singularity matrix test, see Figures 3.18 and 3.19, has been presented by Semlyen and Gustavsen in [20]. In addition, the singularity matrix test requires less computational time and has less numerical errors.

After enforcing the passivity in the third case, all different kinds of tests that have been discussed show a passive network response (see Figures 3.20, 3.21, 3.22, and 3.23). Thus, there is no crossover frequencies or violation regions. To enforce passivity, the residues and the constants matrices are recalculated to obtain a passive rational function and maintaining the best fit to the admittance matrix [18], [24] and [27]

From Figures 3.20, 3.21, 3.22, and 3.23, it is obvious that there are no passivity violation regions or crossover frequencies after applying passivity enforcement. Thus, the two port network obtained from matrix fitting is passive.

Different passivity assessments techniques have been discussed in this chapter. They have their advantages and disadvantages, some of which have been discussed earlier. For

Table 3.4: The values of the passivity assessment tests for S- matrices, T- matrices, M matrices, and Y-matrix after admittance fitting for the third case.

Frequency where $1 < U < 0$	$\omega = eig(M)$ Absolute value of the real part ≈ 0	$\omega = \pm\sqrt{eig(S)}$ Absolute value of the Imaginary value ≈ 0	$\omega = \pm\sqrt{eig(T)}$ Absolute value of the Imaginary value ≈ 0
1.401e+07	-3.814e-05 +5.551e+10i	5.551e+10 -6.806e-07i	5.551e+10 +7.058e-07i
2.599e+09	-1.053e-05 -5.551e+10i	3.139e+10 -2.081e-06i	3.139e+10 +1.191e-06i
2.977e+09	-1.808e-05 +3.139e+10i	3.104e+10 -1.573e-06i	3.104e+10 +1.115e-07i
4.939e+09	-1.814e-05 -3.139e+10i	1.869e+10 +4.296e-06i	1.869e+10 +8.524e-07i
5.003e+09	4.338e-06 +3.104e+10i	1.634e+10 +4.717e-07i	1.634e+10 -4.560e-06i
	1.317e-06 -3.104e+10i		
	6.397e-06 +1.869e+10i		
	-6.575e-07 -1.869e+10i		
	-2.982e-05 +1.634e+10i		
	-2.483e-05 -1.634e+10i		
	-1.758e-06 -4.571e+07i		
	-2.994e-06 +4.571e+07i		
	1.854e-05 +1.181e+07i		
	2.084e-05 -1.181e+07i		
The rest of the values are between 0 and 1, $0 \leq U \leq 1$	The rest of the absolute value of the real value $\gg 0$	The rest of the absolute value of the Imaginary value $\gg 0$	The rest of the absolute value of the Imaginary value $\gg 0$

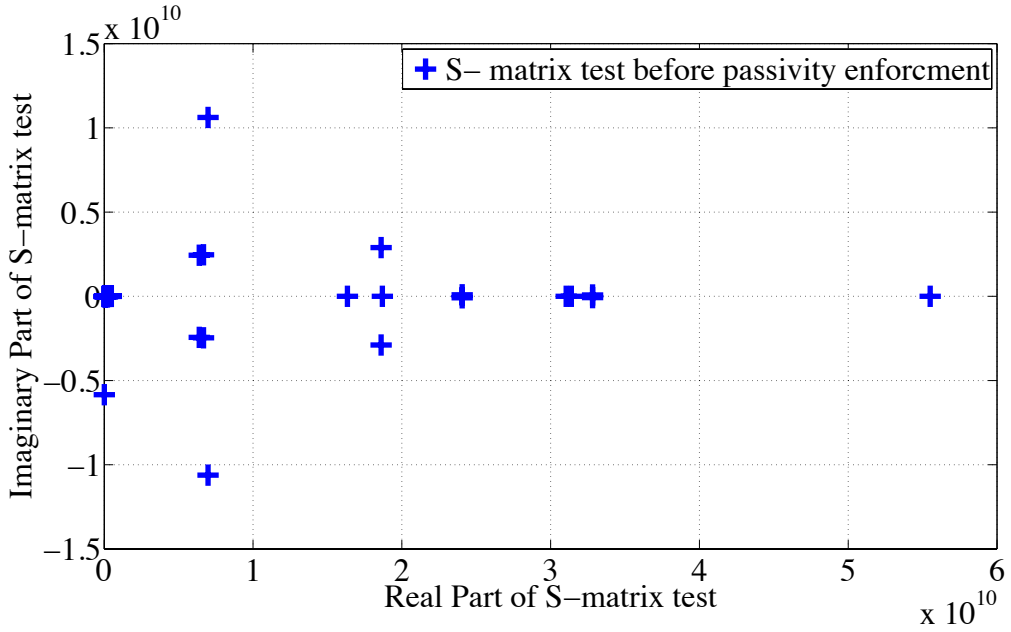

Figure 3.18: S-matrix test before passivity enforcement for case 3. The are many pure real numbers of the eigenvalues of S-matrix which identify passivity violation.

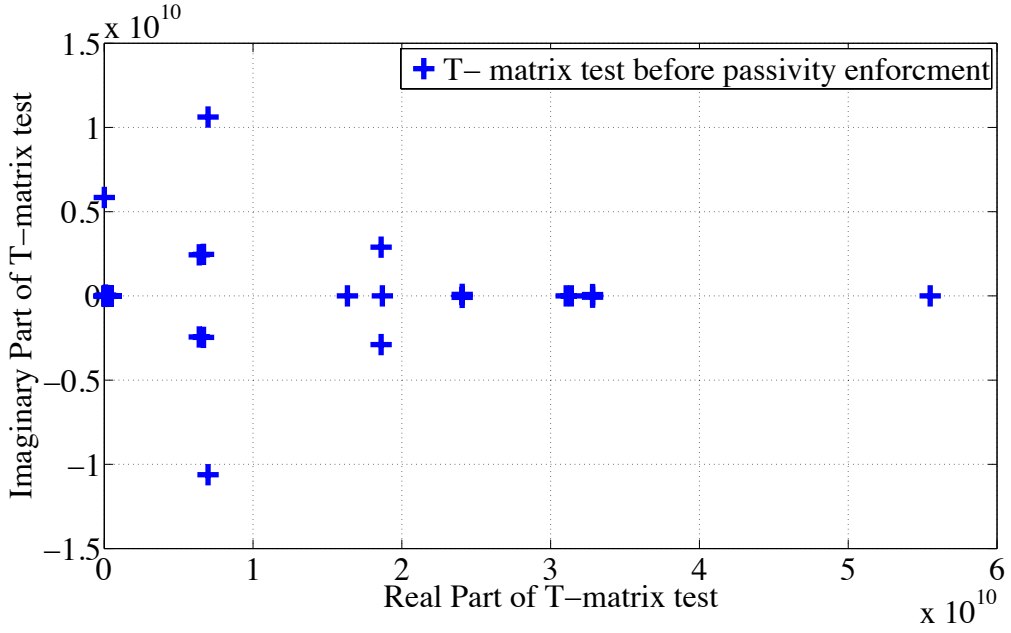

Figure 3.19: T-matrix test before passivity enforcement for case 3. The are many pure real numbers of the eigenvalues of T-matrix which identify passivity violation.

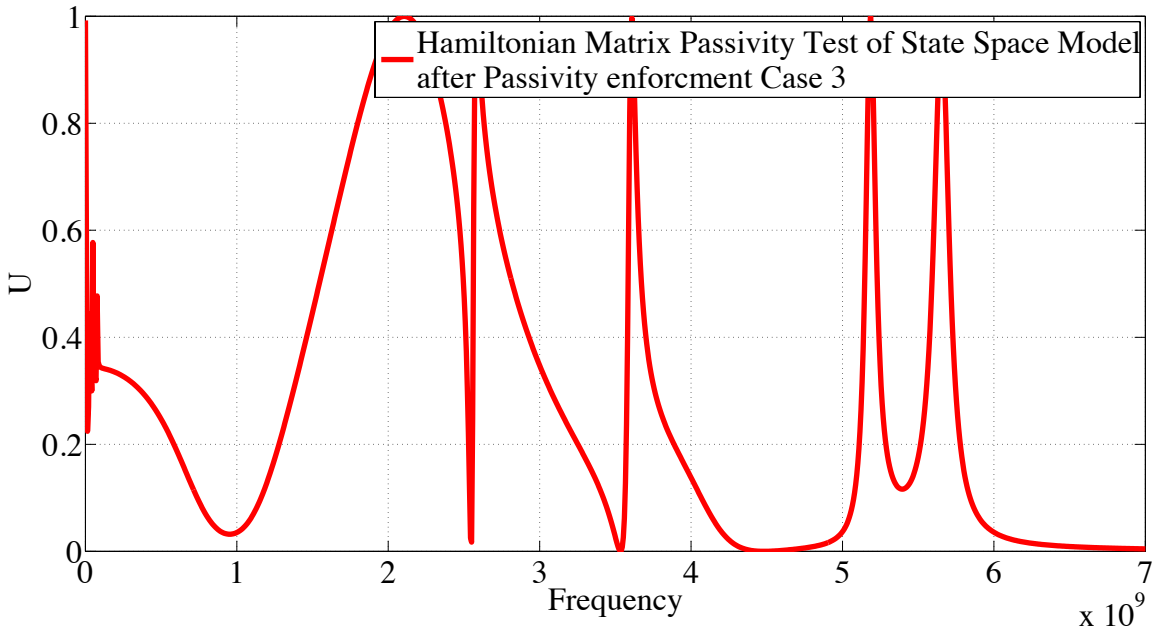

Figure 3.20: Passivity tests after passivity enforcement.

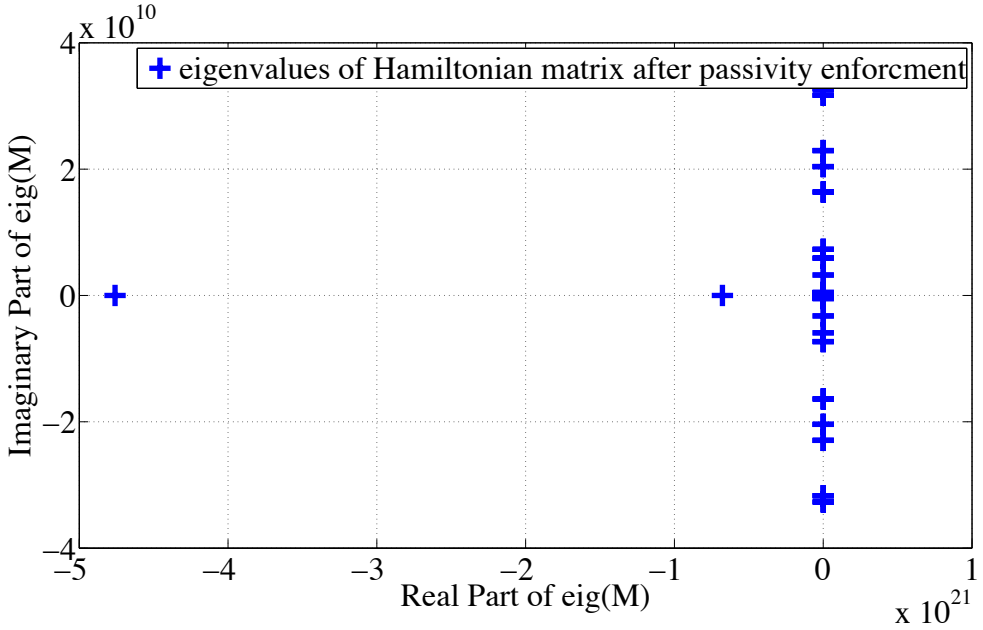

Figure 3.21: eigenvalues of Hamiltonian matrix passivity tests after passivity enforcement. The are not any pure imaginary eigenvalues of the Hamiltonian matrix after enforcing the passivity. It may look like that the values are pure imaginary but that is not the case, it is due to the wide scale of the axes.

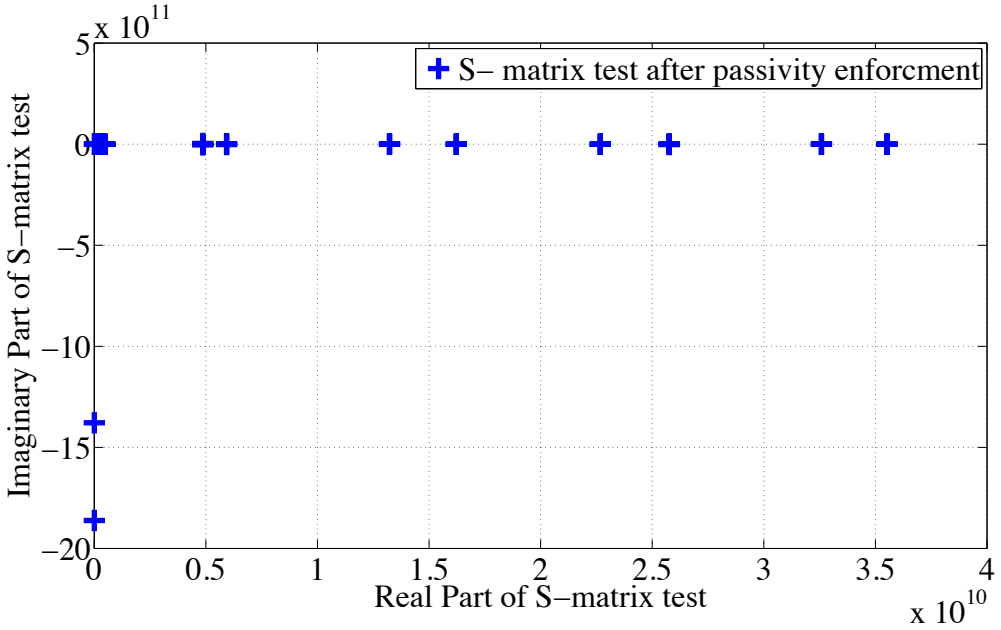

Figure 3.22: S- matrix passivity tests after passivity enforcement. The are not any pure real eigenvalues of the S-matrix after enforcing the passivity. It may look like that the values are pure real but that is not the case, it is due to the wide scale of the axes.

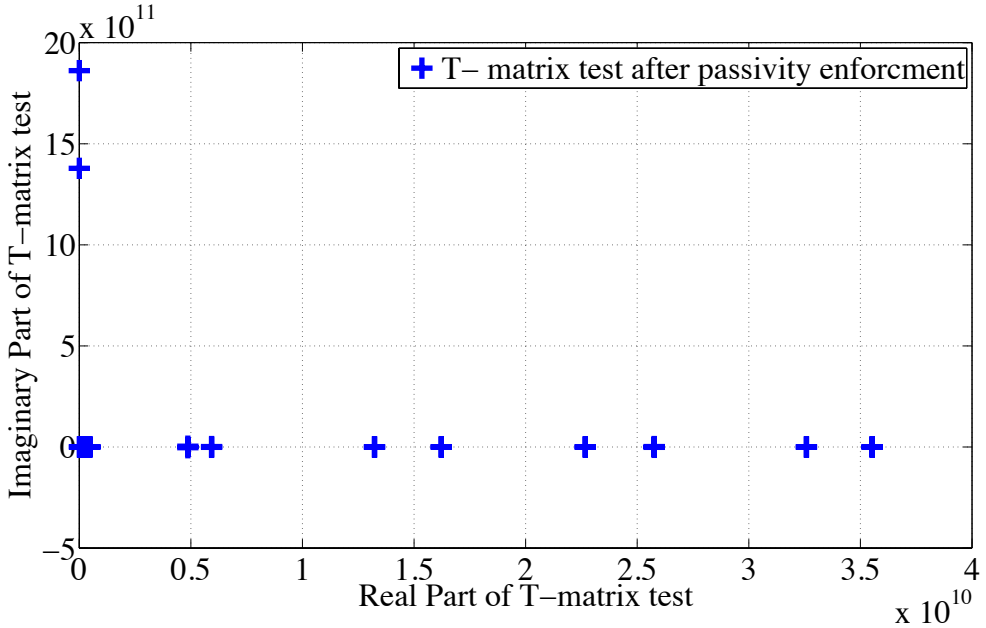

Figure 3.23: T- matrix Passivity tests after passivity enforcement. The are not any pure real eigenvalues of the T-matrix after enforcing the passivity. It may look like that the values are pure real but that is not the case, it is due to the wide scale of the axes.

Table 3.5: Comparisons between different test methods.

Test Methods	Samples	Computational time	Numerical Error	Accuracy
U	1000	high	Low	Low
$\omega = eig(M)$	80	Medium	Medium	Medium
$\omega = \pm\sqrt{eig(S)}$	40	Low	Low	high
$\omega = \pm\sqrt{eig(T)}$	40	Low	Low	high

a summary, see Table A.9.

Chapter 4

Circuit Synthesis

After ensuring the passivity of interest the admittance matrices and thus ensuring its stability over the wide frequency range, a model could be derived from the state-space model which has been obtained from the admittance matrices using Vector Fitting- to represent the transformer. In this chapter, methods will be shown to convert the state-space model to a circuit model which will give the same frequency response as the transformer.

4.1 Background

The circuit modeling of rational functions has been discussed in [33]. The author shows how to represent the same rational function in many different circuit models. In addition, it shows how to model the same rational function if it was an impedance (which known as FOSTER I) [33], [34], or admittance (known as FOSTER II). For more complex system representations such as ladder networks, [33] shows the CauerI and CauerII networks (different types of LC ladder networks) and how to calculate the circuit elements from the rational approximation, either an impedance or an admittance. All these calculations have been carried out for one port networks and calculated according to rational approximation function and not for the state-space model. Such calculations are essential in how the system is represented and how to interpret the circuit elements in the model.

In [35], using the scattering parameters, an equivalent circuit model has been presented

for a potential transformer or a current transformer in the frequency range of 0.1- 11 MHz. To synthesize an equivalent circuit for a potential transformer or a current transformer, the scattering parameters must be transformed to an admittance or an impedance. To study the effect of coupling through the stray capacitance of a potential transformer or a current transformer caused by the very fast transient overvoltage (VFTO), the equivalent circuit should be modeled as a two port network.

Circuit synthesis of different models from state-space equations have been discussed in [36]. The circuit synthesis and the circuit model have been driven and shown for different cases and models. The synthesized circuits have been derived from the state-space model instead of the rational function approximation, which is very useful when dealing with Vector Fitting. The derived circuits and models are presented in admittance or impedance circuits, each with its own calculations and modeling.

In [37], synthesizing an equivalent circuit for Radio Frequency Identification (RFID) antenna from the state space model has been shown. The paper shows how to build the equivalent circuit from real and complex poles and residue pairs. Mathematical derivations of the equivalent circuit model have been provided.

The paper in [38] gives an overview of most of the models in literature, and discusses their development, implementation, and limitations. This paper deals with the circuit model of frequency range below 10 kHz. In addition, this paper shows how to implement an electric circuit model for transformer by using series Foster equivalent circuit to represent the frequency response of a transformer winding and by using the Cauer equivalent circuit model to represent and simulate the eddy current for the iron core.

Current transformers and potential transformers have been simulated in [39] to study the effects of transient of electromagnetic interference between the system primary and secondary which has vital importance for determination of the response in transient con-

ditions. This paper also use scattering parameters to model the current transformer from scattering parameters, which is required to be transformed it to an admittance form. Since the model is considering the transient response of current transformer and potential transformer from the system primary side to the secondary side, it is essential to model the system as a two port system. In this paper, a pi model has been used .

4.2 Equivalent Circuit

Circuit synthesis is a way to obtain a network impedance elements or an equivalent to the original elements [40]. Therefore, the solution for the equivalent network is not unique, i.e. several networks can give the same frequency response with different circuit elements [33], [41], [42].

The equivalent circuit of a system can be calculated from its frequency response. In our case the frequency response is presented in the state space model of the Y-matrix, which is given by [24], [43]:

$$Y(s) = \sum_{m=1}^{n} \frac{R_m}{s - a_m} + D + sE \tag{4.1}$$

$$Y(s) = C(sI - A)^{-1}B + D + sE \tag{4.2}$$

In circuit representation, terms D and E in 4.1 and 4.2 are shunt conductance and capacitance, respectively. However, circuit models must be developed for the poles and residues which will be discussed next.

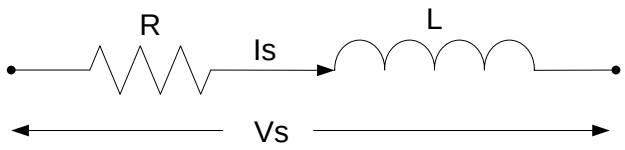

Figure 4.1: RL series circuit [31].

4.3 An Equivalent Circuit for Real Poles and Residues

4.3.1 RL series circuit

Calculating equivalent circuit elements from real poles and residues results in a RL or RC circuit model. The simplification of the circuit by limiting the circuit elements (using R and L, or R and C) it comes with the cost of fitting the frequency response with fewer circuit elements (R and L, or R and C) but more complicated circuit (a circuit with more branches).

Let us consider the RL series circuit represented in Figure 4.1. Calculating the admittance of the circuit, we get

$$Y(s) = \frac{I(s)}{V(s)} \tag{4.3}$$

$$Y(s) = \frac{1}{R + sL} \tag{4.4}$$

$$Y(s) = \frac{\frac{1}{L}}{\frac{R}{L} + s} \tag{4.5}$$

From the fitting algorithm we already have

$$Y(s) = \sum_{m=1}^{n} \frac{R_m}{s - a_m} \tag{4.6}$$

Comparing (4.5) and (4.6) yields

$$a_m = -\frac{R}{L} \quad \text{(poles)} \tag{4.7}$$

$$R_m = \frac{1}{L} \quad \text{(residues)} \tag{4.8}$$

or,

$$L = \frac{1}{R_m} \tag{4.9}$$

$$R = -\frac{a_m}{R_m} \tag{4.10}$$

4.4 An Equivalent Circuit for Complex Pole and Residue Pairs

4.4.1 RLC series circuit model

Let assume a_{m1}, a_{m2}, R_{m1}, and, R_{m2} be the complex and its conjugate poles and residues. Therefore, the admittance transfer function for a pair of poles is

$$Y(s) = \frac{R_{m1}}{s - a_{m1}} + \frac{R_{m2}}{s - a_{m2}} \tag{4.11}$$

$$Y(s) = \frac{R_{m1}(s - a_{m2}) + R_{m2}(s - a_{m1})}{(s - a_{m1})(s - a_{m2})} \tag{4.12}$$

$$Y(s) = \frac{s.(R_{m1} + R_{m2}) - (R_{m1}.a_{m2} + R_{m2}.a_{m1})}{s^2 - s.(a_{m1} + a_{m2}) + (a_{m1}.a_{m2})} \tag{4.13}$$

Assuming

$$a = (R_{m1} + R_{m2}) \tag{4.14}$$

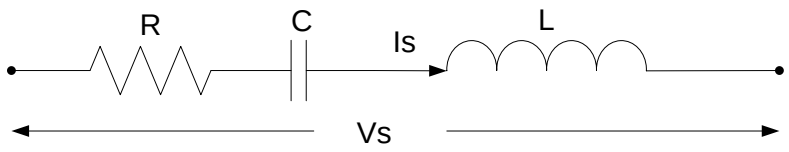

Figure 4.2: RLC series circuit [31].

$$b = -(R_{m1}.a_{m2} + R_{m2}.a_{m1}) \tag{4.15}$$

$$c = -(a_{m1} + a_{m2}) \tag{4.16}$$

$$d = (a_{m1}.a_{m2}) \tag{4.17}$$

We will have

$$Y(s) = \frac{s.a}{s^2 - s.c + d} + \frac{b}{s^2 - s.c + d} \tag{4.18}$$

Now, let's consider the RLC series circuit represented in Figure 4.2. Calculating the admittance of the circuit, we get [31]:

$$Y(s) = \frac{I(s)}{V(s)} \tag{4.19}$$

$$Y(s) = \frac{1}{R + sL + \frac{1}{sC}} \tag{4.20}$$

$$Y(s) = \frac{sC}{s^2LC + sRC + 1} \tag{4.21}$$

$$Y(s) = \frac{\frac{s}{L}}{s^2 + s\frac{R}{L} + \frac{1}{LC}} \tag{4.22}$$

Comparing (4.18) and (4.22), yields

$$a = (R_{m1} + R_{m2}) = \frac{1}{L} \tag{4.23}$$

$$b = -(R_{m1}.a_{m2} + R_{m2}.a_{m1}) = 0 \tag{4.24}$$

$$c = -(a_{m1} + a_{m2}) = \frac{R}{L} \tag{4.25}$$

$$d = (a_{m1}.a_{m2}) = \frac{1}{LC} \tag{4.26}$$

The circuit elements, R, L, and C will be given by

$$L = \frac{1}{(R_{m1} + R_{m2})} \tag{4.27}$$

$$R = -(a_{m1} + a_{m2}).L = \frac{-(a_{m1} + a_{m2})}{(R_{m1} + R_{m2})} \tag{4.28}$$

$$C = \frac{1}{(a_{m1}.a_{m2}).L} = \frac{(R_{m1} + R_{m2})}{(a_{m1}.a_{m2})} \tag{4.29}$$

4.4.2 Series RLC and Parallel Dependent Current Source Circuit Model

The complex conjugate pairs of poles and residues can be alternatively represented by a series RLC circuit in parallel a with dependent current source [31]

Equation 4.18 can be written as

$$Y(s) = \frac{s.a}{s^2 - s.c + d} + \frac{b}{s^2 - s.c + d} = Y_{RLC}(s) + F_{add}(s) \tag{4.30}$$

Let us consider the RLC series circuit represented in Figure 4.3 and let's assume the dependent current source is a function of V_c

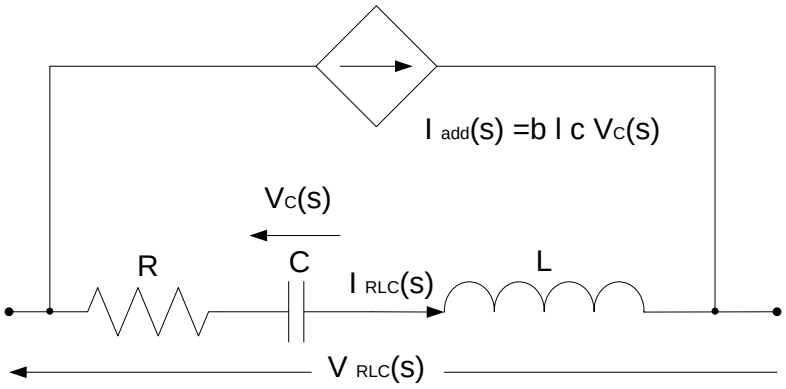

Figure 4.3: RLC series circuit with controlled source [31].

$$V_c(s) = \frac{1}{sC}.I_{RLC} \tag{4.31}$$

$$V_c(s) = \frac{1}{sC}.Y_{RLC}(s).V_{RLC} \tag{4.32}$$

where

$$Y_{RLC}(s) = \left(\frac{\frac{s}{L}}{s^2 + s\frac{R}{L} + \frac{1}{LC}} \right) \tag{4.33}$$

$$V_c(s) = \frac{1}{LC} \left(\frac{1}{s^2 + s\frac{R}{L} + \frac{1}{LC}} \right) V_{RLC} \tag{4.34}$$

$$\left(\frac{1}{s^2 + s\frac{R}{L} + \frac{1}{LC}} \right) = \frac{V_C}{V_{RLC}}\ L\ C \tag{4.35}$$

Since the denominator of Y_{RLC} is equal to the denominator of F_{add}, thus after multiplying (4.35) by b we will get [31]

$$F_{add}(s) = L\ C\ b\ \frac{V_C}{V_{RLC}} \tag{4.36}$$

Since $F_{add}(s)$ is representation of an admittance, we conclude [31]

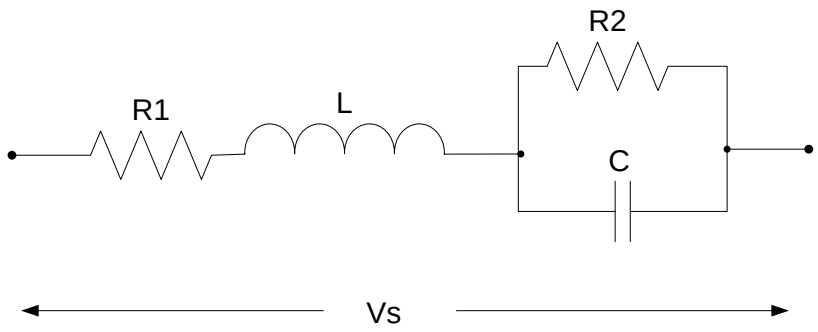

Figure 4.4: R L , R // C equivalent circuit for complex poles and residues pair [31].

$$F_{add}(s) = \frac{I_{add}(s)}{V_{RLC}} \tag{4.37}$$

$$I_{add}(s) = L\ C\ b\ V_C(s) \tag{4.38}$$

Calculating the circuit elements, R, L, and C, we get [31]

$$L = \frac{1}{(R_{m1} + R_{m2})} \tag{4.39}$$

$$R = -\left(a_{m1} + a_{m2}\right).L = \frac{-\left(a_{m1} + a_{m2}\right)}{(R_{m1} + R_{m2})} \tag{4.40}$$

$$C = \frac{1}{(a_{m1}.a_{m2}).L} = \frac{(R_{m1} + R_{m2})}{(a_{m1}.a_{m2})} \tag{4.41}$$

4.4.3 Series RL parallel RC Circuit Model

The complex conjugate pairs of poles and residues can be alternatively represented by a series RL circuit in series with a parallel RC circuit as shown in Figure 4.4 [31].

Let us consider the RLC circuit represented in Figure. 4.4. The admittance of the circuit is given by [31]

$$Y\left(s\right) = \frac{I\left(s\right)}{V\left(s\right)} \tag{4.42}$$

$$Y(s) = \frac{I(s)}{(R_1 + sL)\, I(s) + \left(\frac{R_2 \frac{1}{sC}}{R_2 + \frac{1}{sC}}\right) I(s)}$$

$$Y(s) = \frac{1}{(R_1 + sL) + \left(\frac{R_2 \frac{1}{sC}}{R_2 + \frac{1}{sC}}\right)}$$

$$Y(s) = \frac{1}{(R_1 + sL) + \left(\frac{R_2}{sCR_2 + 1}\right)}$$

$$Y(s) = \frac{sCR_2 + 1}{(R_1 + sL).(sCR_2 + 1) + R_2}$$

$$Y(s) = \frac{sCR_2 + 1}{s^2 LCR_2 + s(L + R_2 R_1 C) + R_1 + R_2}$$

$$Y(s) = \frac{s\frac{1}{L} + \frac{1}{LCR_2}}{s^2 + s\left(\frac{1}{CR_2} + \frac{R_1}{L}\right) + \frac{R_1 + R_2}{LCR_2}} \tag{4.43}$$

Comparing (4.43) with (4.18) yields

$$a = (R_{m1} + R_{m2}) = \frac{1}{L} \tag{4.44}$$

$$b = -(R_{m1}.a_{m2} + R_{m2}.a_{m1}) = \frac{1}{LCR_2} \tag{4.45}$$

$$c = -(a_{m1} + a_{m2}) = \left(\frac{1}{CR_2} + \frac{R_1}{L}\right) \tag{4.46}$$

$$d = (a_{m1}.a_{m2}) = \frac{R_1 + R_2}{LCR_2} = \frac{R_1}{LCR_2} + \frac{1}{LC} \tag{4.47}$$

The circuit elements are calculated as follows [31]

$$L = \frac{1}{(R_{m1} + R_{m2})} \tag{4.48}$$

Calculation of R_1:

$$-(R_{m1}.a_{m2} + R_{m2}.a_{m1})L = \frac{1}{CR_2} \tag{4.49}$$

Thus,

$$\frac{-(R_{m1}.a_{m2} + R_{m2}.a_{m1})}{(R_{m1} + R_{m2})} = \frac{1}{CR_2} \tag{4.50}$$

Using

$$-(a_{m1} + a_{m2}) = \left(\frac{1}{CR_2} + \frac{R_1}{L}\right) \tag{4.51}$$

$$-(a_{m1} + a_{m2}) = \frac{-(R_{m1}.a_{m2} + R_{m2}.a_{m1})}{(R_{m1} + R_{m2})} + \frac{R_1}{L} \tag{4.52}$$

$$-(a_{m1} + a_{m2}) + \frac{(R_{m1}.a_{m2} + R_{m2}.a_{m1})}{(R_{m1} + R_{m2})} = \frac{R_1}{L} \tag{4.53}$$

we get

$$R_1 = \left(-(a_{m1} + a_{m2}) + \frac{(R_{m1} * a_{m2} + R_{m2}.a_{m1})}{(R_{m1} + R_{m2})}\right) \cdot \frac{1}{(R_{m1} + R_{m2})} \tag{4.54}$$

Calculation of C

$$(a_{m1}.a_{m2}) = \frac{R_1}{LCR_2} + \frac{1}{LC} \tag{4.55}$$

$$(a_{m1}.a_{m2})L = \frac{R_1}{CR_2} + \frac{1}{C} \tag{4.56}$$

Since,

$$L = \frac{1}{(R_{m1} + R_{m2})} \tag{4.57}$$

Thus,

$$(a_{m1}.a_{m2})\frac{1}{(R_{m1} + R_{m2})} = \frac{R_1}{CR_2} + \frac{1}{C} \tag{4.58}$$

$$(a_{m1}.a_{m2})\frac{C}{(R_{m1} + R_{m2})} = \frac{R_1}{R_2} + 1 \tag{4.59}$$

$$\frac{R_1}{R_2} = \frac{(a_{m1}.a_{m2}).C}{(R_{m1} + R_{m2})} - 1 \tag{4.60}$$

using

$$LCR_2 = \frac{1}{-(R_{m1}.a_{m2} + R_{m2}.a_{m1})} \tag{4.61}$$

we get

$$R_2 = \frac{1}{LC(-(R_{m1}.a_{m2} + R_{m2}.a_{m1}))} \tag{4.62}$$

Therefore,

$$(L.C.(-(R_{m1}.a_{m2} + R_{m2}.a_{m1})))R_1 = \frac{(a_{m1}.a_{m2}).C}{(R_{m1} + R_{m2})} - 1 \tag{4.63}$$

$$\frac{-(R_{m1}.a_{m2} + R_{m2}.a_{m1})CR_1}{(R_{m1} + R_{m2})} = \frac{(a_{m1}.a_{m2}).C}{(R_{m1} + R_{m2})} - 1 \tag{4.64}$$

Dividing by C yields:

$$\frac{-(R_{m1}.a_{m2} + R_{m2}.a_{m1})R_1}{(R_{m1} + R_{m2})} = \frac{(a_{m1}.a_{m2})}{(R_{m1} + R_{m2})} - \frac{1}{C} \tag{4.65}$$

$$\frac{1}{C} = \frac{(R_{m1}.a_{m2} + R_{m2}.a_{m1})R_1}{(R_{m1} + R_{m2})} + \frac{(a_{m1}.a_{m2})}{(R_{m1} + R_{m2})} \tag{4.66}$$

$$\frac{1}{C} = \frac{(R_{m1}.a_{m2} + R_{m2}.a_{m1})R_1 + (a_{m1}.a_{m2})}{(R_{m1} + R_{m2})} \tag{4.67}$$

$$C = \frac{(R_{m1} + R_{m2})}{(a_{m1}.a_{m2}) + (R_{m1}.a_{m2} + R_{m2}.a_{m1}).R_1} \tag{4.68}$$

by substituting R_1 from (4.54) into (4.68) we get

$$C = \frac{(R_{m1} + R_{m2})}{(a_{m1}.a_{m2}) + \left(-(a_{m1} + a_{m2}) + \frac{(R_{m1}.a_{m2}+R_{m2}.a_{m1})}{(R_{m1}+R_{m2})}\right)\frac{(R_{m1}.a_{m2}+R_{m2}.a_{m1})}{(R_{m1}+R_{m2})}} \tag{4.69}$$

Calculation of R_2 :

Since

$$-(R_{m1}.a_{m2} + R_{m2}.a_{m1}) = \frac{1}{LCR_2} \tag{4.70}$$

and

$$L = \frac{1}{(R_{m1} + R_{m2})} \tag{4.71}$$

thus,

$$\frac{-(R_{m1}.a_{m2} + R_{m2}.a_{m1})}{(R_{m1} + R_{m2})} = \frac{1}{CR_2} \tag{4.72}$$

$$R_2 = \frac{-(R_{m1}.a_{m2} + R_{m2}.a_{m1})}{(R_{m1} + R_{m2})}.\frac{1}{C} \tag{4.73}$$

In dealing with complex circuit models (where we have the real and complex pole and

residue pairs in the same model), many of the circuit models which have been discussed will be used.

Chapter 5

Results

A 13.8 kV / 136.8 kV, 50-MVA single phase distribution transformer will be modeled and tested in this chapter. The obtained frequency responses of the primary and secondary windings were the end-to-end voltage ratio, and transfer voltage ratio in the frequency range of up to 2 MHz (see Figure 5.1 and 5.2)[1]. See Appendix A.1 for the FRA measurements. The provided frequency response analysis data are not in an admittance or impedance form. Thus, to model the transformer as a two port system, it is essential to obtain the admittance response of the distribution transformer. An approximation has to be made (by assuming there are not any leakage current) from the measured data (FRA) to obtain the admittance as discussed in Chapter 2.

The approximation of the measured data is suitable at low frequencies since the stray capacitances have no effects on the frequency response (see Figure 5.3), but even at higher frequencies (up to 2 MHz) the effects of stray capacitances do not have very significant effects on the frequency response. Thus, the calculated admittance from the measured data is an approximation. Using Vector Fitting (VF) method to fit the obtained admittance frequency response (see Figures 5.4 and 5.5) and obtaining the state-space model, we have

$$Y(s) = \sum_{m=1}^{n} \frac{R_m}{s - a_m} + D + s.E \tag{5.1}$$

[1]The measured data has been provided by Manitoba Hydro.

where

R_m are the residues,

a_m are the poles,

D, and E are constants.

where the state-space model is

$$Y(s) = C(sI - A)^{-1}B + D + sE \tag{5.2}$$

where C is a 2x40 residues matrix, (C matrix could be real or complex number) see Appendix A.2.1, A is a 40x40 poles matrix (could be real or complex number), D and E are 2x2 real matrices, I matrix is the identity matrix, B is a matrix of ones.

The order of approximation, N, used in this thesis to fit the calculated admittance from the measured data is 20. This number has been chosen so that the obtained data and the calculated one are approximated with the minimum reasonable number of poles and residues, while keeping the circuit model simple. Notice that in Figure 5.4, at higher frequency, the fitted curves do not match perfectly with the measured one. This will be discussed later in this chapter.

5.1 Passivity Assessment

Since the obtained admittance matrix and the state-space model are based on approximation (i.e. ignoring the stray capacitance), thus the obtained admittance matrices are not an exact match for the actual admittance matrices. To ensure that the obtained model for transient analysis from the admittance matrix is stable in the time domain, a passivity assessment must be carried out. In the case we obtained the actual admittance matrices directly, still the admittance matrices should be tested to ensure an accurate measuring of transformer admittance matrices and detecting if there were any problems in the measured data.

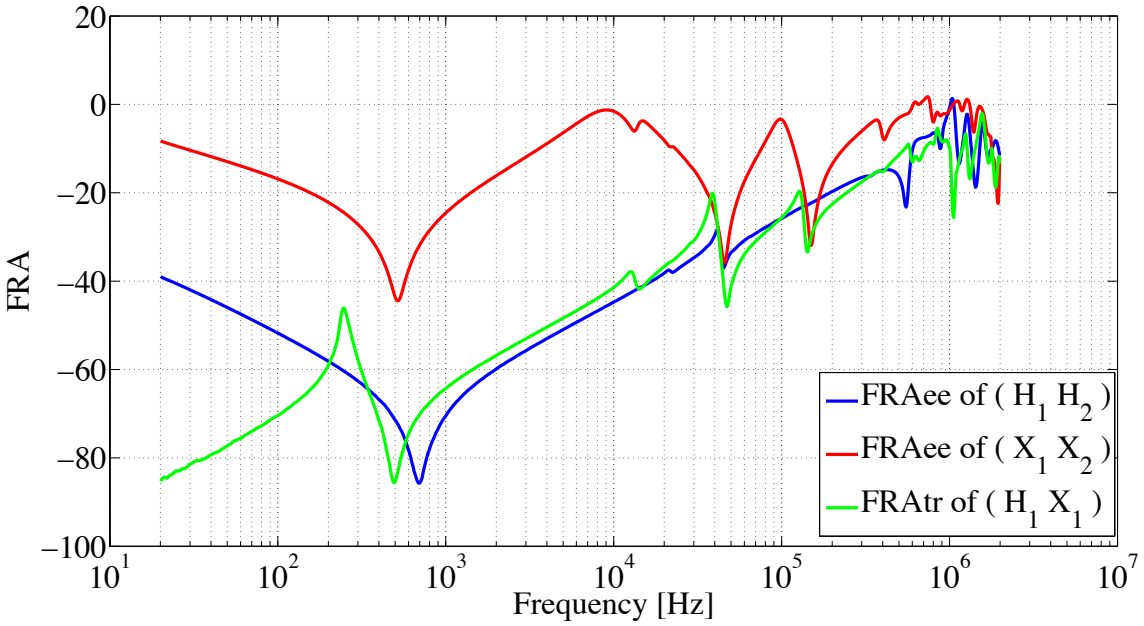

Figure 5.1: The magnitude values of the frequency response measurement (FRA_{ee} and FRA_{tr}).

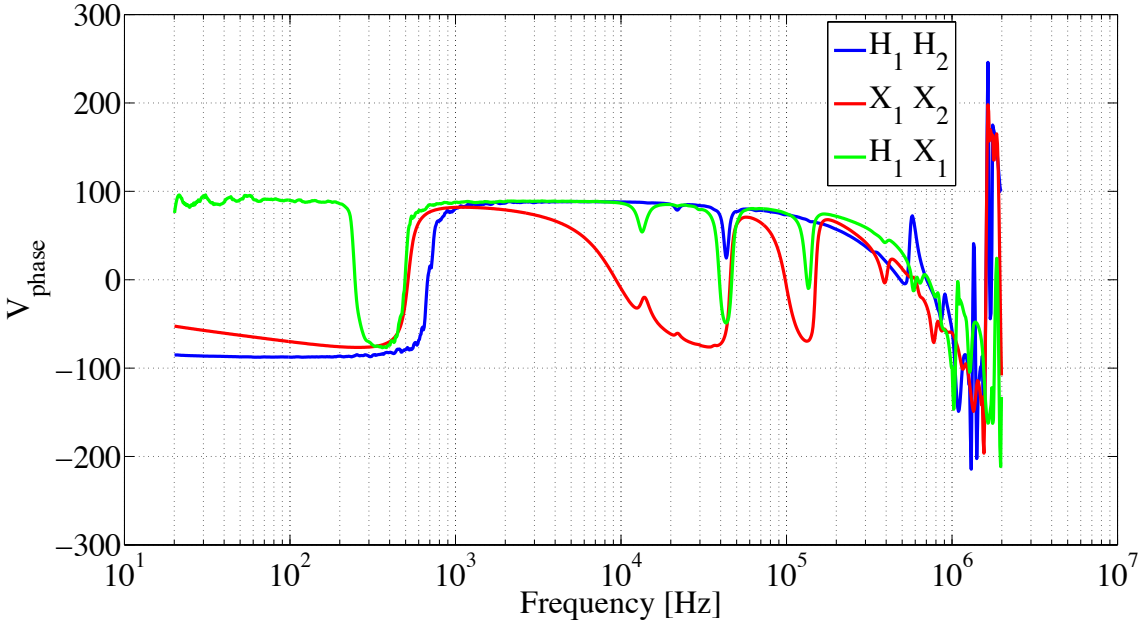

Figure 5.2: The angle values of the frequency response measurement (FRA_{ee} and FRA_{tr}) .

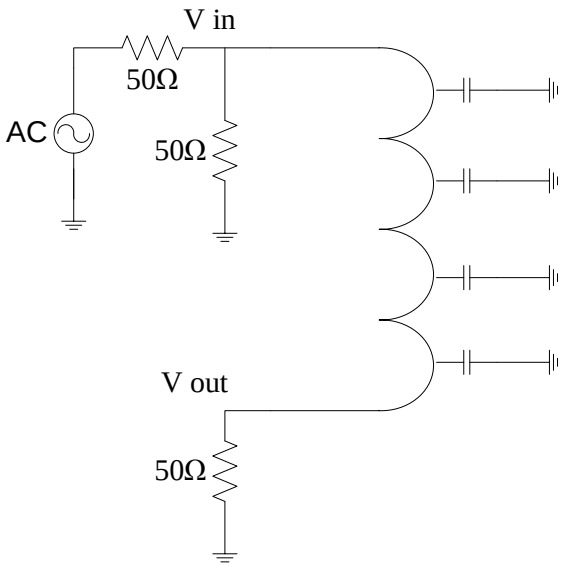

Figure 5.3: Winding stray capacitance.

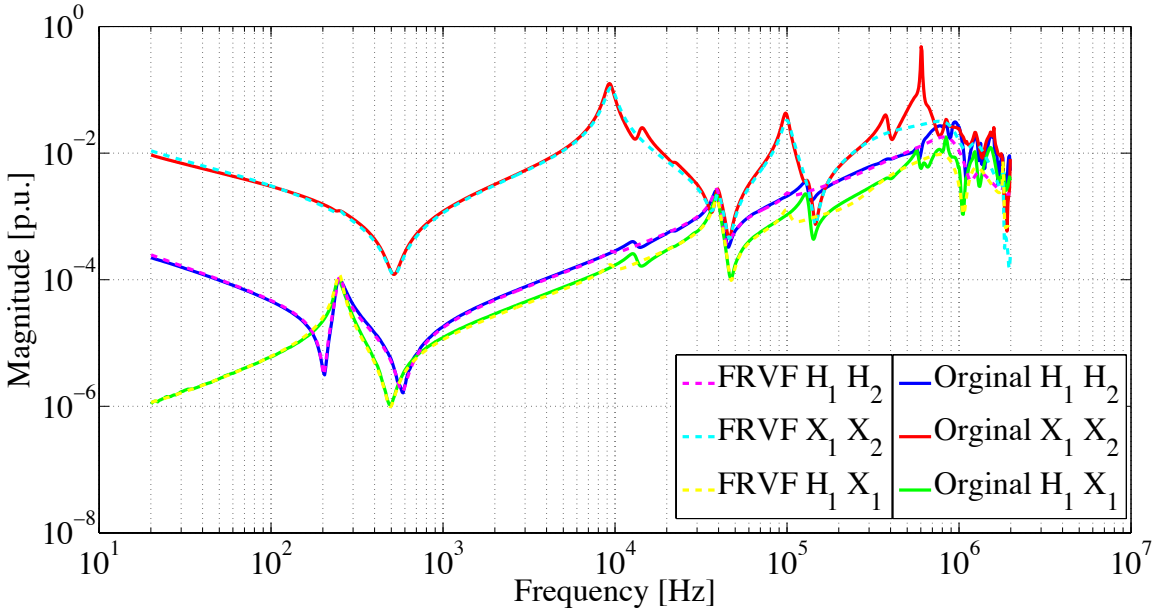

Figure 5.4: The absolute value of calculated admittance and the absolute value of fitted admittance.

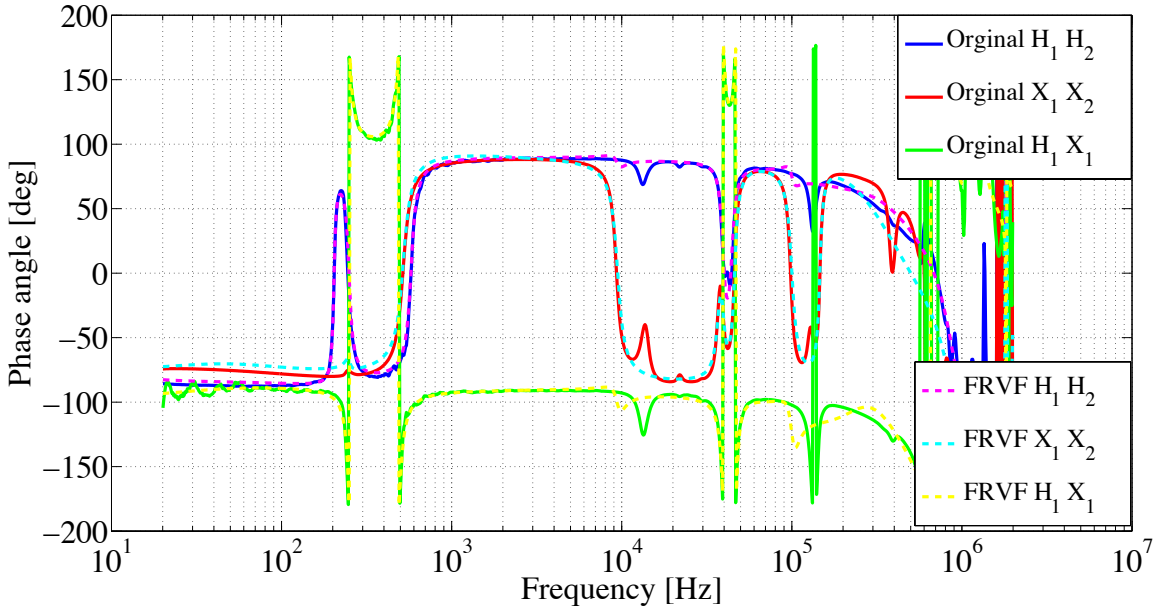

Figure 5.5: Calculated admittance angle and the fitted admittance angle .

5.1.1 Y-matrix test

After calculating the admittance matrix from measured data and before fitting the admittance curve and deriving any equivalent circuit from the data, the admittance matrix should be tested if it is passive or not, because deriving any equivalent circuit from not passive admittance matrix will lead to unstable circuit in the time domain.

As discussed in Chapter 3, the system admittance matrix of a reciprocal network is said to be passive if:

1. Real (Y_{11}) and Real $(Y_{22}) \geq 0$
2. The detriment of $(Y_h) \geq 0$

Y_h is the Hermitian matrix of Y-matrix admittance, which is given by

$$Y_h = \begin{bmatrix} g_{11} & \frac{Y_{12}+\overline{Y_{21}}}{2} \\ \frac{Y_{21}+\overline{Y_{12}}}{2} & g_{22} \end{bmatrix} = \begin{bmatrix} g_{11} & \frac{1}{2}(g_{12}+g_{21}+jb_{12}-jb_{21}) \\ \frac{1}{2}(g_{21}+g_{12}+jb_{21}-jb_{12}) & g_{22} \end{bmatrix} \tag{5.3}$$

For reciprocal network ($Y_{12} = Y_{21}$), the following variable is defined

$$U = \frac{g_{21}\, g_{12}}{g_{11}\, g_{22}} \tag{5.4}$$

To satisfy the passivity condition, the value of U should be

$$0 \leq U \leq 1 \tag{5.5}$$

Thus, the two conditions for a reciprocal network ($Y_{12} = Y_{21}$) can be rewritten as (For more details see chapter 3.)

1. Real (Y_{11}) and Real (Y_{22}) ≥ 0
2. $0 \leq U \leq 1$

By checking the first condition in Figure 5.6, it clearly shows that the admittance matrix is not passive since (Y_{11}) (red curve), and (Y_{22}) (blue curve) are crossing over to the negative values.

By taking a look at the second condition shown in Figure 5.7, it is observed that U values are not between one and zero, thus the second condition is also violated (the blue crosses determine the violation regions (crossover frequencies) and at what frequencies the model is stable or not).

After enforcing the passivity on the admittance matrix, Figure 5.8 it clearly shows that the admittance matrix is passive since (Y_{11}) (red curve), and (Y_{22}) (blue curve) are not crossing-over to the negative values and satisfy the first condition of passivity. Figure 5.9 also shows that U values are between one and zero after enforcing the passivity, thus the second condition is also satisfied. Since both conditions are satisfied, thus admittance matrices are now passive.

5.1.2 Hamiltonian Passivity Test

After fitting the calculated admittance values, and before modeling the equivalent circuit using poles and residues from the obtained state-space model, the constants of the state-

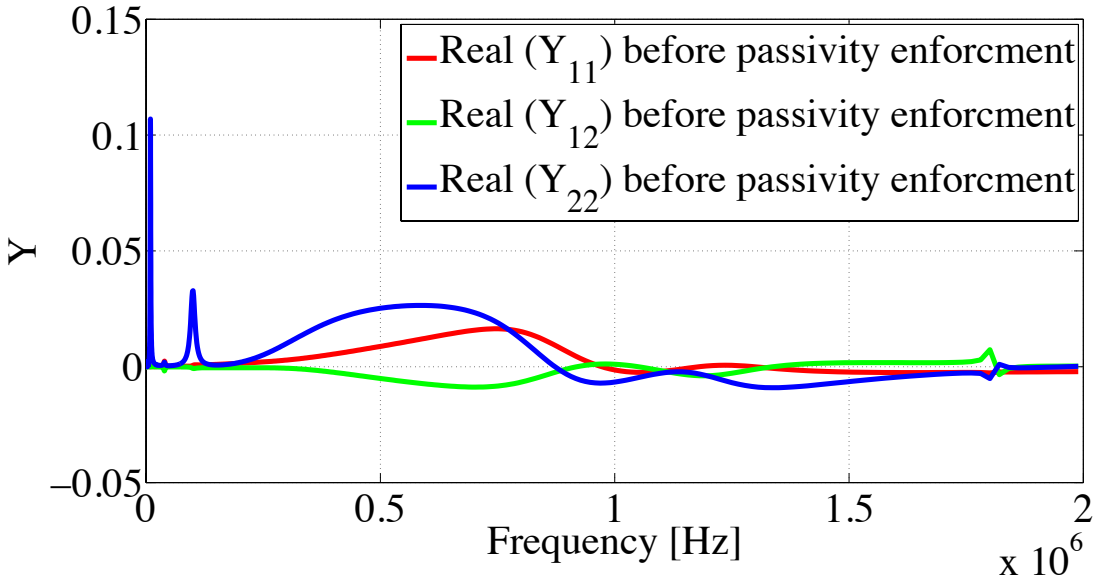

Figure 5.6: Real values of the admittance matrix before passivity enforcement.

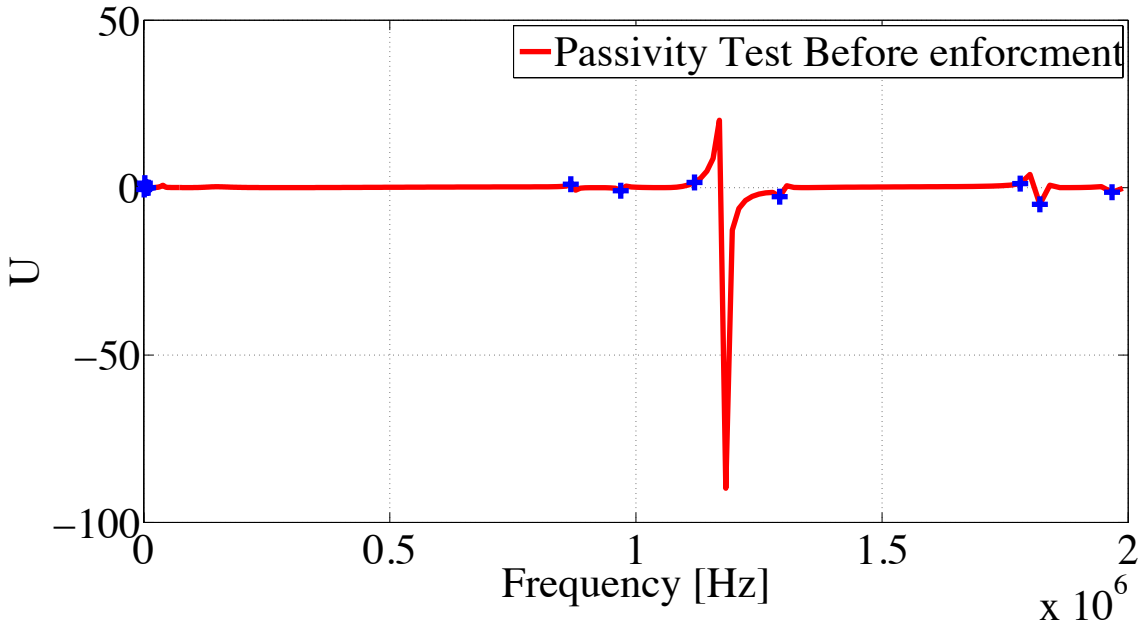

Figure 5.7: Passivity test of Y-matrix before passivity enforcement.

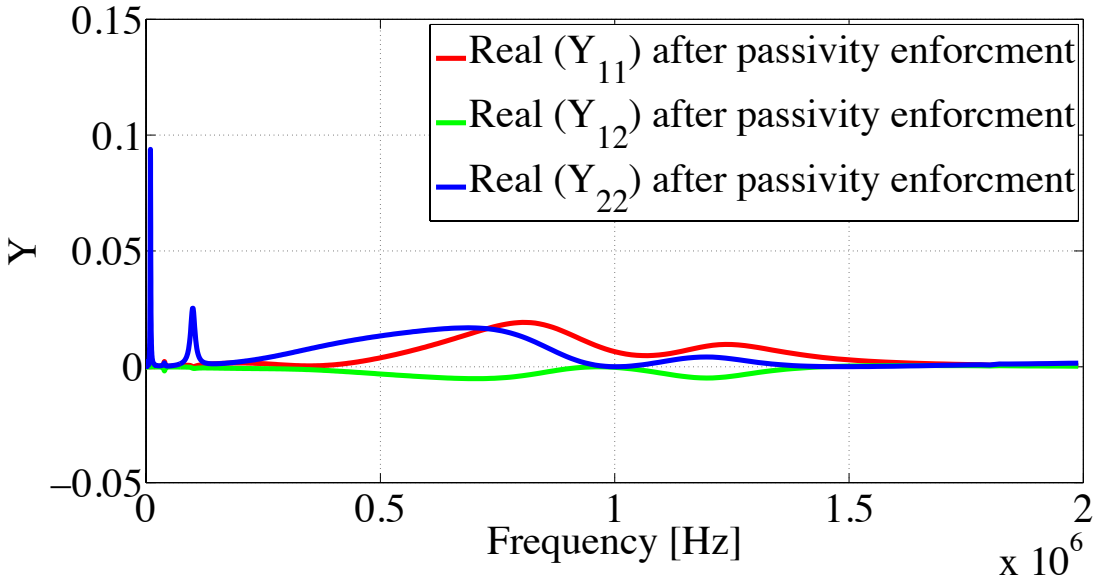

Figure 5.8: Real values of the admittance matrix after passivity enforcement.

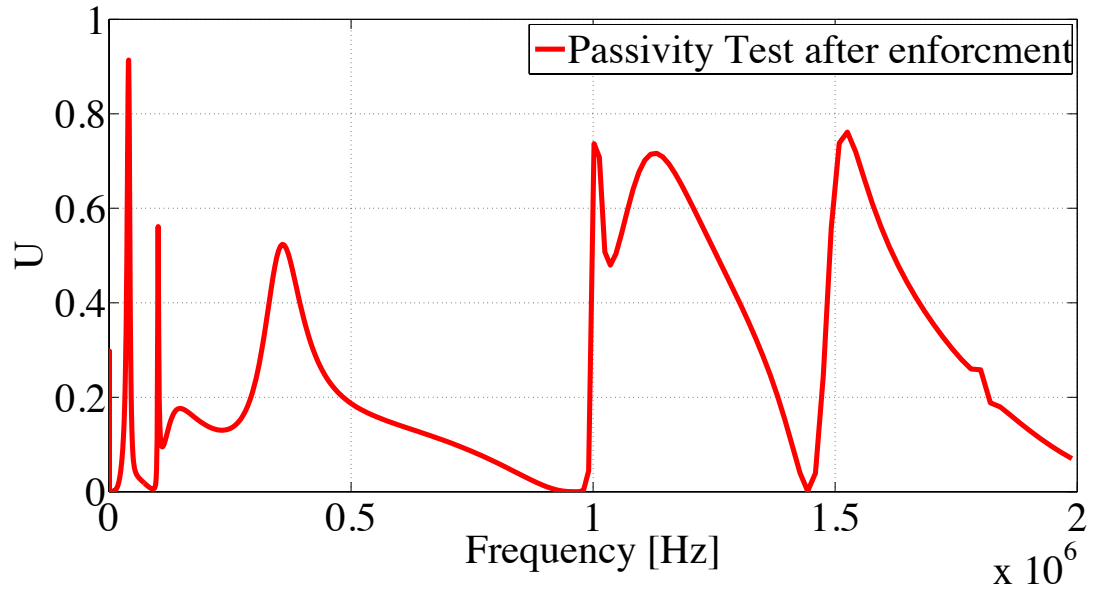

Figure 5.9: Passivity test of Y-matrix after passivity enforcement.

space model have to be tested as well to ensure the obtained equivalent circuit from the state-space model is passive. Also, we might want to ensure that the passive regions for the state-space model are the same passive regions from the first passivity test (Y-matrix test).

As shown earlier, the state-space model matrix is defined as

$$M = \begin{bmatrix} A \ - \ B \ (\ D \ + \ D^T)^{-1} \ C & B \ (\ D \ + \ D^T)^{-1} \ B^T \\ -C^T \ (\ D \ + \ D^T)^{-1} \ C & -A \ + \ C^T \ (\ D \ + \ D^T)^{-1} \ B^T \end{bmatrix} \tag{5.6}$$

where

C contains the residue matrix, see Appendix A.2.2

A contains the pole matrix, see Appendix A.2.1

D, and E are constants, see Appendix A.2.3

I is the unity matrix

For B matrix, see Appendix A.2.3. For testing the passivity of the state space model using Hamiltonian matrix, we calculate

$$CF = eig(M) \tag{5.7}$$

where CF contains the crossover frequencies. After calculating the crossover frequencies of the Hamiltonian matrix, see Appendix A.3 , we obtain a list of complex numbers. To identify if there are any crossover frequencies from this list of complex numbers, the absolute value of the real part should be checked. If the absolute value of the real part is zero or almost zero (≈ 0), then the absolute value of the imaginary part of that complex number divided by 2π gives us the exact crossover frequency. Note that (≈ 0) for determining the absolute value of the real part is due to numerical error associated with this test method, as discussed in the passivity assessment in (Chapter 3).

As shown in Figure 5.10, the calculated crossover frequencies (blue crosses) from Hamiltonian passivity test are plotted over U (red line) which is obtained from the first passivity test (Y - matrix test). By comparing both tests, it is clearly shown that both of the tests identify the same passive regions and a close approximation of the crossover frequencies.

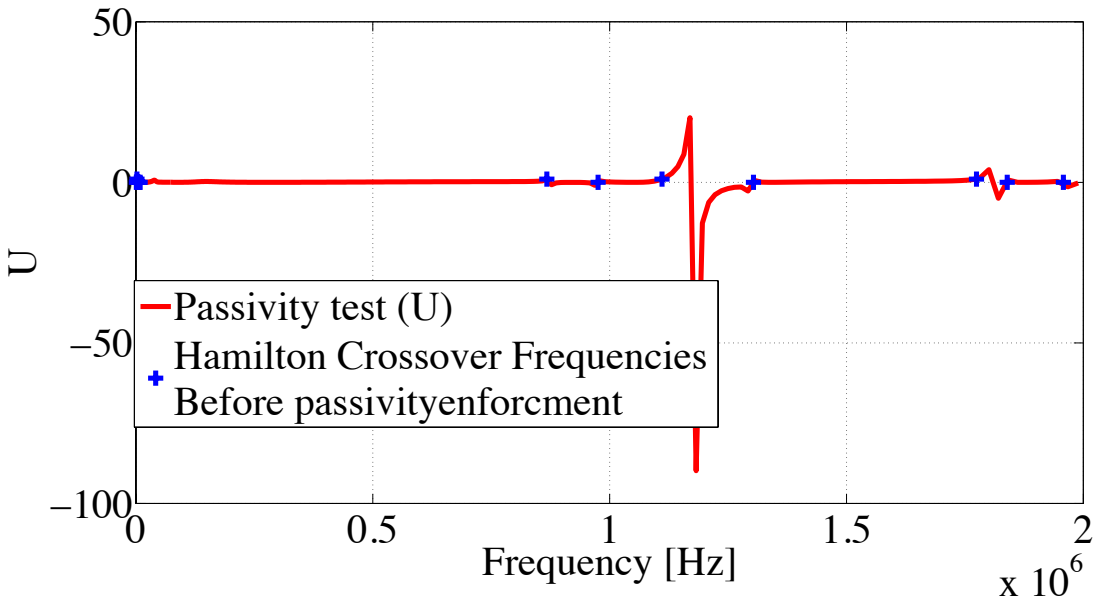

Figure 5.10: Passivity test of Y-matrix and Hamilton matrix before passivity enforcement.

The reason for this will be discussed later in this chapter.

After enforcing the passivity on the state-space model and testing the passivity by Hamiltonian matrix, it is shown in Figure 5.11 that there are no crossover frequencies and thus the state-space model is passive.

5.1.3 Singularity test matrix (S- matrix)

The singularity test matrix (S-matrix) is known as the half-Hamiltonian matrix test, since it has been driven from Hamiltonian matrix. The calculated crossover frequencies from S-matrix should have the same crossover frequencies from Hamiltonian matrix, see Appendix A.4. As discussed earlier, the eigenvalues of the following matrix include the crossover frequencies.

$$S = A\,(\,B\,D^{-1}\,C - A) \tag{5.8}$$

and,

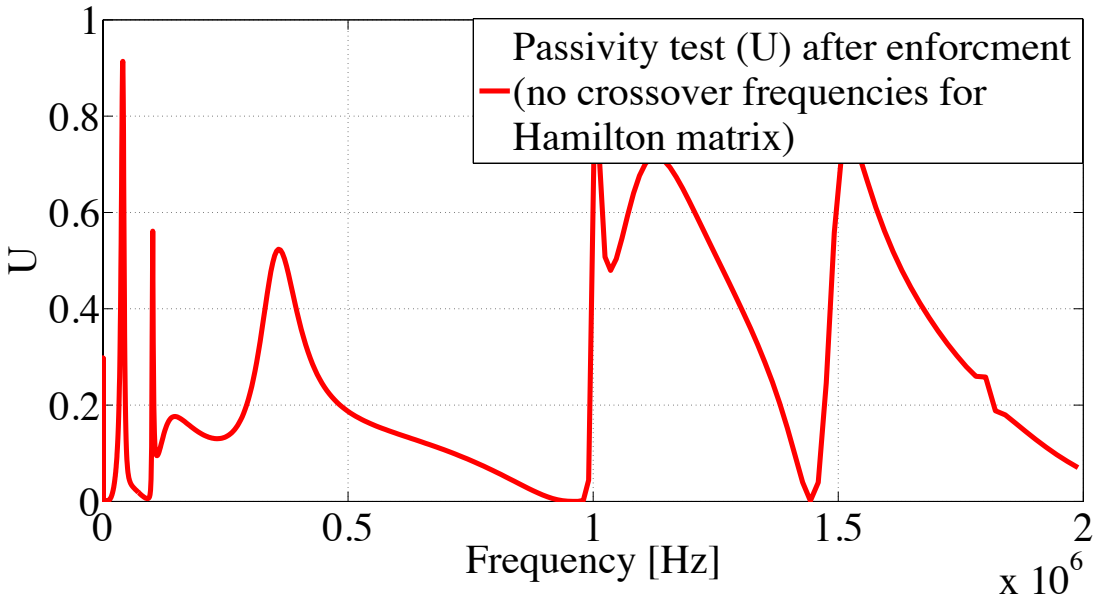

Figure 5.11: Passivity test of Y-matrix and Hamilton matrix after passivity enforcement.

$$CF = eig(M) = \pm\sqrt{eig(S)} \tag{5.9}$$

After calculating the crossover frequencies using (5.8), and (5.9), a list of complex numbers will be obtained. To identify if there are any crossover frequencies from this list of complex numbers, the value of the imaginary part should be checked. If the value of the imaginary part ≈ 0, then the absolute value of the real part of that complex number divided by 2π will provide the crossover frequency.

As show in Figure 5.12, the calculated crossover frequencies (blue crosses) from S-matrix passivity test are plotted over U (red line) which is obtained from the first passivity test (Y-matrix test). By comparing both tests (see Figures 5.12 and 5.7), it is clearly observed that both of the tests identify the same passive regions and a close approximation of the crossover frequencies.

After enforcing the passivity on the state-space model and testing the passivity using S-matrix, we can see from Figure 5.13 that there are no crossover frequencies and thus the state-space model is passive.

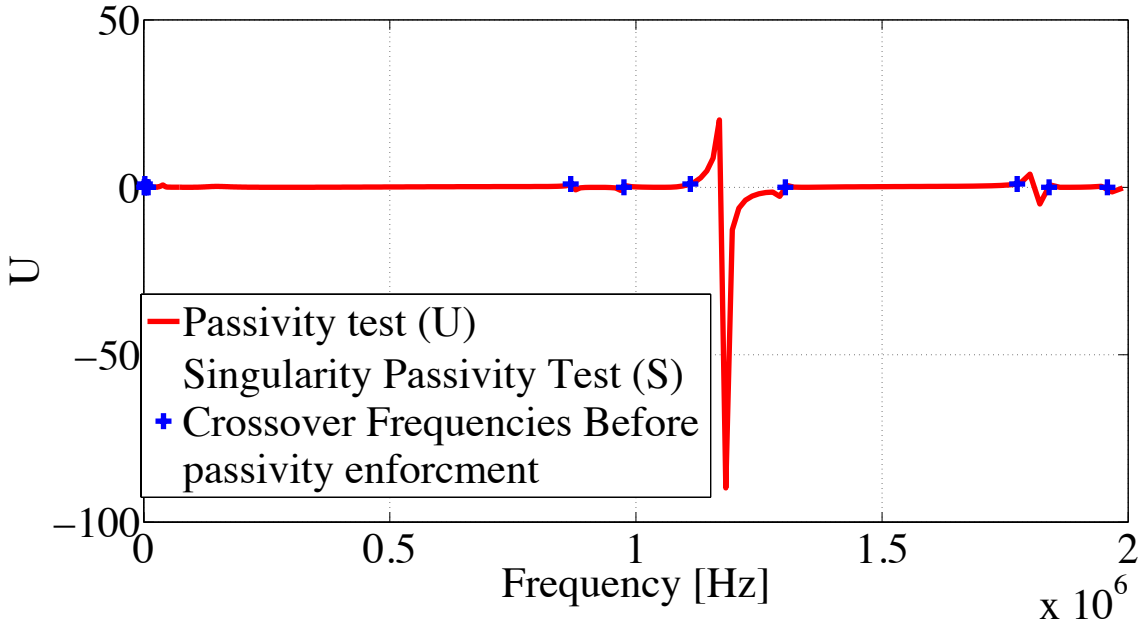

Figure 5.12: Passivity test of Y-matrix and S-matrix before passivity enforcement.

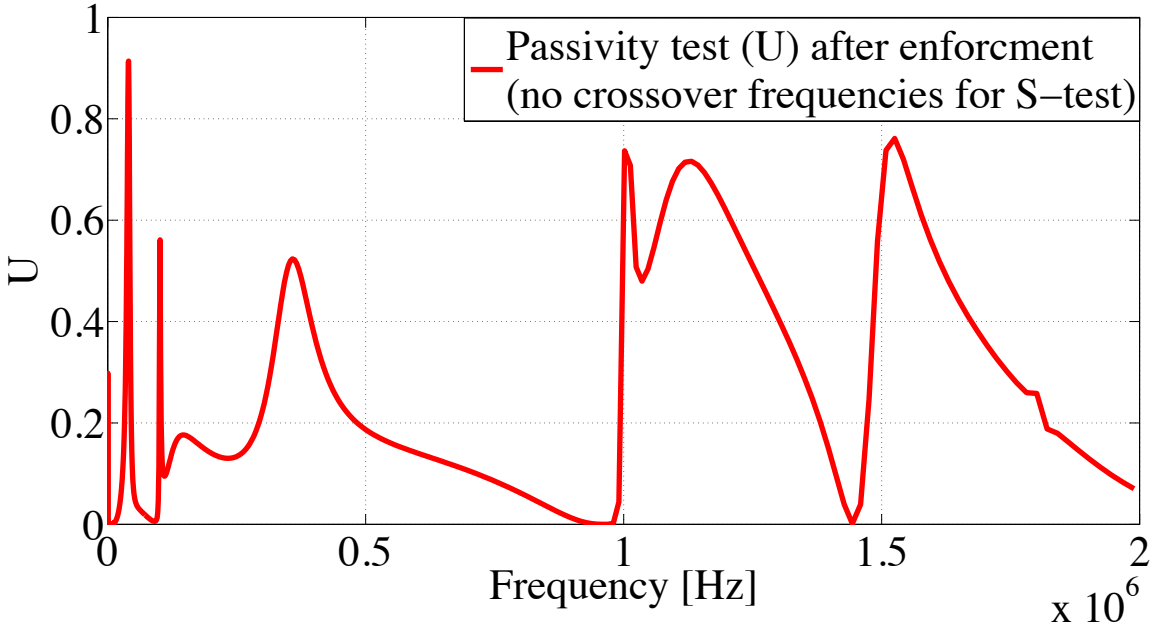

Figure 5.13: Passivity test of Y-matrix and S-matrix after passivity enforcement.

5.1.4 Singularity test matrix (T-matrix)

The singularity test matrix (T-matrix) is also known as the half-Hamiltonian matrix test, since it has been driven from Hamiltonian matrix. The calculated crossover frequencies from T-matrix should have the same crossover frequencies from Hamiltonian matrix, see Appendix A.4. Similar to previous test, the the crossover frequencies are included in the eigenvalues of the following matrix.

$$T \;=\; A\,(\,B\,D^{-1}\,C \;-\; A) \tag{5.10}$$

$$CF = eig(M) = \pm\sqrt{eig(T)} \tag{5.11}$$

Once the eigenvalues are determined, to identify if there are any crossover frequencies, the value of the imaginary part should be checked. If the value of the imaginary part is close to zero, then the absolute value of the real part of that complex number divided by 2π is the exact crossover frequency.

In Figure 5.14, we can see the calculated crossover frequencies (blue crosses) from T-matrix passivity test plotted over U (red line) which is obtained from the first passivity test (Y-matrix test). By comparing both the tests (see Figures 5.14 and 5.7), we can see that both of the tests identify the same passive regions and a close approximation of the crossover frequencies, the reason for the close approximation between the crossover frequencies will be discussed in the next section of this chapter.

After enforcing the passivity on the state-space model and testing the passivity using T-matrix, it shows that from Figure 5.15 there are not any crossover frequencies and thus the state-space model is passive.

5.2 Comparisons of All Passivity Tests

Figure 5.16 shows that Hamiltonian passivity test, and Singularity test matrix (S-matrix, and T-matrix) provided more accurate result than the Y-matrix test. As it has been

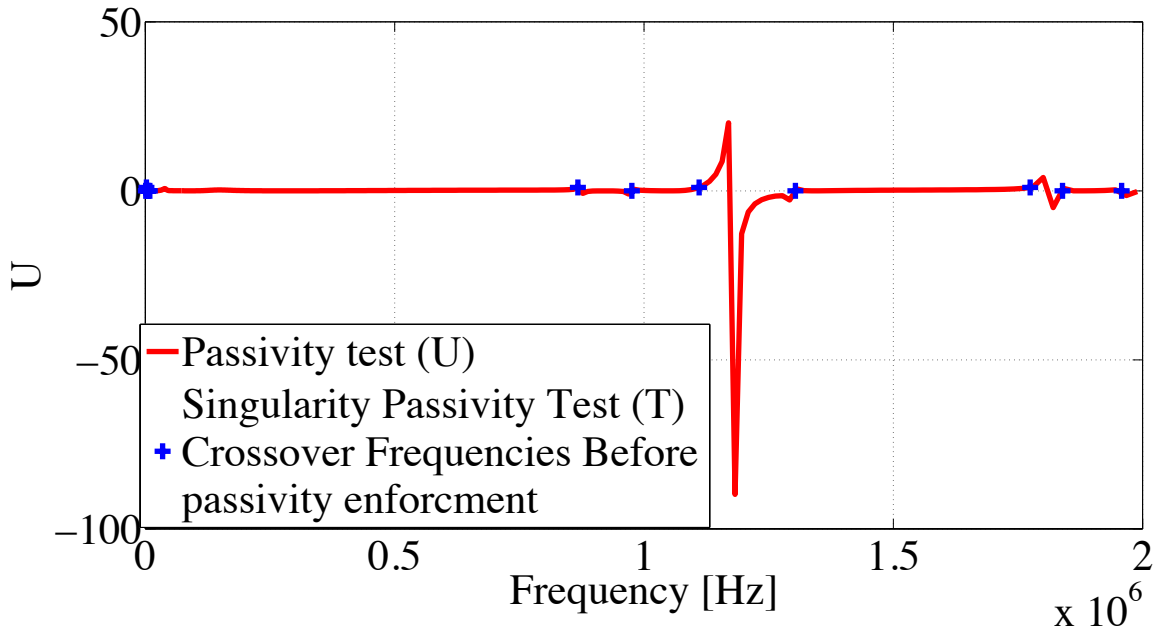

Figure 5.14: Passivity test of Y-matrix and T-matrix before passivity enforcement.

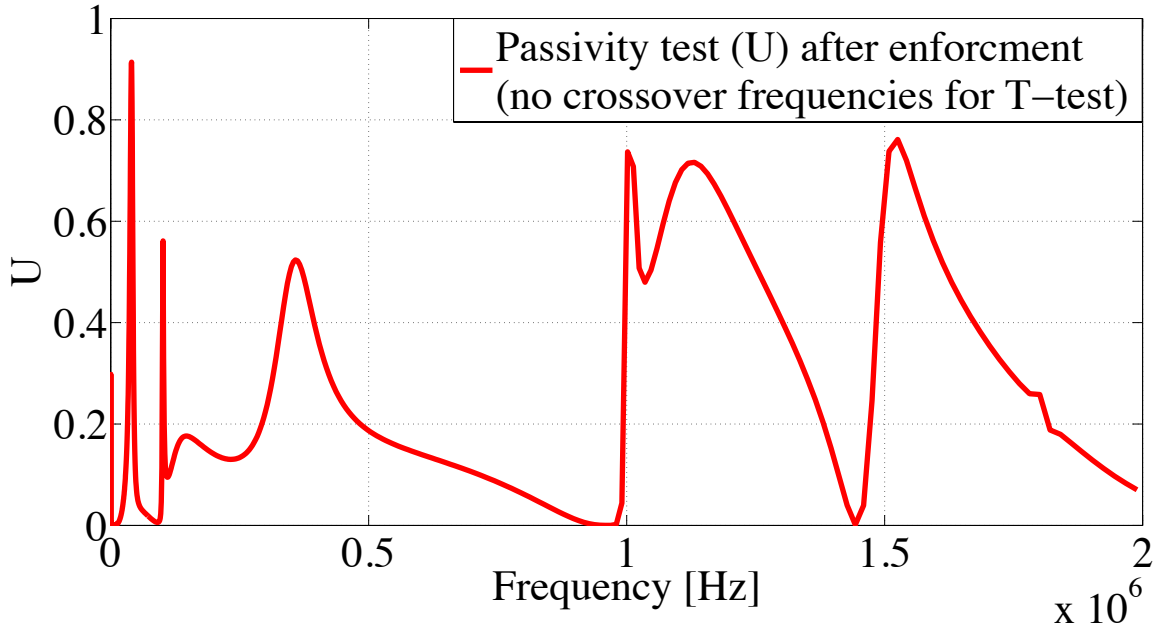

Figure 5.15: Passivity test of Y-matrix and T-matrix after passivity enforcement.

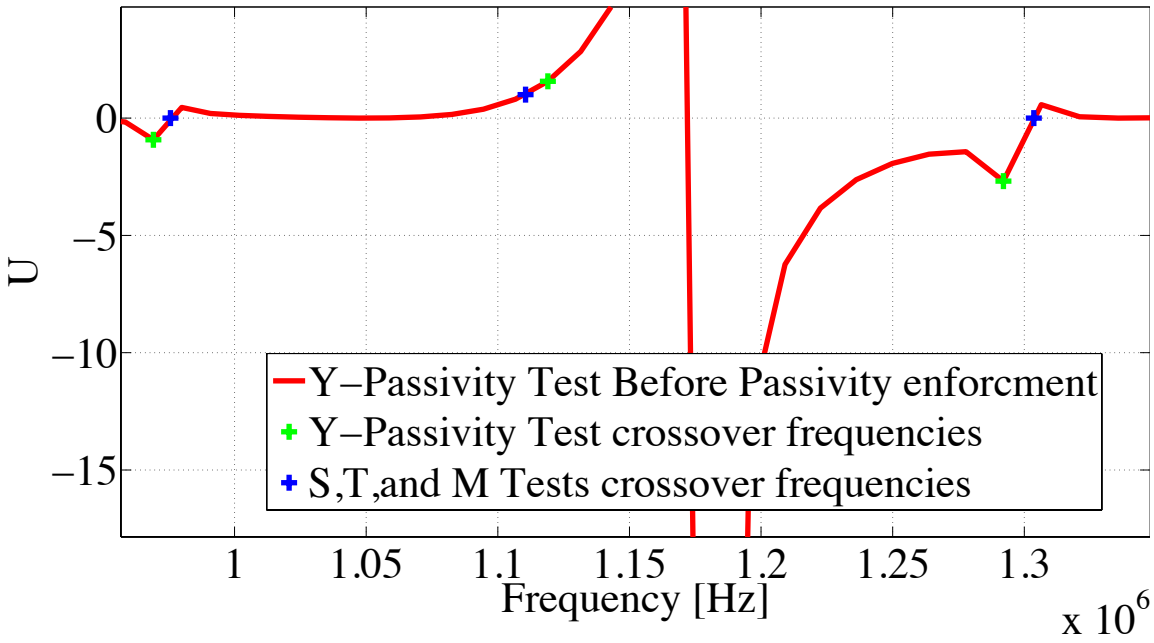

Figure 5.16: Comparisons between all passivity tests.

discussed before in the passivity chapter, to obtain accurate results for the crossover frequencies using Y-matrix test, the sampling of the admittance matrix through the frequency range should be very fine. Thus, the longest computational time of all the test methods belongs to the Y-matrix test.

Although the singularity test matrix (S-matrix, and T-matrix) are derived from the Hamiltonian passivity test and have the same results, the Singularity test matrix requires less computational time since it has only half the crossover frequencies compared to the Hamiltonian matrix. Table 5.1 provides the crossover frequencies for all the passivity test methods which have been carried out in this thesis. Also, the Singularity test matrix has less numerical error in determining the crossover frequencies.

5.3 Admittance Calculations

After testing the system passivity and ensuring that the system is passive, we model the system as a two port network. To obtain a model which has the same frequency response as the transformer admittance, each of the transformers winding has to be modeled based

Table 5.1: The values of S- matrix, T- matrix, Y- matrix, and Hamilton matrix after admittance fitting.

$eig(M)$ Absolute value of the real value ≈ 0	$\sqrt{eig(S)} = \sqrt{eig(T)}$ Absolute value of the Imaginary value ≈ 0	$f = \frac{\omega}{2 * \pi}$	U
9.53e-09 + 1.23e+07i	1.23e+07 + 6.76e-10i	1.957 MHz	1.967 MHz
1.52e-08 - 1.23e+07i			
-1.48e-08 + 1.15e+07i	1.15e+07 - 1.56e-09i	1.839 MHz	1.820 MHz
-1.74e-09 - 1.15e+07i			
6.30e-09 + 1.11e+07i	1.11e+07 + 1.02e-09i	1.774 MHz	1.780 MHz
8.82e-09 - 1.11e+07i			
-4.65e-09 + 8.19e+06i	8.19e+06 + 1.33e-09i	1.303 MHz	1.292 MHz
8.58e-09 - 8.19e+06i			
-9.20e-10 + 6.97e+06i	6.97e+06 + 2.84e-10i	1.110 MHz	1.119 MHz
-1.15e-09 - 6.97e+06i			
-2.01e-09 + 6.13e+06i	6.13e+06 + 1.31e-09i	0.975MHz	0.969 MHz
-1.18e-09 - 6.13e+06i			
8.26e-10 - 5.45e+06i	5.45e+06 - 6.35e-10i	0.867MHz	0.867 MHz
1.75e-09 + 5.45e+06i			
1.52e-10 + 5.61e+04i	5.61e+04 - 2.19e-08i	0.893 MHz	0.890 MHz
2.68e-11 - 5.61e+04i			
-2.72e-09 + 3.55e+04i	3.55e+04 - 5.01e-07i	5.652 kHz	5.657 kHz
-1.04e-09 - 3.55e+04i			
-3.70e-09 + 1.40e+04i	1.40e+04 + 9.36e-10i	2.235 kHz	2.233 kHz
2.55e-09 - 1.40e+04i			
1.44e-09 + 6.21e+03i	6.21e+03 - 1.07e-11i	988.74 Hz	996.3 Hz
-2.37e-10 - 6.21e+03i			

on the fitted data poles and residues.

Each of the transformer windings and the coupling between windings will be modeled, as shown in Figure 5.17, see Appendix A.5 for the circuit elements, using the circuit synthesis methods described in Section 4.3, 4.4.1, and 4.5.3. For the sake of convenience and self containing of this chapter the final formulas are repeated here

Consider the state space model (admittance), that has been derived from the measured data.

$$Y(s) = \sum_{m=1}^{n} \frac{R_m}{s - a_m} + D + sE \tag{5.12}$$

D and E are represented as shunt conductance and capacitance. R and C branches are calculated as follows

$$R = \frac{1}{D} \tag{5.13}$$

$$C = E \tag{5.14}$$

For the real poles and residues we have RL branches:

$$L = \frac{1}{R_m} \tag{5.15}$$

$$R = -\frac{a_m}{R_m} \tag{5.16}$$

Complex conjugates poles we have RLRC branches.

$$L = \frac{1}{(R_{m1} + R_{m2})} \tag{5.17}$$

$$R_1 = \left(-(a_{m1} + a_{m2}) + \frac{(R_{m1}.a_{m2} + R_{m2}.a_{m1})}{(R_{m1} + R_{m2})} \right) . \frac{1}{(R_{m1} + R_{m2})} \tag{5.18}$$

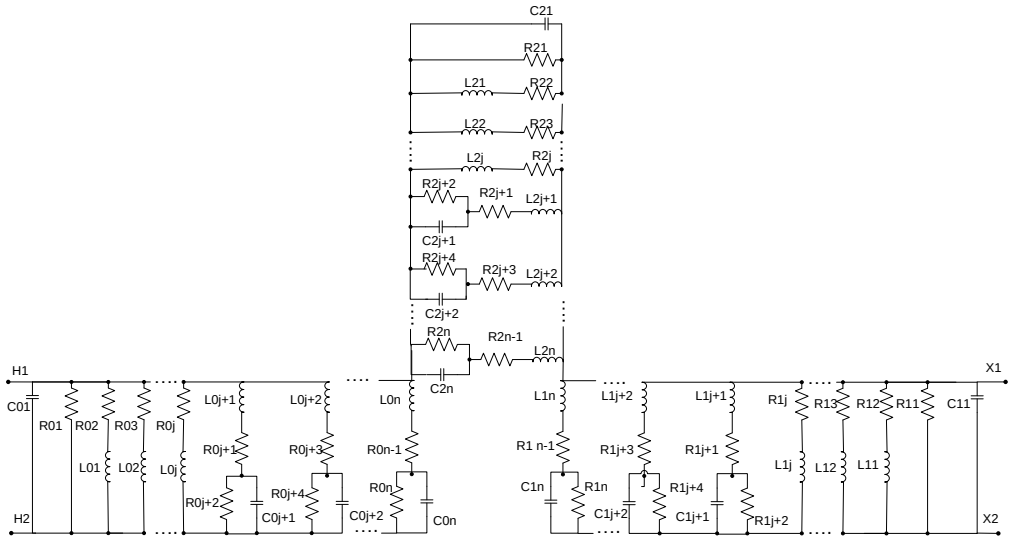

Figure 5.17: Detailed circuit elements for the proposed model. The values of circuit elements are provided in Appendix A.5

$$C = \frac{(R_{m1} + R_{m2})}{(a_{m1}.a_{m2}) + \left(-(a_{m1} + a_{m2}) + \frac{(R_{m1}.a_{m2}+R_{m2}.a_{m1})}{(R_{m1}+R_{m2})}\right)\frac{(R_{m1}.a_{m2}+R_{m2}.a_{m1})}{(R_{m1}+R_{m2})}} \tag{5.19}$$

$$R_2 = \frac{-(R_{m1}.a_{m2} + R_{m2}.a_{m1})}{(R_{m1} + R_{m2})}.\frac{1}{C} \tag{5.20}$$

After calculating all the proposed model elements, testing their frequency response is carried out to ensure that the proposed model has the same frequency response as the original data as shown in Figures 5.18 and 5.20. PSpice[2] has been used to determine the frequency response of the proposed model. The Figures 5.18 and 5.20 shows that the frequency response of the equivalent circuit and the transformer are almost matching. In the high frequency range, there is some difference between the measured admittance response and the equivalent circuit response. This is due to the order of approximation (which was discussed before). In other words, if the order of approximation increases the curves will fit in the high frequency range but it will complicate the equivalent circuit.

[2]PSpice is a commonly-used circuit simulator.

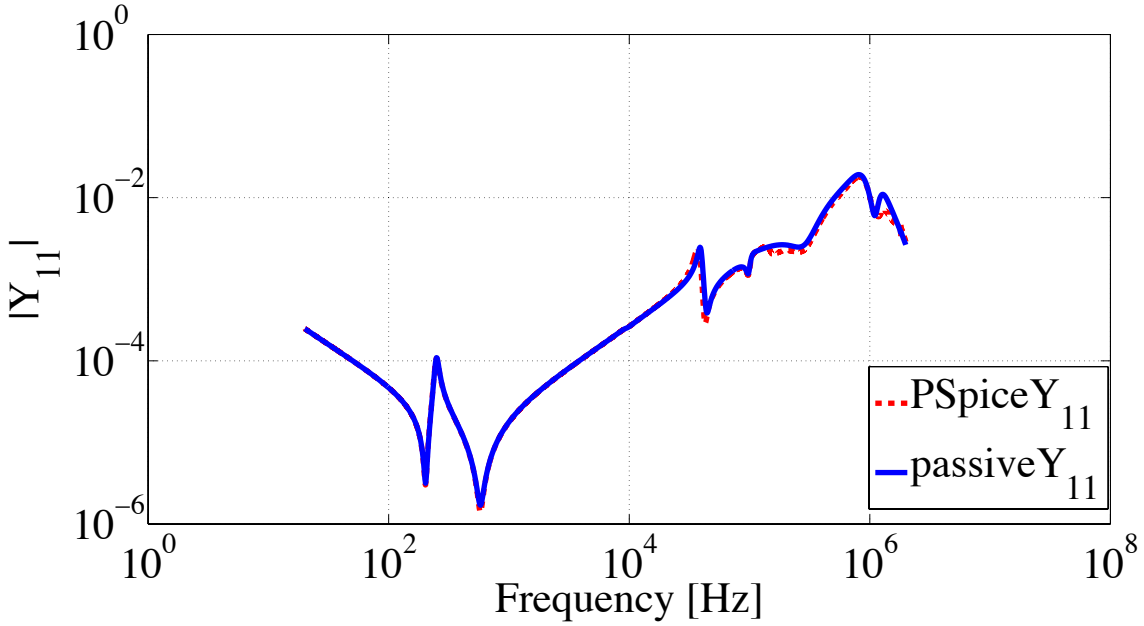

Figure 5.18: The proposed model response of Y_{11} compare to the calculated passive Y_{11}.

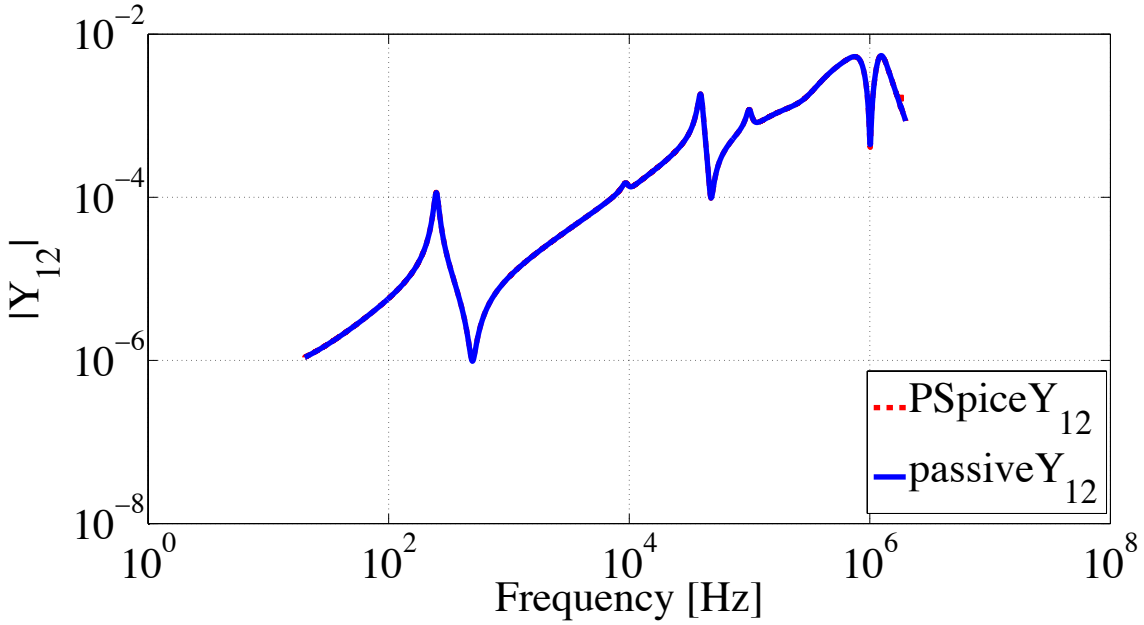

Figure 5.19: The proposed model response of Y_{12} compare to the calculated passive Y_{12}.

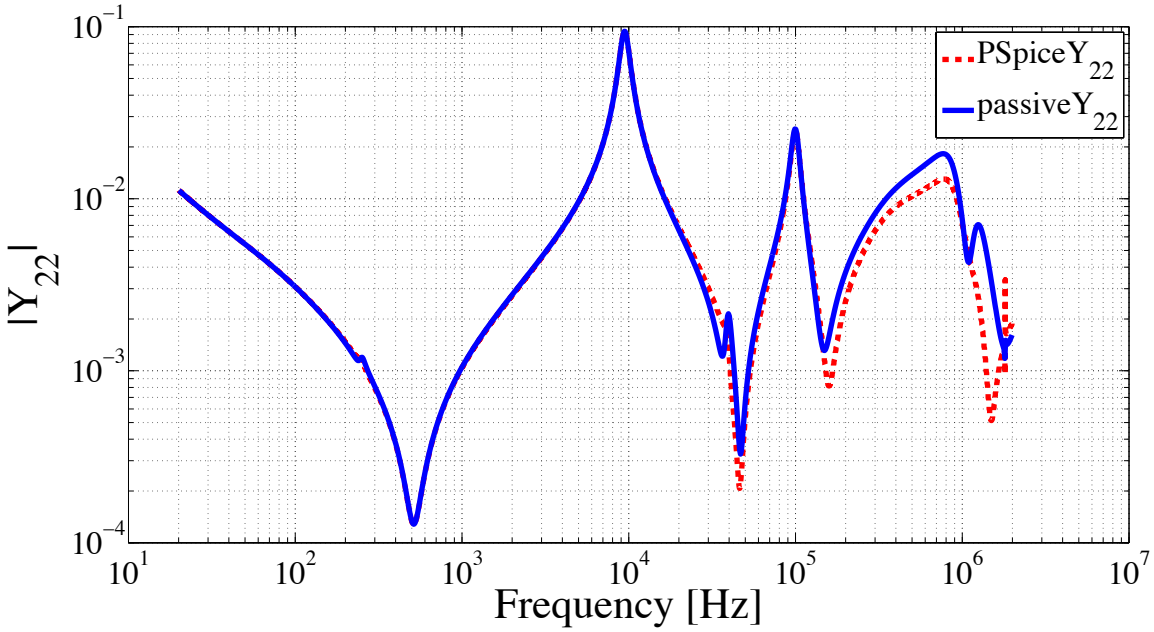

Figure 5.20: The proposed model response of Y_{22} compare to the calculated passive Y_{22}.

5.4 Transient Response of the Proposed Model and the Capacitive Model

To demonstrate an application of the proposed model, a comparison is made between this model and the capacitive model shown in Figure 5.21. A schematic of the proposed model is shown in Figure 5.22. This model has been tested for transient analysis (lightning and switching) and compared to the capacitive models, of Figure 5.21. The capacitive model is used for testing the transient response of a transformer by industry, and transformer manufacturers usually provide the capacitive values of their products.

In our case, the capacitive values were not provided from the transformer manufacturers, thus the capacitive values have to be calculated from the admittance response at low frequencies.

To calculate C_{12}, we considered the first value of Y_{12} admittance at f_{11} =20.074 Hz:

$$Y_{12} = 2.718.10^{-7} + 1.0575.10^{-6} j \ S \tag{5.21}$$

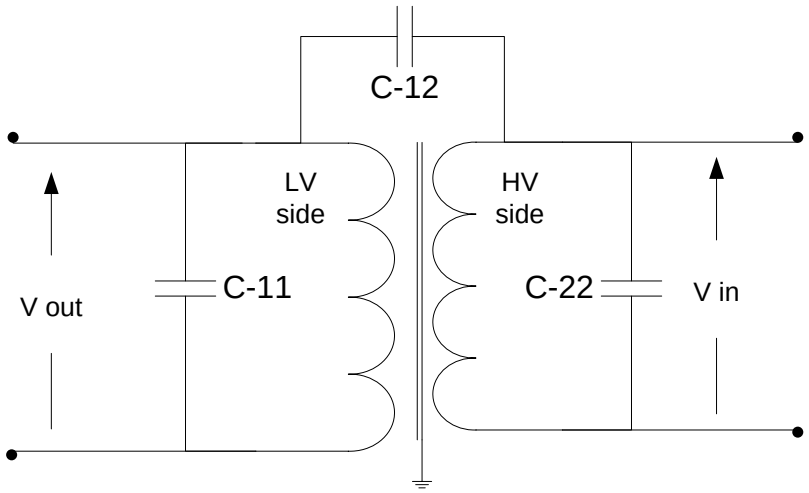

Figure 5.21: Capacitive model.

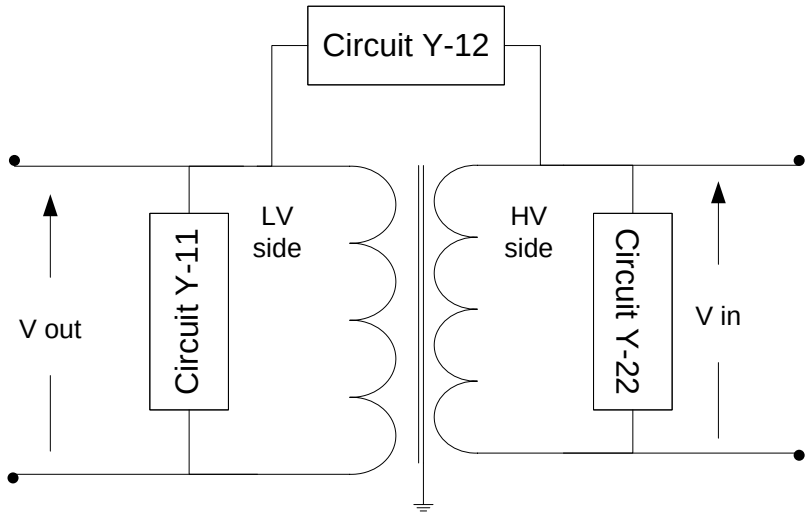

Figure 5.22: Proposed model.

$$Z_{12} = \frac{1}{Y_{12}} = 2.2797.10^5 - 8.87.10^5 j\ \Omega \tag{5.22}$$

Since the impedance of Z_{12} at low frequency is capacitive, thus

$$\frac{1}{2\pi f_{11} C_{12}} = 8.87.10^5 \tag{5.23}$$

or,

$$C_{12} = 8.9385\ nF \tag{5.24}$$

To calculate C-22, we considered the first value of the admittance at 20.074 Hz:

$$Y_{22} = 0.0025 - 0.0090 j\ S \tag{5.25}$$

$$Z_{22} = \frac{1}{Y_{22}} = 28.905 + 102.72 j\ \Omega \tag{5.26}$$

The impedance of Z_{22} at low frequency (20.074 Hz) is an inductive, thus:

$$L_{22} = 102.72/(2\pi f) = 0.81441\ H \tag{5.27}$$

To calculate the capacitance value, the first resonance of the admittance response must be known which takes place at

$$f_{22} = 9306\ Hz \tag{5.28}$$

from [44], we can calculate

$$f_{22} = \frac{1}{2\pi\sqrt{L_{22} C_{22}}} \tag{5.29}$$

$$C_{22} = 0.3591476\ nF \tag{5.30}$$

Similarly for C-11, we have

$$Y_{11} = 1.6339.10^{-5} + 2.2484.10^{-4}j\ S \tag{5.31}$$

Thus,

$$Z_{11} = \frac{1}{Y_{11}} = 321.52 + 4424.3j\ \Omega \tag{5.32}$$

The impedance of Z_{11} at low frequencies (20.074 Hz) is inductive, thus:

$$L_{11} = 4424.3/(2\pi f) = 35.0777\ H \tag{5.33}$$

To calculate the capacitance value, the first resonance of the admittance response must be known. The first resonance frequency is

$$f_{11} = 21330\ Hz \tag{5.34}$$

from [44], we can calculate

$$f_{11} = \frac{1}{2\pi\sqrt{L_{11}C_{11}}} \tag{5.35}$$

$$C_{11} = 1.5872\ pF \tag{5.36}$$

Therefore, the capacitance values for the capacitive model are:

$$C_{12} = 8.9385\ nF \tag{5.37}$$

$$C_{22} = 0.3591476\ nF \tag{5.38}$$

$$C_{11} = 1.5872\ pF \tag{5.39}$$

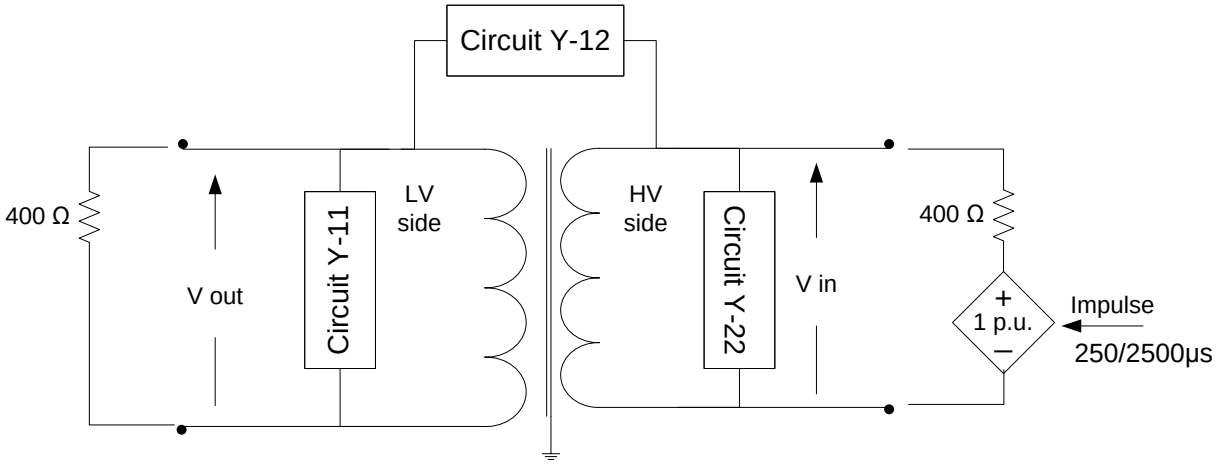

Figure 5.23: Implemented circuit to study the effects of applying $250/2500\mu s$ switching impulse to the proposed model.

5.4.1 Switching Response

After obtaining the proposed model and the the capacitive model, we test both of them and compare their results (see Figures A.1 and 5.24) -PSCAD/EMTDC was used for time-domain simulations.

For switching response of both of the high voltage side and low voltage side, a $250/2500\mu s$ [45] impulse is applied to the high voltage side and the both of the input voltage and the output voltage are evaluated and plotted. The results are shown in Figures 5.25 - 5.26.

From Figure 5.25, where the input voltage for the capacitive model and the proposed model are shown, we can see that both models give an almost the same maximum value for the switching peak, and both of them require almost the same time form the peak to reach zero. A similar observation can be made for the output voltages shown in Figure 5.26.

5.4.2 Lightning Response

As a second test for the proposed model and comparison with the capacitive model, a $1.2/50\mu s$ lightning impulse test [45] was implemented using PSCAD/EMTDC. Figures 5.27, and 5.28 shows the schematic of both models.

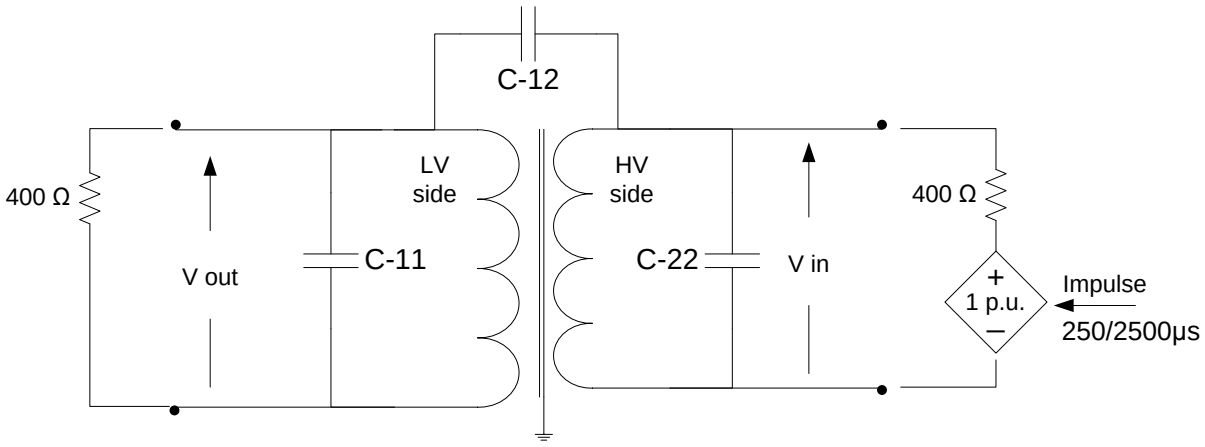

Figure 5.24: Implemented circuit to study the effects of applying $250/2500\mu s$ switching impulse to the capacitive model.

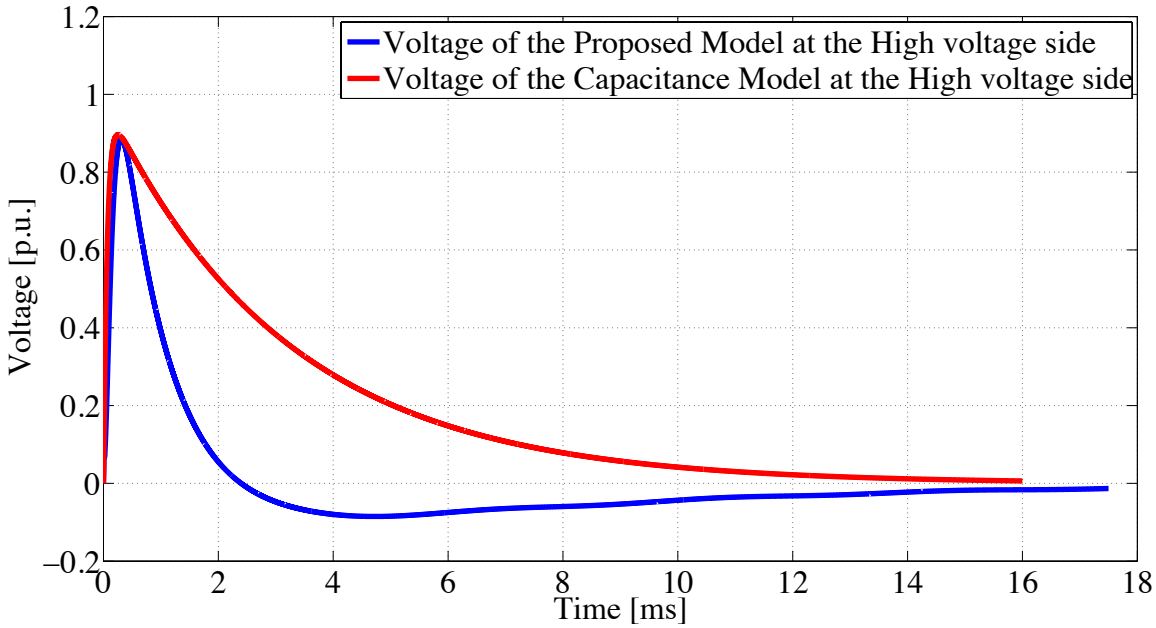

Figure 5.25: Capacitive model and proposed model high voltage side switching transient voltage waveform response.

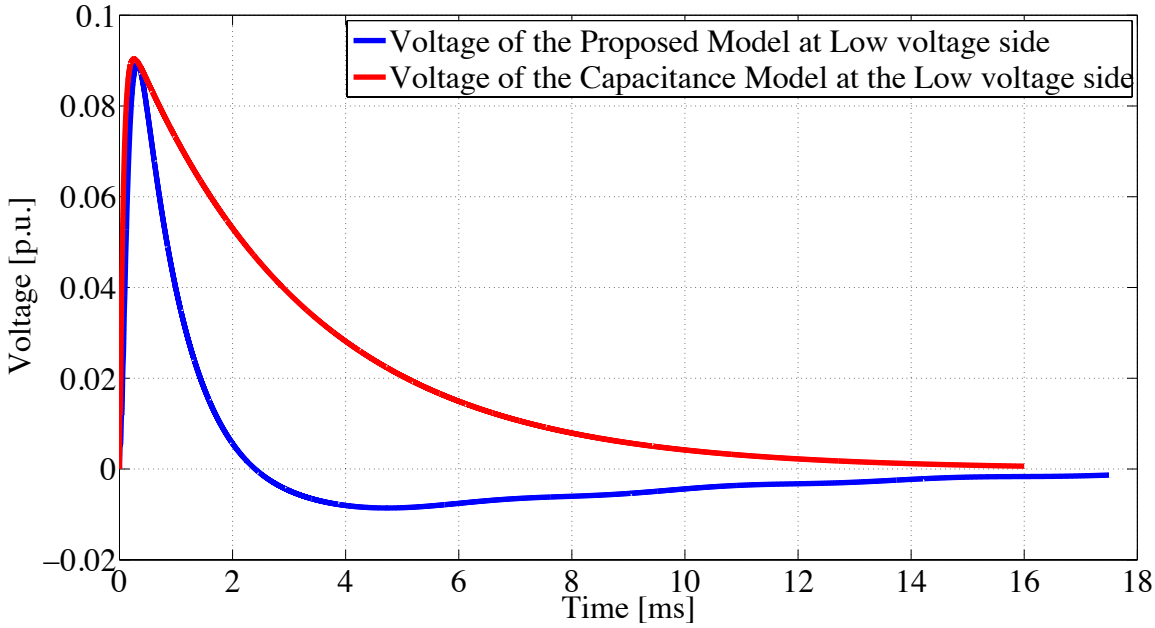

Figure 5.26: Capacitive model and proposed model low voltage side switching transient voltage waveform response.

Figures 5.29 and 5.31 show the input voltages on the high voltage side of the transformer for the capacitive model and the proposed model, respectively, in case of applying a 30 kA, 1.2/50μs lightning impulse. As shown in Figure 5.29 the maximum amplitude of the input voltage for the capacitive model is about 1 MV while the maximum peak of the input voltage for the proposed model is about 0.5 MV. Also, the waveform of lightning impulse is more oscillatory in the proposed model than the capacitive model. Keep in mind that this capacitive model is more concerned about the effect of the lightning on the other side of the transformer (not where the lightning hit). In other words, it only care about the waveform on the other side of the transformer and not about the waveform of lightning which hit the transformer.

For the output voltage waveform, the maximum peak of output voltage for the capacitive model on the low voltage side is about 5 times that of the proposed model (see Figures 5.32 and 5.30), see Appendix A.6, but by looking closely at the waveform of both response, it clearly shows that both have the same waveform. Also, by looking at the time required for both waveform to reach zero, it shows that both of them required almost the same time.

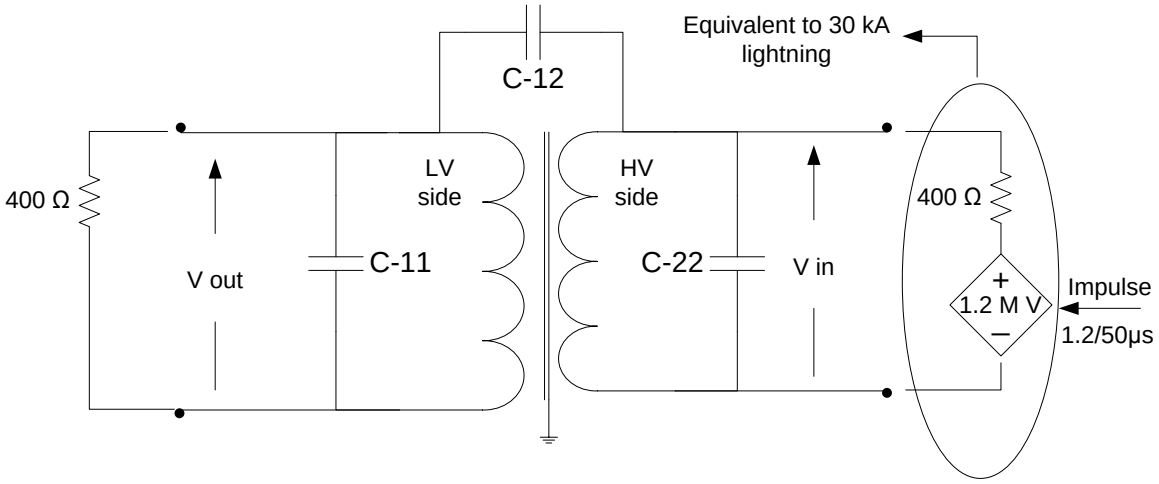

Figure 5.27: Implemented circuit to study the effects of applying $1.2/50\mu s$ lightning impulse to the capacitive model.

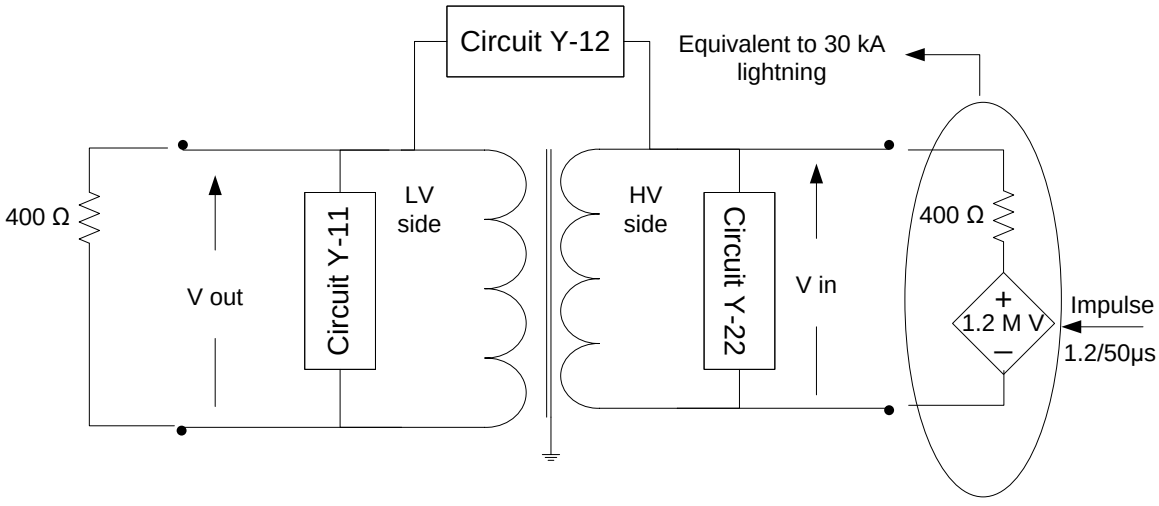

Figure 5.28: Implemented circuit to study the effects of applying $1.2/50\mu s$ lightning impulse to the proposed model.

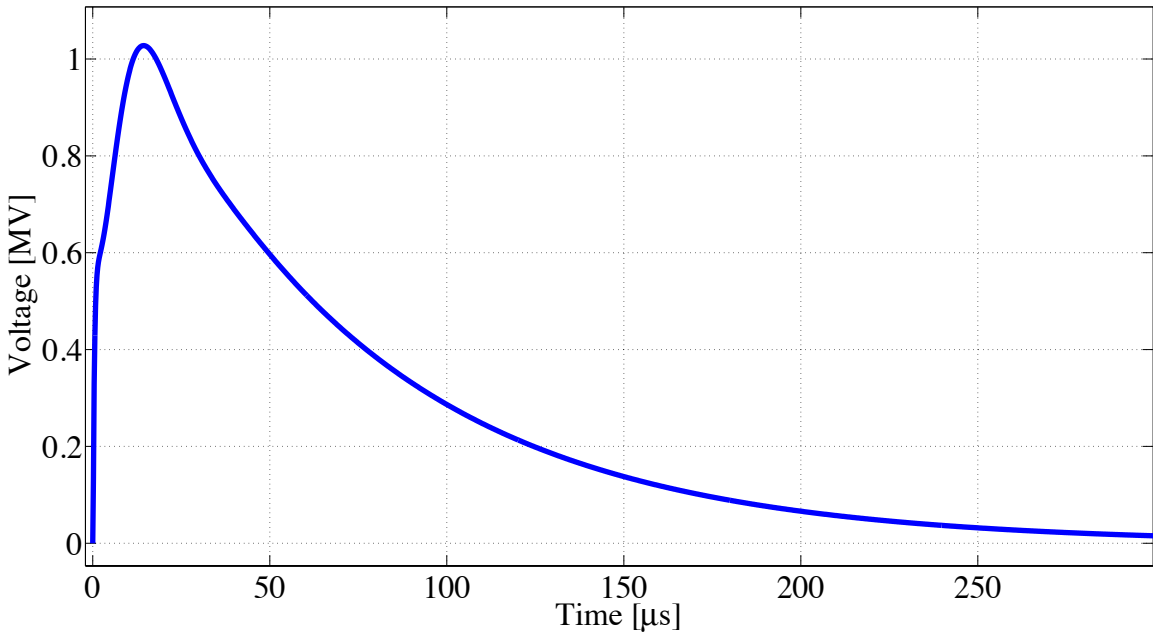

Figure 5.29: Capacitive model high voltage side transient voltage waveform response.

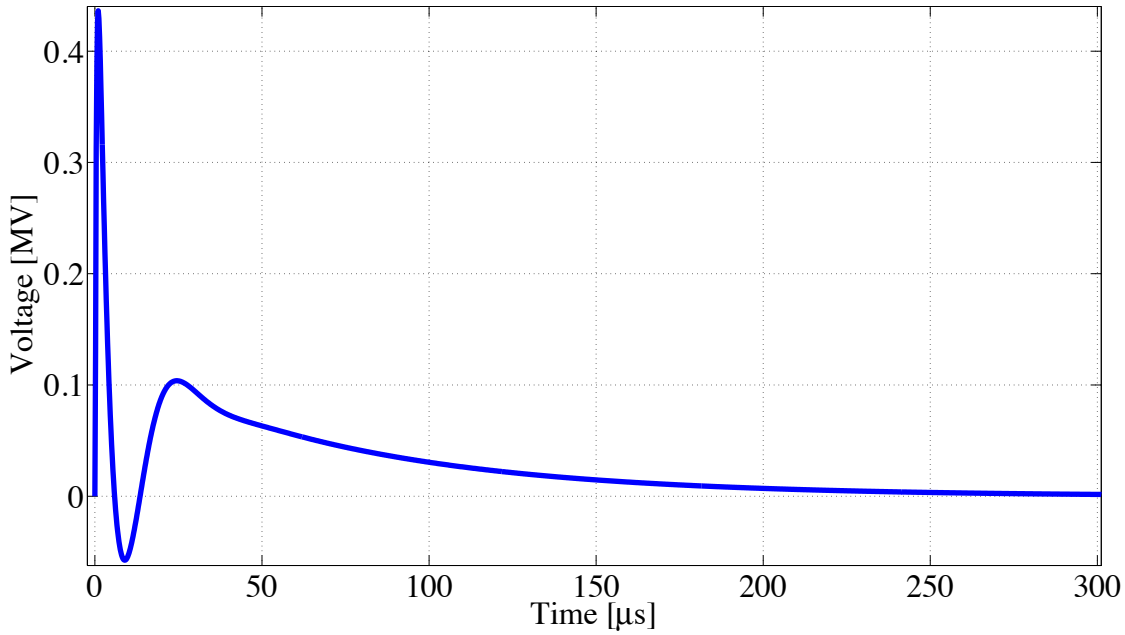

Figure 5.30: Capacitive model low voltage side transient voltage waveform response.

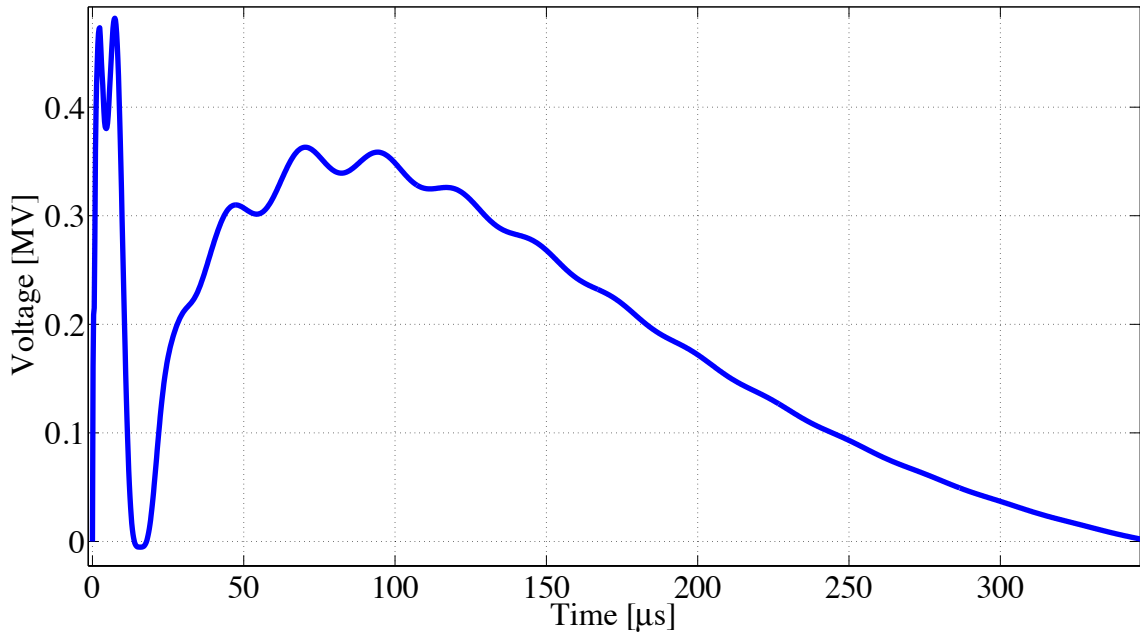

Figure 5.31: Proposed model high voltage side transient voltage waveform response.

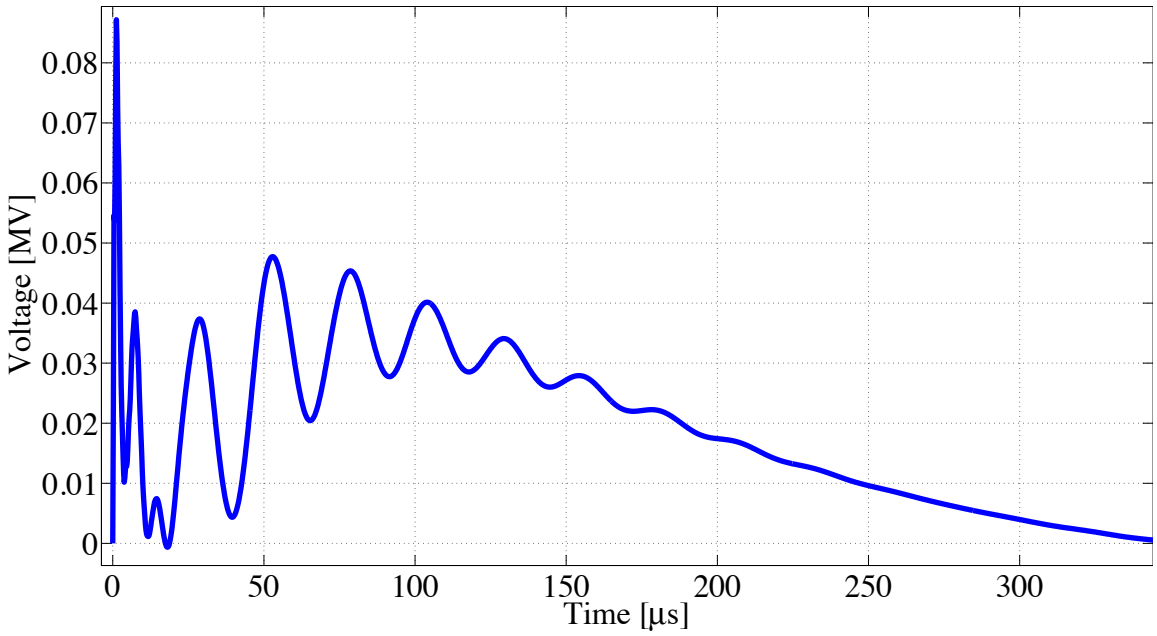

Figure 5.32: Proposed model low voltage side transient voltage waveform response.

Chapter 6

Conclusions and Future Work

6.1 Conclusions

Vector Fitting was employed to approximate the Frequency Response Analysis (FRA) measurement data of a 13.8 kV/136.8 kV, 50-MVA single phase transformer. The frequency response of the primary and secondary coils as well the coupling between the coils had been measured in the frequency range of up to 2 MHz. The measured data included the stray capacitances that exist between the coils. A synthesis model was used to represent the measured data in the form of a two-port passive RLC network. The derived network was implemented in a commonly used power system transient simulator (PSCAD/EMTDC). The proposed RLC model is passive to ensure the stability of the network. The model was used to investigate transient response of the transformer including the simulation of switching and lightning over voltage transients. The results were compared with those derived from existing simple models.

The proposed model presented in this thesis has many advantages over the existing model (the capacitive model). The proposed model provide more realistic waveform transient response than the smooth transient response for the capacitive model. The capacitive model is simpler than the proposed model but it gives an overestimate transient response in ,for example, lightning studies. In this case, for this transformer it was found to be 5 times the peak of the transient response from the capacitor model. Also, the capacitive

model do not give an accurate waveform of the lightning waveform entering to the transformer. The waveform of the lightning induced waveform given by the proposed model is more realistic than the one provided by the capacitive model, see [4] for measured waveform. The capacitive model has wide range of capacitance values and all of these values must be simulated to ensure the maximum peak of the transient waveform will not exceed what have been simulated. In addition, when the transformer ages or faces catastrophic failures these capacitance values may not give an accurate transient response. To overcome all these problem, the proposed model is based on direct measurements of the transformer FRA. In addition, to over come any overestimated values and to have an optimum and cost effective design, the proposed model gives a more realistic and accurate transient response for the transformer.

6.2 Future work

In this thesis, a two port model for transformer was proposed based on end-to-end voltage ratio and transfer voltage ratio measurement which is then employed to calculate approximation to the input admittance matrix. To avoid such calculation and approximation and to have more an accurate model, an input admittance measurement should be carried out for the high voltage side, the low voltage side, and the admittance between the high voltage winding and the low voltage winding.

The proposed model was made for a single phase transformer, thus to have a more complete model for most of the power transformer, a three phase model should be investigated.

Appendix A

A.1 FRA Measurements

Table A.1 shows the FRA measurements data. $|H_1H_2|_{dB}$ which is $|FRA_{ee}|_{dB}$ is the high voltage side measurements. $|X_1X_2|_{dB}$ which is $|FRA_{ee}|_{dB}$ is the low voltage side measurements. $|X_1H_1|_{dB}$ which is $|FRA_{tr}|_{dB}$ is the voltage transfer measurements between the high voltage side and the low voltage side.

Table A.1: FRA measurements .

Frequency [Hz]	$\lvert H_1H_2\rvert$ [dB]	$\angle H_1H_2$ [degrees]	$\lvert X_1X_2\rvert$ [dB]	$\angle X_1X_2$ [degrees]	$\lvert H_1X_2\rvert$ [dB]	$\angle H_1X_2$ [degrees]
20.074	-38.968	-85.200	-8.268	-52.471	-85.257	75.583
20.298	-39.075	-85.165	-8.340	-52.623	-84.952	81.906
20.523	-39.176	-85.149	-8.411	-52.774	-84.707	87.110
20.752	-39.272	-85.154	-8.479	-52.922	-84.525	91.156
20.983	-39.361	-85.178	-8.545	-53.067	-84.407	94.003
21.216	-39.445	-85.225	-8.610	-53.210	-84.357	95.610
21.452	-39.523	-85.292	-8.672	-53.349	-84.375	95.935
21.690	-39.595	-85.383	-8.732	-53.486	-84.465	94.935
21.932	-39.660	-85.497	-8.790	-53.619	-84.629	92.565
22.176	-39.733	-85.509	-8.841	-53.741	-84.294	92.315
22.422	-39.810	-85.540	-8.900	-53.878	-84.169	89.257
22.672	-39.888	-85.568	-8.958	-54.011	-83.994	86.819
22.924	-39.965	-85.610	-9.016	-54.146	-83.946	87.346
23.179	-40.043	-85.683	-9.073	-54.278	-83.773	85.087
23.437	-40.121	-85.724	-9.130	-54.412	-83.637	86.036
23.697	-40.201	-85.739	-9.186	-54.543	-83.586	83.863
23.961	-40.281	-85.774	-9.242	-54.676	-83.451	84.882
24.227	-40.362	-85.805	-9.298	-54.808	-83.161	84.398
24.497	-40.443	-85.832	-9.354	-54.938	-83.061	82.715
24.769	-40.523	-85.869	-9.410	-55.069	-82.911	81.851
25.045	-40.604	-85.902	-9.465	-55.199	-82.974	82.770
25.323	-40.685	-85.941	-9.521	-55.326	-82.941	84.778
25.605	-40.765	-85.966	-9.576	-55.455	-83.005	84.453
25.890	-40.846	-85.986	-9.631	-55.583	-82.920	84.238
26.178	-40.928	-85.992	-9.686	-55.712	-82.911	86.849
26.469	-41.010	-86.005	-9.741	-55.839	-82.735	84.462
26.763	-41.091	-86.027	-9.797	-55.968	-82.604	85.382
27.061	-41.173	-86.050	-9.852	-56.095	-82.467	87.968
27.362	-41.255	-86.097	-9.907	-56.223	-82.416	87.251
27.666	-41.337	-86.117	-9.962	-56.350	-82.422	88.216
27.974	-41.420	-86.153	-10.017	-56.477	-82.386	90.408
28.285	-41.503	-86.177	-10.072	-56.603	-82.280	89.229
28.600	-41.587	-86.196	-10.127	-56.729	-82.135	88.472
28.918	-41.671	-86.233	-10.182	-56.856	-81.996	90.813
29.240	-41.755	-86.274	-10.238	-56.981	-81.933	93.084
29.565	-41.843	-86.310	-10.293	-57.106	-81.592	93.622
29.894	-41.927	-86.343	-10.348	-57.231	-81.467	94.851
30.226	-42.011	-86.390	-10.403	-57.356	-81.344	94.234
30.562	-42.095	-86.423	-10.458	-57.482	-81.309	92.889
30.902	-42.178	-86.435	-10.513	-57.606	-81.236	95.995

Frequency [Hz]	$\lvert H_1H_2\rvert$ [dB]	$\angle H_1H_2$ [degrees]	$\lvert X_1X_2\rvert$ [dB]	$\angle X_1X_2$ [degrees]	$\lvert H_1X_2\rvert$ [dB]	$\angle H_1X_2$ [degrees]
31.246	-42.263	-86.442	-10.569	-57.730	-81.047	93.489
31.594	-42.348	-86.474	-10.624	-57.854	-80.920	92.531
31.945	-42.432	-86.485	-10.679	-57.978	-80.846	90.854
32.300	-42.515	-86.500	-10.735	-58.102	-80.736	90.247
32.660	-42.600	-86.529	-10.790	-58.225	-80.649	88.645
33.023	-42.685	-86.554	-10.846	-58.349	-80.565	87.783
33.390	-42.765	-86.565	-10.901	-58.472	-80.659	86.899
33.762	-42.851	-86.571	-10.957	-58.596	-80.588	87.342
34.137	-42.937	-86.559	-11.012	-58.718	-80.573	87.285
34.517	-43.022	-86.569	-11.068	-58.840	-80.539	85.106
34.901	-43.108	-86.565	-11.123	-58.963	-80.472	85.045
35.289	-43.195	-86.596	-11.179	-59.085	-80.487	85.803
35.681	-43.281	-86.583	-11.235	-59.207	-80.434	85.702
36.078	-43.368	-86.620	-11.290	-59.329	-80.283	85.439
36.480	-43.453	-86.649	-11.346	-59.452	-80.195	85.527
36.885	-43.540	-86.648	-11.402	-59.574	-80.104	85.128
37.296	-43.626	-86.637	-11.458	-59.695	-80.020	85.237
37.710	-43.712	-86.668	-11.514	-59.815	-79.894	84.602
38.130	-43.797	-86.691	-11.570	-59.937	-79.859	85.320
38.554	-43.883	-86.730	-11.626	-60.059	-79.709	85.703
38.983	-43.969	-86.721	-11.682	-60.178	-79.538	86.014
39.416	-44.056	-86.741	-11.738	-60.300	-79.438	86.619
39.855	-44.142	-86.761	-11.794	-60.420	-79.313	87.596
40.298	-44.230	-86.814	-11.851	-60.539	-79.199	87.942
40.746	-44.316	-86.830	-11.907	-60.658	-79.122	90.619
41.199	-44.405	-86.847	-11.963	-60.778	-79.081	90.903
41.658	-44.492	-86.843	-12.020	-60.901	-78.985	91.816
42.121	-44.580	-86.888	-12.076	-61.019	-78.882	92.322
42.590	-44.667	-86.902	-12.133	-61.141	-78.860	92.717
43.063	-44.757	-86.918	-12.190	-61.258	-78.720	93.118
43.542	-44.846	-86.893	-12.247	-61.376	-78.649	93.347
44.027	-44.935	-86.941	-12.303	-61.496	-78.613	94.030
44.516	-45.023	-86.970	-12.360	-61.613	-78.485	91.740
45.011	-45.112	-87.013	-12.417	-61.733	-78.423	90.440
45.512	-45.200	-87.022	-12.474	-61.853	-78.262	91.262
46.018	-45.288	-87.028	-12.531	-61.971	-78.148	90.320
46.530	-45.377	-87.029	-12.589	-62.089	-77.985	89.800
47.048	-45.466	-87.082	-12.646	-62.205	-77.876	89.185
47.571	-45.555	-87.129	-12.703	-62.324	-77.828	88.606
48.100	-45.644	-87.128	-12.761	-62.441	-77.678	88.924

Frequency [Hz]	$\lvert H_1H_2\rvert$ [dB]	$\angle H_1H_2$ [degrees]	$\lvert X_1X_2\rvert$ [dB]	$\angle X_1X_2$ [degrees]	$\lvert H_1X_2\rvert$ [dB]	$\angle H_1X_2$ [degrees]
48.635	-45.732	-87.176	-12.818	-62.560	-77.612	89.249
49.176	-45.820	-87.233	-12.876	-62.678	-77.471	89.008
49.723	-45.909	-87.296	-12.934	-62.797	-77.355	90.592
50.276	-45.999	-87.273	-12.992	-62.916	-77.263	90.752
50.835	-46.088	-87.295	-13.050	-63.033	-77.082	91.411
51.401	-46.177	-87.275	-13.107	-63.150	-76.991	91.613
51.972	-46.265	-87.271	-13.166	-63.268	-76.909	91.303
52.550	-46.356	-87.277	-13.224	-63.389	-76.830	93.422
53.135	-46.447	-87.283	-13.282	-63.507	-76.637	95.276
53.726	-46.537	-87.214	-13.340	-63.624	-76.408	95.348
54.324	-46.628	-87.256	-13.399	-63.743	-76.314	95.030
54.928	-46.718	-87.238	-13.457	-63.859	-76.230	94.153
55.539	-46.808	-87.249	-13.516	-63.978	-76.160	94.873
56.156	-46.898	-87.234	-13.574	-64.095	-76.044	94.755
56.781	-46.985	-87.322	-13.633	-64.214	-75.989	95.319
57.413	-47.075	-87.293	-13.692	-64.332	-75.872	95.386
58.051	-47.167	-87.353	-13.751	-64.450	-75.800	94.310
58.697	-47.257	-87.382	-13.810	-64.567	-75.706	94.458
59.350	-47.345	-87.508	-13.869	-64.682	-75.595	92.762
60.010	-47.435	-87.545	-13.928	-64.798	-75.587	91.022
60.677	-47.526	-87.603	-13.987	-64.915	-75.489	90.430
61.352	-47.616	-87.601	-14.047	-65.031	-75.387	90.224
62.035	-47.706	-87.619	-14.107	-65.147	-75.237	90.353
62.725	-47.797	-87.640	-14.167	-65.264	-75.085	90.137
63.422	-47.889	-87.615	-14.227	-65.379	-74.941	88.966
64.128	-47.985	-87.591	-14.287	-65.494	-74.801	88.801
64.841	-48.077	-87.608	-14.347	-65.610	-74.748	88.507
65.562	-48.170	-87.613	-14.408	-65.727	-74.648	88.845
66.291	-48.264	-87.599	-14.469	-65.843	-74.532	88.803
67.029	-48.357	-87.510	-14.530	-65.958	-74.424	89.034
67.774	-48.447	-87.428	-14.590	-66.079	-74.277	90.375
68.528	-48.539	-87.432	-14.650	-66.200	-74.193	90.546
69.290	-48.630	-87.390	-14.711	-66.320	-74.070	91.275
70.061	-48.724	-87.356	-14.772	-66.438	-73.959	91.078
70.840	-48.818	-87.365	-14.834	-66.556	-73.873	91.333
71.628	-48.910	-87.407	-14.895	-66.674	-73.796	91.038
72.425	-49.000	-87.441	-14.957	-66.790	-73.658	90.855
73.230	-49.094	-87.470	-15.019	-66.906	-73.507	91.212
74.045	-49.183	-87.407	-15.082	-67.021	-73.421	90.977
74.869	-49.276	-87.453	-15.144	-67.136	-73.307	90.892

Frequency [Hz]	$\lvert H_1H_2\rvert$ [dB]	$\angle H_1H_2$ [degrees]	$\lvert X_1X_2\rvert$ [dB]	$\angle X_1X_2$ [degrees]	$\lvert H_1X_2\rvert$ [dB]	$\angle H_1X_2$ [degrees]
75.701	-49.369	-87.483	-15.207	-67.253	-73.205	90.970
76.543	-49.465	-87.506	-15.271	-67.363	-73.123	90.617
77.395	-49.560	-87.507	-15.335	-67.474	-73.023	91.224
78.255	-49.656	-87.543	-15.399	-67.585	-72.910	90.508
79.126	-49.749	-87.588	-15.463	-67.699	-72.827	90.736
80.006	-49.841	-87.538	-15.528	-67.810	-72.727	90.895
80.896	-49.937	-87.516	-15.592	-67.924	-72.606	91.242
81.796	-50.034	-87.455	-15.656	-68.038	-72.517	91.635
82.705	-50.122	-87.444	-15.721	-68.152	-72.422	91.277
83.625	-50.219	-87.504	-15.786	-68.265	-72.278	90.782
84.555	-50.313	-87.487	-15.851	-68.380	-72.179	90.665
85.496	-50.406	-87.406	-15.916	-68.495	-72.059	90.203
86.447	-50.498	-87.403	-15.981	-68.608	-71.956	90.175
87.408	-50.596	-87.373	-16.047	-68.717	-71.764	89.518
88.381	-50.689	-87.367	-16.113	-68.831	-71.641	89.763
89.364	-50.784	-87.355	-16.179	-68.944	-71.485	89.499
90.358	-50.879	-87.376	-16.245	-69.059	-71.362	89.589
91.363	-50.971	-87.355	-16.312	-69.170	-71.245	89.219
92.379	-51.061	-87.430	-16.379	-69.281	-71.146	89.388
93.406	-51.160	-87.423	-16.446	-69.392	-71.017	89.897
94.445	-51.255	-87.446	-16.514	-69.504	-70.914	89.928
95.496	-51.349	-87.422	-16.582	-69.614	-70.781	89.922
96.558	-51.446	-87.462	-16.650	-69.727	-70.679	90.353
97.632	-51.542	-87.541	-16.718	-69.837	-70.579	89.877
98.718	-51.631	-87.594	-16.787	-69.951	-70.541	89.810
99.816	-51.729	-87.585	-16.856	-70.061	-70.435	89.752
100.926	-51.826	-87.618	-16.926	-70.172	-70.346	89.686
102.049	-51.922	-87.637	-16.995	-70.281	-70.229	89.146
103.184	-52.016	-87.626	-17.065	-70.390	-70.105	89.308
104.331	-52.115	-87.527	-17.136	-70.499	-69.978	89.039
105.492	-52.212	-87.492	-17.206	-70.610	-69.844	88.612
106.665	-52.316	-87.571	-17.279	-70.727	-69.723	88.123
107.852	-52.411	-87.390	-17.351	-70.829	-69.570	88.347
109.051	-52.501	-87.288	-17.422	-70.941	-69.426	89.088
110.264	-52.600	-87.214	-17.495	-71.048	-69.290	89.652
111.490	-52.696	-87.224	-17.568	-71.151	-69.138	89.959
112.731	-52.799	-87.228	-17.641	-71.255	-69.007	90.300
113.984	-52.905	-87.337	-17.714	-71.363	-68.888	90.389
115.252	-53.002	-87.453	-17.787	-71.471	-68.769	90.071
116.534	-53.098	-87.588	-17.861	-71.578	-68.656	90.156

Frequency [Hz]	$\lvert H_1H_2\rvert$ [dB]	$\angle H_1H_2$ [degrees]	$\lvert X_1X_2\rvert$ [dB]	$\angle X_1X_2$ [degrees]	$\lvert H_1X_2\rvert$ [dB]	$\angle H_1X_2$ [degrees]
117.830	-53.195	-87.655	-17.935	-71.683	-68.516	88.961
119.141	-53.293	-87.695	-18.010	-71.793	-68.377	88.227
120.466	-53.387	-87.627	-18.085	-71.898	-68.223	88.231
121.806	-53.478	-87.574	-18.160	-72.004	-68.042	88.038
123.161	-53.577	-87.591	-18.236	-72.106	-67.881	87.499
124.531	-53.675	-87.499	-18.314	-72.206	-67.743	87.694
125.916	-53.776	-87.463	-18.390	-72.308	-67.607	87.885
127.316	-53.874	-87.457	-18.468	-72.415	-67.489	87.766
128.732	-53.970	-87.361	-18.545	-72.514	-67.378	88.158
130.164	-54.063	-87.357	-18.623	-72.616	-67.270	88.386
131.612	-54.170	-87.410	-18.702	-72.718	-67.111	88.074
133.076	-54.270	-87.401	-18.782	-72.818	-66.951	88.690
134.556	-54.376	-87.373	-18.862	-72.914	-66.799	88.908
136.053	-54.476	-87.265	-18.942	-73.011	-66.623	89.578
137.566	-54.578	-87.335	-19.024	-73.103	-66.455	89.367
139.096	-54.682	-87.312	-19.106	-73.196	-66.305	89.360
140.643	-54.780	-87.308	-19.188	-73.292	-66.153	89.700
142.207	-54.880	-87.442	-19.270	-73.389	-66.013	89.561
143.789	-54.982	-87.280	-19.354	-73.482	-65.881	89.457
145.388	-55.079	-87.209	-19.437	-73.575	-65.737	88.900
147.006	-55.183	-87.352	-19.522	-73.672	-65.551	88.429
148.641	-55.273	-87.434	-19.607	-73.767	-65.367	88.241
150.294	-55.377	-87.308	-19.693	-73.859	-65.192	87.806
151.966	-55.473	-87.217	-19.779	-73.955	-64.986	88.098
153.656	-55.585	-87.195	-19.866	-74.041	-64.799	87.772
155.365	-55.692	-87.145	-19.955	-74.129	-64.621	87.645
157.093	-55.798	-87.112	-20.043	-74.216	-64.436	87.737
158.840	-55.909	-87.253	-20.132	-74.302	-64.253	87.897
160.607	-56.022	-87.289	-20.221	-74.386	-64.080	87.663
162.393	-56.133	-87.275	-20.311	-74.467	-63.908	87.737
164.200	-56.227	-87.381	-20.402	-74.554	-63.718	87.823
166.026	-56.323	-87.193	-20.493	-74.639	-63.527	88.027
167.873	-56.422	-87.073	-20.586	-74.722	-63.319	88.530
169.740	-56.525	-87.199	-20.678	-74.799	-63.105	89.079
171.628	-56.634	-87.221	-20.773	-74.878	-62.882	88.717
173.537	-56.754	-87.051	-20.869	-74.959	-62.647	88.508
175.467	-56.863	-87.341	-20.967	-75.043	-62.392	88.490
177.419	-56.971	-87.388	-21.067	-75.126	-62.148	88.124
179.392	-57.082	-87.464	-21.167	-75.207	-61.904	87.547
181.387	-57.181	-87.317	-21.269	-75.290	-61.652	87.576

Frequency [Hz]	$\lvert H_1H_2\rvert$ [dB]	$\angle H_1H_2$ [degrees]	$\lvert X_1X_2\rvert$ [dB]	$\angle X_1X_2$ [degrees]	$\lvert H_1X_2\rvert$ [dB]	$\angle H_1X_2$ [degrees]
183.405	-57.280	-87.347	-21.370	-75.365	-61.372	87.973
185.445	-57.394	-87.072	-21.473	-75.434	-61.105	88.013
187.507	-57.500	-87.093	-21.575	-75.500	-60.832	88.085
189.593	-57.605	-87.199	-21.676	-75.556	-60.556	87.931
191.702	-57.720	-86.924	-21.780	-75.614	-60.272	87.325
193.834	-57.837	-86.663	-21.884	-75.674	-59.975	87.072
195.990	-57.940	-86.683	-21.989	-75.733	-59.646	86.819
198.170	-58.060	-86.469	-22.096	-75.792	-59.333	86.347
200.374	-58.172	-86.481	-22.203	-75.854	-58.990	85.971
202.603	-58.278	-86.477	-22.311	-75.914	-58.611	85.751
204.856	-58.378	-86.936	-22.420	-75.970	-58.204	85.638
207.135	-58.492	-87.071	-22.531	-76.025	-57.798	85.303
209.439	-58.598	-87.168	-22.643	-76.077	-57.382	84.593
211.768	-58.698	-87.323	-22.756	-76.126	-56.926	84.042
214.124	-58.814	-87.076	-22.870	-76.170	-56.455	83.253
216.505	-58.921	-87.065	-22.986	-76.217	-55.937	82.433
218.913	-59.045	-86.728	-23.102	-76.260	-55.365	81.534
221.348	-59.173	-86.914	-23.220	-76.299	-54.762	80.716
223.810	-59.282	-86.721	-23.339	-76.337	-54.071	79.428
226.300	-59.386	-86.525	-23.460	-76.371	-53.263	77.821
228.817	-59.493	-86.698	-23.581	-76.403	-52.300	75.514
231.362	-59.615	-86.884	-23.705	-76.430	-51.157	71.821
233.935	-59.743	-87.189	-23.830	-76.454	-49.895	65.421
236.537	-59.859	-87.291	-23.956	-76.477	-48.630	56.045
239.168	-59.983	-86.763	-24.084	-76.497	-47.520	43.848
241.828	-60.104	-86.638	-24.214	-76.519	-46.684	29.716
244.518	-60.231	-85.989	-24.345	-76.538	-46.193	14.981
247.238	-60.353	-86.014	-24.478	-76.556	-46.094	0.548
249.988	-60.463	-85.393	-24.612	-76.571	-46.348	-12.404
252.768	-60.576	-84.821	-24.749	-76.586	-46.864	-23.076
255.580	-60.707	-84.943	-24.887	-76.591	-47.527	-31.188
258.422	-60.836	-85.477	-25.027	-76.591	-48.239	-37.322
261.297	-60.972	-85.849	-25.169	-76.585	-48.959	-42.269
264.203	-61.088	-86.117	-25.314	-76.580	-49.697	-46.755
267.142	-61.204	-85.799	-25.461	-76.566	-50.439	-50.812
270.113	-61.318	-85.746	-25.610	-76.550	-51.191	-54.582
273.117	-61.444	-85.857	-25.761	-76.530	-51.940	-57.738
276.155	-61.582	-85.875	-25.915	-76.510	-52.683	-60.730
279.227	-61.709	-85.828	-26.071	-76.480	-53.414	-63.439
282.332	-61.839	-85.015	-26.229	-76.450	-54.136	-65.644

Frequency [Hz]	$\lvert H_1H_2\rvert$ [dB]	$\angle H_1H_2$ [degrees]	$\lvert X_1X_2\rvert$ [dB]	$\angle X_1X_2$ [degrees]	$\lvert H_1X_2\rvert$ [dB]	$\angle H_1X_2$ [degrees]
285.473	-61.978	-84.937	-26.390	-76.416	-54.836	-67.358
288.648	-62.123	-85.118	-26.554	-76.371	-55.516	-68.540
291.858	-62.278	-85.289	-26.720	-76.325	-56.179	-69.212
295.105	-62.415	-85.909	-26.890	-76.274	-56.827	-69.617
298.387	-62.540	-86.067	-27.063	-76.209	-57.463	-70.019
301.706	-62.671	-86.822	-27.239	-76.141	-58.085	-70.468
305.062	-62.807	-87.100	-27.418	-76.065	-58.685	-71.118
308.455	-62.930	-86.932	-27.600	-75.984	-59.248	-71.851
311.886	-63.049	-86.884	-27.786	-75.892	-59.795	-73.029
315.355	-63.192	-85.712	-27.975	-75.806	-60.341	-73.688
318.862	-63.346	-85.032	-28.170	-75.700	-60.881	-74.411
322.409	-63.503	-84.807	-28.366	-75.583	-61.423	-74.984
325.995	-63.673	-84.751	-28.565	-75.467	-61.955	-75.462
329.621	-63.842	-85.614	-28.767	-75.334	-62.489	-75.482
333.287	-63.983	-85.267	-28.973	-75.188	-63.017	-75.050
336.994	-64.137	-85.124	-29.184	-75.033	-63.525	-74.893
340.742	-64.260	-84.726	-29.400	-74.854	-64.031	-75.212
344.532	-64.415	-84.605	-29.622	-74.673	-64.525	-75.704
348.364	-64.576	-84.580	-29.851	-74.470	-65.010	-76.080
352.239	-64.768	-84.360	-30.088	-74.261	-65.494	-75.409
356.157	-64.952	-84.466	-30.335	-74.028	-65.979	-75.825
360.118	-65.105	-83.869	-30.585	-73.780	-66.465	-76.845
364.124	-65.272	-83.847	-30.842	-73.521	-66.909	-76.748
368.174	-65.452	-84.439	-31.106	-73.227	-67.407	-76.331
372.269	-65.601	-83.371	-31.378	-72.903	-67.894	-75.879
376.409	-65.743	-82.767	-31.659	-72.560	-68.403	-76.153
380.596	-65.900	-82.425	-31.947	-72.189	-68.946	-76.833
384.829	-66.101	-82.252	-32.246	-71.793	-69.524	-76.568
389.110	-66.293	-82.309	-32.552	-71.360	-70.087	-74.792
393.438	-66.498	-82.611	-32.870	-70.894	-70.663	-73.926
397.814	-66.701	-82.431	-33.198	-70.379	-71.260	-73.769
402.238	-66.869	-82.138	-33.539	-69.802	-71.776	-74.081
406.712	-67.014	-82.153	-33.891	-69.198	-72.250	-70.253
411.236	-67.178	-82.760	-34.257	-68.502	-72.745	-69.026
415.810	-67.366	-82.754	-34.637	-67.766	-73.299	-69.287
420.435	-67.553	-83.436	-35.033	-66.923	-73.990	-70.051
425.111	-67.739	-83.581	-35.445	-65.997	-74.751	-71.072
429.840	-67.913	-82.894	-35.874	-64.977	-75.525	-69.866
434.621	-68.119	-81.710	-36.323	-63.853	-76.459	-64.224
439.455	-68.372	-80.109	-36.792	-62.609	-77.393	-65.062

Frequency [Hz]	$\lvert H_1H_2\rvert$ [dB]	$\angle H_1H_2$ [degrees]	$\lvert X_1X_2\rvert$ [dB]	$\angle X_1X_2$ [degrees]	$\lvert H_1X_2\rvert$ [dB]	$\angle H_1X_2$ [degrees]
444.343	-68.631	-78.740	-37.283	-61.191	-78.343	-63.165
449.285	-68.861	-78.548	-37.797	-59.591	-79.149	-57.900
454.282	-69.053	-78.648	-38.335	-57.738	-79.973	-50.265
459.335	-69.342	-78.407	-38.898	-55.636	-80.783	-46.584
464.444	-69.614	-79.299	-39.486	-53.267	-81.760	-42.295
469.610	-69.901	-81.897	-40.096	-50.402	-82.975	-39.996
474.833	-70.131	-81.892	-40.727	-47.134	-83.975	-39.258
480.115	-70.402	-80.641	-41.372	-43.317	-84.686	-30.123
485.455	-70.713	-79.991	-42.019	-38.921	-85.334	-16.738
490.854	-70.996	-79.344	-42.650	-33.853	-85.579	-12.130
496.314	-71.273	-79.634	-43.236	-27.965	-85.564	1.605
501.834	-71.537	-78.981	-43.745	-21.272	-85.189	17.486
507.416	-71.778	-78.484	-44.138	-13.844	-84.622	31.669
513.060	-72.132	-76.694	-44.386	-5.892	-83.849	44.652
518.767	-72.376	-77.858	-44.465	2.365	-83.073	55.700
524.537	-72.692	-79.403	-44.365	10.709	-82.339	60.882
530.371	-73.083	-79.353	-44.098	18.716	-81.463	62.537
536.270	-73.460	-77.990	-43.686	26.183	-80.562	68.810
542.235	-73.767	-79.095	-43.162	32.867	-79.854	72.014
548.266	-74.097	-78.232	-42.562	38.737	-79.165	69.287
554.364	-74.476	-77.202	-41.919	43.831	-78.563	70.306
560.530	-74.962	-73.232	-41.259	48.207	-77.993	70.630
566.765	-75.400	-71.658	-40.600	51.908	-77.398	72.391
573.069	-75.899	-70.982	-39.956	55.111	-76.806	75.021
579.443	-76.369	-72.627	-39.331	57.876	-76.227	75.941
585.888	-76.907	-74.021	-38.729	60.292	-75.665	76.267
592.404	-77.579	-72.539	-38.152	62.414	-75.141	75.995
598.993	-78.109	-68.494	-37.600	64.266	-74.657	78.125
605.656	-78.668	-67.640	-37.072	65.903	-74.259	78.694
612.392	-79.291	-63.029	-36.567	67.346	-73.872	77.973
619.204	-79.984	-61.551	-36.083	68.639	-73.487	77.668
626.091	-80.788	-55.269	-35.619	69.785	-73.133	77.852
633.055	-81.408	-53.638	-35.176	70.780	-72.725	78.883
640.096	-82.069	-56.811	-34.749	71.700	-72.399	78.598
647.215	-82.947	-53.570	-34.338	72.537	-72.104	78.871
654.414	-83.454	-43.504	-33.942	73.293	-71.788	79.354
661.693	-84.096	-28.371	-33.561	73.997	-71.479	80.112
669.053	-84.656	-14.519	-33.193	74.631	-71.221	81.852
676.494	-85.204	-3.700	-32.837	75.224	-70.974	82.434
684.019	-85.542	4.939	-32.493	75.752	-70.709	83.818

Frequency [Hz]	$\lvert H_1H_2\rvert$ [dB]	$\angle H_1H_2$ [degrees]	$\lvert X_1X_2\rvert$ [dB]	$\angle X_1X_2$ [degrees]	$\lvert H_1X_2\rvert$ [dB]	$\angle H_1X_2$ [degrees]
691.627	-85.746	9.235	-32.159	76.240	-70.445	84.825
699.320	-85.665	15.076	-31.836	76.665	-70.192	84.778
707.098	-85.398	15.876	-31.523	77.072	-69.902	84.814
714.963	-85.045	13.320	-31.219	77.445	-69.657	84.488
722.915	-84.503	22.396	-30.923	77.796	-69.417	84.421
730.956	-83.564	32.874	-30.635	78.119	-69.160	84.205
739.086	-82.718	45.732	-30.355	78.420	-68.936	84.930
747.307	-81.964	54.276	-30.082	78.699	-68.753	84.515
755.619	-81.272	59.728	-29.816	78.962	-68.569	84.724
764.023	-80.529	62.246	-29.556	79.199	-68.380	85.875
772.521	-79.846	65.233	-29.301	79.416	-68.198	86.169
781.114	-79.111	66.500	-29.054	79.621	-68.007	85.876
789.802	-78.597	65.930	-28.814	79.822	-67.791	85.882
798.586	-78.099	66.141	-28.579	80.007	-67.590	86.154
807.469	-77.527	67.753	-28.350	80.180	-67.384	86.014
816.450	-77.029	67.672	-28.126	80.346	-67.210	85.743
825.531	-76.503	69.429	-27.906	80.492	-67.028	86.437
834.713	-76.092	70.766	-27.690	80.631	-66.856	86.328
843.997	-75.724	71.726	-27.477	80.758	-66.695	86.846
853.385	-75.297	72.408	-27.266	80.875	-66.522	87.510
862.877	-74.877	75.208	-27.058	80.982	-66.353	87.390
872.474	-74.410	75.731	-26.854	81.083	-66.170	87.309
882.178	-74.064	76.819	-26.654	81.166	-65.981	87.211
891.991	-73.735	78.602	-26.456	81.249	-65.812	87.297
901.912	-73.378	77.834	-26.262	81.321	-65.647	86.668
911.944	-72.975	77.416	-26.071	81.402	-65.484	86.321
922.087	-72.599	75.947	-25.882	81.467	-65.330	86.701
932.343	-72.269	76.771	-25.697	81.531	-65.176	86.393
942.713	-71.947	76.765	-25.514	81.596	-65.036	86.367
953.198	-71.630	76.607	-25.334	81.655	-64.887	86.522
963.801	-71.344	77.879	-25.156	81.706	-64.758	86.902
974.521	-71.073	78.155	-24.980	81.753	-64.618	87.383
985.360	-70.831	79.571	-24.807	81.789	-64.486	87.637
996.320	-70.603	80.141	-24.636	81.824	-64.356	87.652
1007.401	-70.341	81.202	-24.467	81.853	-64.198	87.637
1018.606	-70.017	81.819	-24.300	81.886	-64.047	87.767
1029.936	-69.767	80.989	-24.135	81.905	-63.913	87.636
1041.392	-69.496	81.474	-23.972	81.930	-63.751	87.210
1052.975	-69.239	81.983	-23.810	81.953	-63.598	87.580
1064.687	-69.004	82.803	-23.651	81.970	-63.457	87.361

Frequency [Hz]	$\lvert H_1H_2\rvert$ [dB]	$\angle H_1H_2$ [degrees]	$\lvert X_1X_2\rvert$ [dB]	$\angle X_1X_2$ [degrees]	$\lvert H_1X_2\rvert$ [dB]	$\angle H_1X_2$ [degrees]
1076.529	-68.759	83.613	-23.493	81.979	-63.324	87.778
1088.503	-68.526	83.187	-23.336	81.988	-63.187	87.873
1100.610	-68.266	83.114	-23.181	81.992	-63.064	87.943
1112.851	-68.067	82.162	-23.028	81.995	-62.926	87.852
1125.229	-67.863	82.828	-22.876	81.986	-62.790	88.138
1137.745	-67.639	82.966	-22.726	81.982	-62.661	88.062
1150.399	-67.439	83.224	-22.576	81.970	-62.529	88.316
1163.195	-67.234	83.750	-22.429	81.959	-62.400	88.318
1176.133	-67.087	84.471	-22.282	81.945	-62.259	88.605
1189.215	-66.875	85.475	-22.137	81.930	-62.139	88.480
1202.442	-66.674	85.788	-21.993	81.913	-62.009	88.547
1215.816	-66.472	85.253	-21.850	81.890	-61.876	88.275
1229.339	-66.256	85.352	-21.708	81.871	-61.745	88.109
1243.013	-66.091	84.599	-21.567	81.848	-61.616	87.934
1256.838	-65.906	85.261	-21.427	81.818	-61.504	87.948
1270.818	-65.714	85.269	-21.288	81.790	-61.374	87.649
1284.953	-65.540	85.385	-21.151	81.757	-61.258	87.440
1299.245	-65.373	85.332	-21.014	81.724	-61.153	87.363
1313.696	-65.207	85.194	-20.879	81.691	-61.034	87.299
1328.308	-65.025	84.872	-20.744	81.659	-60.923	87.245
1343.082	-64.880	84.815	-20.607	81.624	-60.804	87.453
1358.020	-64.703	84.786	-20.470	81.583	-60.676	87.484
1373.125	-64.548	84.762	-20.334	81.543	-60.551	87.541
1388.398	-64.397	84.613	-20.197	81.500	-60.437	87.656
1403.841	-64.255	85.082	-20.062	81.455	-60.319	87.871
1419.455	-64.099	85.114	-19.928	81.403	-60.204	87.767
1435.243	-63.957	85.070	-19.796	81.349	-60.091	87.840
1451.207	-63.798	85.348	-19.666	81.293	-59.986	87.779
1467.348	-63.642	85.291	-19.539	81.237	-59.871	87.875
1483.669	-63.496	85.280	-19.412	81.182	-59.746	88.079
1500.172	-63.338	85.752	-19.285	81.123	-59.635	88.462
1516.857	-63.175	86.025	-19.158	81.065	-59.508	88.393
1533.729	-63.026	86.142	-19.032	81.004	-59.387	88.399
1550.788	-62.884	85.931	-18.907	80.943	-59.270	88.173
1568.037	-62.741	85.971	-18.782	80.879	-59.166	88.243
1585.478	-62.599	85.650	-18.658	80.809	-59.069	87.998
1603.112	-62.465	85.486	-18.534	80.738	-58.966	87.886
1620.943	-62.332	85.266	-18.410	80.668	-58.863	87.575
1638.972	-62.210	85.256	-18.287	80.596	-58.751	87.634
1657.202	-62.072	85.399	-18.165	80.517	-58.644	87.674

Frequency [Hz]	$\lvert H_1H_2\rvert$ [dB]	$\angle H_1H_2$ [degrees]	$\lvert X_1X_2\rvert$ [dB]	$\angle X_1X_2$ [degrees]	$\lvert H_1X_2\rvert$ [dB]	$\angle H_1X_2$ [degrees]
1675.635	-61.940	85.797	-18.043	80.438	-58.532	87.772
1694.272	-61.798	86.697	-17.922	80.359	-58.407	87.839
1713.117	-61.658	87.336	-17.800	80.280	-58.299	87.658
1732.171	-61.518	87.450	-17.680	80.198	-58.206	87.594
1751.438	-61.376	87.792	-17.559	80.118	-58.109	87.891
1770.918	-61.249	87.373	-17.439	80.034	-58.005	88.017
1790.616	-61.113	87.226	-17.320	79.950	-57.902	88.229
1810.532	-60.992	86.656	-17.200	79.863	-57.803	88.384
1830.670	-60.879	86.381	-17.081	79.773	-57.693	88.593
1851.032	-60.752	86.177	-16.963	79.678	-57.580	88.786
1871.620	-60.632	86.161	-16.844	79.584	-57.458	88.682
1892.438	-60.504	86.291	-16.726	79.488	-57.341	88.503
1913.487	-60.383	86.460	-16.608	79.390	-57.242	88.216
1934.770	-60.249	86.455	-16.491	79.287	-57.138	88.234
1956.290	-60.127	86.600	-16.374	79.186	-57.031	88.145
1978.049	-60.001	86.548	-16.257	79.082	-56.933	88.267
2000.050	-59.868	86.826	-16.140	78.974	-56.822	88.361
2022.296	-59.733	86.968	-16.023	78.864	-56.712	88.576
2044.789	-59.593	87.781	-15.906	78.753	-56.596	88.823
2067.533	-59.465	88.022	-15.790	78.641	-56.486	89.057
2090.529	-59.350	88.287	-15.674	78.527	-56.378	88.918
2113.781	-59.240	88.285	-15.558	78.410	-56.269	88.856
2137.292	-59.125	88.334	-15.442	78.290	-56.164	89.052
2161.065	-59.022	88.126	-15.327	78.167	-56.063	88.962
2185.101	-58.917	87.802	-15.212	78.046	-55.969	89.024
2209.405	-58.813	87.621	-15.096	77.922	-55.868	88.982
2233.980	-58.689	87.399	-14.981	77.793	-55.767	89.040
2258.828	-58.559	87.359	-14.866	77.661	-55.666	88.984
2283.952	-58.431	87.685	-14.751	77.527	-55.566	88.974
2309.355	-58.312	87.654	-14.636	77.393	-55.469	88.837
2335.042	-58.197	87.485	-14.521	77.253	-55.364	88.706
2361.014	-58.085	87.393	-14.407	77.110	-55.259	88.621
2387.274	-57.973	87.452	-14.292	76.968	-55.155	88.757
2413.827	-57.867	87.405	-14.177	76.822	-55.051	88.706
2440.675	-57.765	87.260	-14.061	76.676	-54.953	88.708
2467.822	-57.667	87.393	-13.946	76.527	-54.839	88.770
2495.271	-57.549	87.395	-13.831	76.371	-54.731	88.852
2523.025	-57.438	87.595	-13.715	76.213	-54.624	88.853
2551.088	-57.321	87.764	-13.601	76.057	-54.521	88.957
2579.463	-57.210	87.895	-13.486	75.897	-54.420	88.907

Frequency [Hz]	$\lvert H_1H_2\rvert$ [dB]	$\angle H_1H_2$ [degrees]	$\lvert X_1X_2\rvert$ [dB]	$\angle X_1X_2$ [degrees]	$\lvert H_1X_2\rvert$ [dB]	$\angle H_1X_2$ [degrees]
2608.153	-57.097	87.906	-13.372	75.730	-54.317	88.891
2637.163	-56.988	87.874	-13.258	75.564	-54.218	88.885
2666.495	-56.881	87.956	-13.144	75.395	-54.122	88.816
2696.153	-56.766	88.020	-13.029	75.222	-54.021	88.781
2726.142	-56.652	87.970	-12.915	75.044	-53.923	88.738
2756.464	-56.543	87.889	-12.801	74.864	-53.813	88.742
2787.123	-56.426	88.024	-12.686	74.680	-53.707	88.822
2818.123	-56.319	88.068	-12.572	74.495	-53.609	88.922
2849.468	-56.217	87.888	-12.457	74.309	-53.505	88.825
2881.162	-56.113	87.645	-12.343	74.118	-53.407	88.692
2913.208	-56.020	87.397	-12.228	73.924	-53.308	88.686
2945.611	-55.924	87.193	-12.113	73.729	-53.212	88.723
2978.374	-55.821	87.323	-11.999	73.528	-53.114	88.716
3011.501	-55.710	87.366	-11.884	73.323	-53.011	88.826
3044.997	-55.598	87.408	-11.769	73.114	-52.906	88.765
3078.865	-55.490	87.586	-11.654	72.901	-52.803	88.753
3113.111	-55.369	87.842	-11.538	72.685	-52.693	88.860
3147.737	-55.256	87.967	-11.423	72.463	-52.592	88.813
3182.748	-55.143	87.904	-11.307	72.239	-52.485	88.808
3218.149	-55.031	88.043	-11.192	72.010	-52.387	88.744
3253.943	-54.930	87.903	-11.076	71.778	-52.284	88.865
3290.135	-54.826	87.785	-10.960	71.541	-52.188	89.013
3326.730	-54.731	87.664	-10.844	71.298	-52.091	89.158
3363.733	-54.622	87.856	-10.728	71.050	-51.995	89.117
3401.146	-54.523	87.959	-10.612	70.798	-51.896	89.001
3438.976	-54.424	88.075	-10.496	70.542	-51.795	88.962
3477.227	-54.315	88.128	-10.379	70.282	-51.692	88.919
3515.903	-54.213	88.149	-10.262	70.015	-51.589	88.788
3555.009	-54.108	88.134	-10.145	69.744	-51.485	88.699
3594.550	-54.003	88.204	-10.027	69.468	-51.380	88.648
3634.531	-53.901	87.951	-9.910	69.190	-51.286	88.637
3674.956	-53.802	87.796	-9.792	68.906	-51.189	88.730
3715.832	-53.702	87.815	-9.674	68.614	-51.093	88.781
3757.162	-53.589	88.049	-9.556	68.316	-50.995	88.765
3798.951	-53.487	88.119	-9.438	68.013	-50.898	88.840
3841.206	-53.384	88.114	-9.320	67.703	-50.796	88.866
3883.930	-53.280	88.173	-9.201	67.388	-50.697	88.909
3927.130	-53.174	88.112	-9.082	67.062	-50.589	88.910
3970.810	-53.074	88.065	-8.962	66.733	-50.482	88.933
4014.976	-52.973	88.121	-8.843	66.397	-50.378	88.934

Frequency [Hz]	$\lvert H_1H_2\rvert$ [dB]	$\angle H_1H_2$ [degrees]	$\lvert X_1X_2\rvert$ [dB]	$\angle X_1X_2$ [degrees]	$\lvert H_1X_2\rvert$ [dB]	$\angle H_1X_2$ [degrees]
4059.633	-52.868	88.106	-8.723	66.058	-50.284	88.767
4104.787	-52.764	88.110	-8.603	65.712	-50.179	88.685
4150.443	-52.661	88.158	-8.483	65.358	-50.076	88.598
4196.607	-52.559	88.184	-8.363	64.996	-49.974	88.605
4243.285	-52.455	88.240	-8.242	64.626	-49.873	88.608
4290.481	-52.355	88.256	-8.121	64.248	-49.773	88.641
4338.203	-52.253	88.254	-8.000	63.860	-49.676	88.760
4386.455	-52.151	88.177	-7.879	63.464	-49.571	88.846
4435.244	-52.058	88.153	-7.757	63.061	-49.471	88.849
4484.576	-51.960	88.211	-7.635	62.650	-49.376	88.835
4534.456	-51.857	88.213	-7.513	62.231	-49.276	88.785
4584.892	-51.760	88.209	-7.390	61.799	-49.174	88.704
4635.888	-51.660	88.206	-7.267	61.361	-49.072	88.700
4687.451	-51.559	88.190	-7.144	60.910	-48.971	88.718
4739.588	-51.458	88.156	-7.020	60.452	-48.869	88.704
4792.305	-51.359	88.148	-6.897	59.985	-48.769	88.712
4845.608	-51.258	88.208	-6.773	59.507	-48.669	88.770
4899.504	-51.151	88.236	-6.650	59.020	-48.568	88.840
4954.000	-51.050	88.244	-6.526	58.520	-48.466	88.828
5009.101	-50.952	88.257	-6.402	58.010	-48.364	88.747
5064.816	-50.847	88.350	-6.278	57.485	-48.260	88.719
5121.150	-50.745	88.388	-6.154	56.947	-48.157	88.609
5178.111	-50.642	88.468	-6.029	56.400	-48.051	88.605
5235.705	-50.541	88.474	-5.904	55.836	-47.948	88.527
5293.940	-50.443	88.478	-5.779	55.261	-47.848	88.472
5352.823	-50.344	88.511	-5.655	54.673	-47.748	88.462
5412.360	-50.246	88.517	-5.530	54.071	-47.649	88.504
5472.560	-50.144	88.465	-5.405	53.455	-47.549	88.571
5533.430	-50.046	88.383	-5.280	52.820	-47.448	88.595
5594.976	-49.951	88.230	-5.155	52.174	-47.345	88.523
5657.207	-49.850	88.234	-5.031	51.513	-47.239	88.580
5720.130	-49.751	88.197	-4.906	50.837	-47.135	88.576
5783.753	-49.655	88.227	-4.782	50.145	-47.031	88.598
5848.084	-49.557	88.223	-4.658	49.433	-46.929	88.539
5913.130	-49.460	88.209	-4.535	48.704	-46.826	88.545
5978.900	-49.359	88.226	-4.411	47.960	-46.722	88.574
6045.401	-49.259	88.278	-4.288	47.193	-46.620	88.553
6112.642	-49.158	88.319	-4.166	46.409	-46.516	88.548
6180.631	-49.057	88.292	-4.044	45.604	-46.415	88.498
6249.376	-48.956	88.170	-3.923	44.783	-46.310	88.458

Frequency [Hz]	$\lvert H_1H_2\rvert$ [dB]	$\angle H_1H_2$ [degrees]	$\lvert X_1X_2\rvert$ [dB]	$\angle X_1X_2$ [degrees]	$\lvert H_1X_2\rvert$ [dB]	$\angle H_1X_2$ [degrees]
6318.886	-48.858	88.192	-3.802	43.942	-46.206	88.450
6389.169	-48.759	88.188	-3.683	43.077	-46.103	88.438
6460.233	-48.660	88.204	-3.564	42.191	-45.998	88.394
6532.088	-48.561	88.226	-3.447	41.285	-45.893	88.406
6604.742	-48.457	88.257	-3.331	40.356	-45.789	88.411
6678.205	-48.359	88.414	-3.216	39.405	-45.682	88.470
6752.484	-48.264	88.501	-3.102	38.429	-45.576	88.456
6827.590	-48.169	88.409	-2.990	37.430	-45.463	88.468
6903.531	-48.072	88.314	-2.880	36.412	-45.355	88.582
6980.316	-47.975	88.274	-2.772	35.369	-45.246	88.661
7057.956	-47.878	88.216	-2.665	34.300	-45.137	88.688
7136.459	-47.778	88.164	-2.562	33.206	-45.028	88.690
7215.836	-47.677	88.176	-2.460	32.089	-44.921	88.630
7296.095	-47.574	88.158	-2.361	30.946	-44.815	88.550
7377.247	-47.468	88.187	-2.264	29.777	-44.709	88.452
7459.301	-47.372	88.314	-2.171	28.581	-44.601	88.361
7542.269	-47.276	88.280	-2.080	27.363	-44.495	88.213
7626.159	-47.176	88.212	-1.994	26.118	-44.381	88.109
7710.982	-47.077	88.222	-1.910	24.852	-44.272	88.162
7796.749	-46.979	88.199	-1.831	23.557	-44.162	88.125
7883.469	-46.881	88.178	-1.756	22.240	-44.051	88.085
7971.154	-46.781	88.167	-1.685	20.900	-43.939	88.070
8059.815	-46.680	88.166	-1.619	19.538	-43.827	88.039
8149.461	-46.581	88.147	-1.558	18.154	-43.713	87.981
8240.105	-46.483	88.127	-1.502	16.747	-43.599	87.956
8331.757	-46.384	88.120	-1.451	15.323	-43.483	87.913
8424.428	-46.284	88.119	-1.405	13.879	-43.367	87.862
8518.130	-46.184	88.137	-1.366	12.415	-43.250	87.804
8612.874	-46.086	88.116	-1.332	10.938	-43.133	87.738
8708.673	-45.987	88.080	-1.305	9.444	-43.016	87.686
8805.536	-45.888	88.116	-1.284	7.939	-42.896	87.620
8903.477	-45.789	88.129	-1.269	6.422	-42.775	87.582
9002.507	-45.691	88.146	-1.262	4.897	-42.653	87.532
9102.639	-45.593	88.127	-1.261	3.360	-42.530	87.465
9203.885	-45.495	88.106	-1.267	1.814	-42.405	87.386
9306.257	-45.395	88.094	-1.281	0.266	-42.279	87.324
9409.767	-45.294	88.064	-1.302	-1.286	-42.152	87.235
9514.428	-45.194	88.033	-1.331	-2.841	-42.024	87.137
9620.254	-45.095	88.001	-1.368	-4.391	-41.893	87.029
9727.257	-44.995	87.960	-1.412	-5.936	-41.763	86.922

Frequency [Hz]	$\lvert H_1H_2\rvert$ [dB]	$\angle H_1H_2$ [degrees]	$\lvert X_1X_2\rvert$ [dB]	$\angle X_1X_2$ [degrees]	$\lvert H_1X_2\rvert$ [dB]	$\angle H_1X_2$ [degrees]
9835.450	-44.897	87.987	-1.464	-7.471	-41.627	86.802
9944.846	-44.799	87.982	-1.525	-8.998	-41.490	86.661
10055.460	-44.701	87.988	-1.593	-10.514	-41.350	86.514
10167.303	-44.604	87.947	-1.670	-12.018	-41.207	86.352
10280.390	-44.506	87.935	-1.755	-13.507	-41.061	86.167
10394.736	-44.406	87.932	-1.848	-14.980	-40.913	85.985
10510.353	-44.306	87.921	-1.950	-16.431	-40.761	85.760
10627.256	-44.206	87.909	-2.061	-17.863	-40.606	85.519
10745.459	-44.107	87.890	-2.180	-19.270	-40.445	85.249
10864.977	-44.008	87.864	-2.309	-20.647	-40.281	84.940
10985.825	-43.909	87.840	-2.448	-21.987	-40.111	84.579
11108.016	-43.809	87.831	-2.596	-23.285	-39.935	84.171
11231.567	-43.709	87.818	-2.755	-24.543	-39.754	83.700
11356.492	-43.609	87.809	-2.924	-25.755	-39.568	83.154
11482.806	-43.509	87.801	-3.105	-26.910	-39.375	82.521
11610.526	-43.409	87.788	-3.298	-27.996	-39.176	81.771
11739.666	-43.309	87.759	-3.504	-29.005	-38.971	80.877
11870.242	-43.209	87.743	-3.723	-29.914	-38.764	79.805
12002.271	-43.109	87.730	-3.956	-30.706	-38.555	78.523
12135.768	-43.008	87.722	-4.203	-31.356	-38.350	76.974
12270.750	-42.907	87.708	-4.464	-31.824	-38.157	75.104
12407.233	-42.805	87.691	-4.737	-32.069	-37.990	72.852
12545.234	-42.703	87.674	-5.019	-32.032	-37.870	70.175
12684.771	-42.600	87.654	-5.301	-31.647	-37.829	67.063
12825.859	-42.496	87.636	-5.572	-30.842	-37.906	63.630
12968.517	-42.392	87.617	-5.808	-29.561	-38.139	60.145
13112.761	-42.287	87.581	-5.980	-27.805	-38.545	57.041
13258.610	-42.181	87.531	-6.050	-25.690	-39.106	54.820
13406.081	-42.075	87.468	-5.989	-23.471	-39.761	53.921
13555.192	-41.970	87.397	-5.789	-21.506	-40.419	54.512
13705.962	-41.865	87.321	-5.471	-20.176	-40.990	56.433
13858.409	-41.763	87.234	-5.083	-19.739	-41.410	59.256
14012.551	-41.664	87.134	-4.686	-20.268	-41.661	62.471
14168.408	-41.569	87.032	-4.331	-21.639	-41.764	65.643
14325.998	-41.477	86.941	-4.054	-23.611	-41.758	68.527
14485.342	-41.389	86.884	-3.864	-25.925	-41.682	71.052
14646.457	-41.300	86.857	-3.756	-28.367	-41.560	73.262
14809.365	-41.210	86.855	-3.719	-30.802	-41.405	75.190
14974.084	-41.115	86.873	-3.738	-33.152	-41.225	76.861
15140.636	-41.017	86.891	-3.801	-35.362	-41.027	78.281

Frequency [Hz]	$\lvert H_1H_2\rvert$ [dB]	$\angle H_1H_2$ [degrees]	$\lvert X_1X_2\rvert$ [dB]	$\angle X_1X_2$ [degrees]	$\lvert H_1X_2\rvert$ [dB]	$\angle H_1X_2$ [degrees]
15309.040	-40.915	86.900	-3.897	-37.421	-40.818	79.469
15479.317	-40.812	86.905	-4.017	-39.319	-40.607	80.444
15651.488	-40.707	86.897	-4.155	-41.068	-40.397	81.242
15825.575	-40.603	86.877	-4.306	-42.683	-40.192	81.903
16001.597	-40.498	86.846	-4.466	-44.179	-39.992	82.447
16179.577	-40.393	86.811	-4.632	-45.567	-39.799	82.890
16359.537	-40.288	86.775	-4.803	-46.856	-39.611	83.257
16541.499	-40.183	86.741	-4.976	-48.058	-39.431	83.569
16725.484	-40.077	86.712	-5.152	-49.190	-39.256	83.844
16911.516	-39.972	86.680	-5.329	-50.254	-39.085	84.084
17099.617	-39.865	86.645	-5.507	-51.261	-38.917	84.300
17289.810	-39.757	86.607	-5.686	-52.216	-38.750	84.490
17482.119	-39.648	86.562	-5.865	-53.119	-38.585	84.647
17676.567	-39.538	86.514	-6.045	-53.979	-38.422	84.775
17873.177	-39.427	86.466	-6.225	-54.808	-38.261	84.885
18071.974	-39.314	86.409	-6.406	-55.601	-38.103	84.975
18272.983	-39.201	86.339	-6.588	-56.362	-37.945	85.047
18476.227	-39.086	86.259	-6.772	-57.095	-37.790	85.101
18681.732	-38.969	86.175	-6.957	-57.796	-37.635	85.141
18889.522	-38.851	86.081	-7.143	-58.464	-37.481	85.160
19099.624	-38.730	85.974	-7.332	-59.099	-37.327	85.171
19312.063	-38.606	85.851	-7.523	-59.711	-37.174	85.173
19526.864	-38.479	85.681	-7.717	-60.295	-37.021	85.163
19744.055	-38.346	85.517	-7.915	-60.842	-36.867	85.164
19963.661	-38.214	85.303	-8.118	-61.358	-36.713	85.093
20185.710	-38.075	84.980	-8.326	-61.821	-36.560	84.944
20410.229	-37.928	84.487	-8.542	-62.217	-36.406	84.822
20637.245	-37.780	83.931	-8.767	-62.522	-36.250	84.698
20866.786	-37.630	83.075	-9.005	-62.662	-36.093	84.530
21098.880	-37.511	81.985	-9.245	-62.504	-35.946	84.217
21333.556	-37.478	80.623	-9.450	-61.967	-35.824	83.911
21570.842	-37.559	79.418	-9.579	-61.226	-35.727	83.578
21810.767	-37.728	78.730	-9.620	-60.649	-35.650	83.334
22053.361	-37.899	78.904	-9.601	-60.559	-35.571	83.394
22298.653	-38.007	79.835	-9.580	-61.078	-35.477	83.589
22546.673	-38.014	81.116	-9.605	-62.070	-35.349	83.854
22797.452	-37.926	82.250	-9.698	-63.226	-35.198	84.113
23051.020	-37.801	83.170	-9.843	-64.286	-35.034	84.357
23307.409	-37.667	83.653	-10.014	-65.183	-34.875	84.532
23566.649	-37.532	83.934	-10.195	-65.972	-34.716	84.450

Frequency [Hz]	$\lvert H_1H_2\rvert$ [dB]	$\angle H_1H_2$ [degrees]	$\lvert X_1X_2\rvert$ [dB]	$\angle X_1X_2$ [degrees]	$\lvert H_1X_2\rvert$ [dB]	$\angle H_1X_2$ [degrees]
23828.773	-37.391	84.116	-10.385	-66.690	-34.555	84.452
24093.812	-37.248	84.387	-10.580	-67.328	-34.394	84.500
24361.800	-37.111	84.515	-10.780	-67.902	-34.222	84.501
24632.768	-36.976	84.675	-10.980	-68.420	-34.044	84.406
24906.750	-36.845	84.873	-11.181	-68.906	-33.866	84.214
25183.779	-36.716	84.982	-11.383	-69.363	-33.695	84.044
25463.889	-36.582	84.900	-11.587	-69.797	-33.527	83.729
25747.116	-36.454	84.881	-11.794	-70.203	-33.357	83.581
26033.492	-36.329	84.919	-12.002	-70.587	-33.183	83.518
26323.054	-36.206	84.880	-12.213	-70.950	-33.001	83.393
26615.836	-36.083	84.824	-12.425	-71.297	-32.808	83.293
26911.875	-35.956	84.872	-12.640	-71.628	-32.611	83.146
27211.207	-35.832	84.805	-12.858	-71.939	-32.412	83.053
27513.867	-35.707	84.672	-13.078	-72.225	-32.204	82.859
27819.895	-35.585	84.622	-13.303	-72.497	-31.988	82.553
28129.326	-35.461	84.548	-13.532	-72.726	-31.767	82.171
28442.199	-35.327	84.409	-13.761	-72.893	-31.551	81.502
28758.552	-35.199	84.261	-13.982	-73.018	-31.365	80.771
29078.423	-35.073	84.146	-14.194	-73.168	-31.214	80.040
29401.853	-34.943	84.094	-14.402	-73.383	-31.084	79.485
29728.880	-34.822	83.906	-14.616	-73.677	-30.951	79.261
30059.544	-34.701	83.824	-14.844	-74.036	-30.790	79.252
30393.886	-34.576	83.717	-15.091	-74.404	-30.596	79.348
30731.947	-34.447	83.582	-15.353	-74.729	-30.357	79.382
31073.768	-34.318	83.626	-15.623	-74.986	-30.095	79.309
31419.391	-34.187	83.601	-15.896	-75.211	-29.814	79.138
31768.858	-34.047	83.524	-16.176	-75.396	-29.513	78.842
32122.212	-33.908	83.375	-16.461	-75.564	-29.198	78.484
32479.496	-33.768	83.125	-16.754	-75.724	-28.870	77.977
32840.755	-33.619	82.981	-17.056	-75.870	-28.525	77.359
33206.031	-33.464	82.767	-17.369	-75.982	-28.162	76.617
33575.371	-33.307	82.598	-17.691	-76.057	-27.776	75.774
33948.818	-33.139	82.411	-18.024	-76.094	-27.364	74.828
34326.419	-32.965	82.128	-18.369	-76.096	-26.919	73.724
34708.220	-32.782	81.867	-18.732	-76.056	-26.442	72.412
35094.268	-32.591	81.417	-19.112	-75.886	-25.929	70.832
35484.610	-32.402	80.893	-19.495	-75.511	-25.371	68.887
35879.293	-32.227	80.299	-19.855	-75.008	-24.763	66.554
36278.366	-32.067	79.704	-20.197	-74.562	-24.100	63.632
36681.878	-31.912	79.218	-20.538	-74.307	-23.377	59.955

Frequency [Hz]	$\lvert H_1H_2\rvert$ [dB]	$\angle H_1H_2$ [degrees]	$\lvert X_1X_2\rvert$ [dB]	$\angle X_1X_2$ [degrees]	$\lvert H_1X_2\rvert$ [dB]	$\angle H_1X_2$ [degrees]
37089.878	-31.737	78.772	-20.903	-74.292	-22.602	55.238
37502.416	-31.530	78.379	-21.313	-74.420	-21.792	49.034
37919.543	-31.275	77.874	-21.780	-74.539	-21.014	40.888
38341.309	-30.985	77.141	-22.292	-74.462	-20.401	30.462
38767.766	-30.664	76.146	-22.837	-74.195	-20.128	17.976
39198.967	-30.320	74.716	-23.415	-73.773	-20.341	4.367
39634.964	-29.944	72.820	-24.033	-73.206	-21.085	-8.986
40075.810	-29.534	70.260	-24.692	-72.456	-22.287	-20.760
40521.559	-29.089	66.720	-25.396	-71.498	-23.797	-30.192
40972.267	-28.655	61.635	-26.159	-70.259	-25.448	-37.197
41427.987	-28.377	54.315	-26.980	-68.667	-27.130	-42.132
41888.777	-28.508	44.951	-27.862	-66.630	-28.799	-45.519
42354.691	-29.298	35.034	-28.819	-64.065	-30.455	-47.688
42825.788	-30.812	27.309	-29.862	-60.790	-32.113	-48.811
43302.125	-32.799	24.514	-31.012	-56.518	-33.794	-48.937
43783.760	-34.771	27.781	-32.281	-50.714	-35.516	-48.006
44270.751	-36.246	35.917	-33.618	-42.486	-37.296	-45.859
44763.160	-36.978	46.155	-34.845	-31.044	-39.151	-42.144
45261.045	-37.036	55.716	-35.690	-16.519	-41.082	-36.133
45764.468	-36.679	63.042	-35.929	-0.225	-42.971	-26.833
46273.491	-36.172	68.004	-35.490	15.803	-44.561	-13.827
46788.175	-35.669	71.267	-34.493	29.662	-45.562	2.012
47308.584	-35.212	73.501	-33.184	40.352	-45.809	18.659
47834.782	-34.798	75.089	-31.804	48.002	-45.346	33.809
48366.832	-34.417	76.197	-30.496	53.431	-44.397	45.816
48904.799	-34.066	76.860	-29.299	57.367	-43.259	54.182
49448.751	-33.764	77.135	-28.213	60.246	-42.179	59.543
49998.752	-33.522	77.189	-27.235	62.382	-41.265	63.054
50554.871	-33.337	77.232	-26.354	64.029	-40.519	65.628
51117.176	-33.191	77.441	-25.553	65.389	-39.900	67.853
51685.735	-33.053	77.870	-24.808	66.582	-39.350	70.009
52260.618	-32.897	78.431	-24.102	67.642	-38.820	72.088
52841.895	-32.716	78.965	-23.426	68.542	-38.286	73.921
53429.637	-32.522	79.360	-22.777	69.248	-37.762	75.358
54023.917	-32.331	79.621	-22.164	69.777	-37.266	76.442
54624.807	-32.146	79.784	-21.579	70.162	-36.803	77.266
55232.380	-31.969	79.880	-21.017	70.430	-36.373	77.861
55846.711	-31.800	79.935	-20.477	70.607	-35.980	78.287
56467.875	-31.637	79.964	-19.959	70.709	-35.623	78.618
57095.947	-31.478	79.973	-19.464	70.749	-35.297	78.924

Frequency [Hz]	$\lvert H_1H_2\rvert$ [dB]	$\angle H_1H_2$ [degrees]	$\lvert X_1X_2\rvert$ [dB]	$\angle X_1X_2$ [degrees]	$\lvert H_1X_2\rvert$ [dB]	$\angle H_1X_2$ [degrees]
57731.006	-31.323	79.969	-18.990	70.734	-34.992	79.255
58373.129	-31.171	79.938	-18.538	70.674	-34.696	79.599
59022.393	-31.022	79.882	-18.101	70.567	-34.405	79.925
59678.879	-30.877	79.805	-17.674	70.420	-34.117	80.178
60342.667	-30.735	79.707	-17.259	70.234	-33.838	80.349
61013.838	-30.596	79.609	-16.855	70.012	-33.572	80.457
61692.474	-30.457	79.480	-16.460	69.756	-33.313	80.521
62378.658	-30.317	79.285	-16.074	69.465	-33.063	80.522
63072.475	-30.186	79.007	-15.697	69.132	-32.826	80.456
63774.008	-30.073	78.689	-15.327	68.765	-32.605	80.349
64483.345	-29.980	78.410	-14.964	68.362	-32.404	80.242
65200.571	-29.901	78.242	-14.608	67.936	-32.217	80.187
65925.775	-29.825	78.219	-14.257	67.490	-32.037	80.211
66659.045	-29.738	78.303	-13.910	67.019	-31.855	80.292
67400.471	-29.634	78.407	-13.566	66.517	-31.666	80.392
68150.143	-29.517	78.480	-13.225	65.980	-31.473	80.465
68908.154	-29.396	78.499	-12.886	65.405	-31.279	80.496
69674.596	-29.272	78.478	-12.550	64.792	-31.087	80.486
70449.563	-29.150	78.425	-12.216	64.141	-30.900	80.440
71233.149	-29.030	78.359	-11.884	63.455	-30.718	80.378
72025.451	-28.909	78.276	-11.553	62.729	-30.541	80.312
72826.566	-28.788	78.176	-11.222	61.957	-30.367	80.249
73636.591	-28.670	78.063	-10.891	61.140	-30.195	80.191
74455.626	-28.552	77.929	-10.560	60.269	-30.023	80.133
75283.770	-28.438	77.790	-10.228	59.341	-29.851	80.062
76121.126	-28.327	77.650	-9.897	58.353	-29.680	79.977
76967.795	-28.220	77.498	-9.564	57.302	-29.511	79.878
77823.882	-28.114	77.339	-9.231	56.181	-29.342	79.762
78689.491	-28.010	77.163	-8.896	54.989	-29.175	79.631
79564.727	-27.909	76.980	-8.560	53.717	-29.010	79.485
80449.698	-27.809	76.810	-8.222	52.359	-28.848	79.332
81344.513	-27.710	76.667	-7.881	50.898	-28.685	79.176
82249.280	-27.612	76.561	-7.540	49.330	-28.526	79.028
83164.111	-27.510	76.471	-7.197	47.637	-28.368	78.886
84089.117	-27.404	76.383	-6.856	45.810	-28.213	78.736
85024.412	-27.294	76.282	-6.517	43.850	-28.058	78.571
85970.109	-27.181	76.160	-6.179	41.747	-27.903	78.397
86926.325	-27.068	76.015	-5.844	39.481	-27.746	78.218
87893.177	-26.955	75.850	-5.512	37.032	-27.587	78.036
88870.783	-26.843	75.662	-5.186	34.380	-27.424	77.855

Frequency [Hz]	$\lvert H_1H_2\rvert$ [dB]	$\angle H_1H_2$ [degrees]	$\lvert X_1X_2\rvert$ [dB]	$\angle X_1X_2$ [degrees]	$\lvert H_1X_2\rvert$ [dB]	$\angle H_1X_2$ [degrees]
89859.263	-26.731	75.463	-4.869	31.505	-27.260	77.671
90858.737	-26.618	75.244	-4.567	28.391	-27.092	77.468
91869.327	-26.507	74.986	-4.286	25.039	-26.921	77.237
92891.159	-26.401	74.689	-4.030	21.449	-26.749	76.972
93924.355	-26.303	74.361	-3.805	17.626	-26.577	76.674
94969.044	-26.220	74.030	-3.616	13.578	-26.407	76.343
96025.352	-26.149	73.766	-3.469	9.315	-26.241	76.001
97093.409	-26.083	73.615	-3.372	4.853	-26.076	75.678
98173.346	-26.009	73.571	-3.332	0.229	-25.907	75.356
99265.295	-25.921	73.577	-3.356	-4.497	-25.734	75.020
100369.389	-25.818	73.572	-3.444	-9.254	-25.558	74.663
101485.764	-25.706	73.521	-3.597	-13.975	-25.380	74.293
102614.555	-25.590	73.399	-3.811	-18.613	-25.197	73.918
103755.902	-25.479	73.230	-4.082	-23.131	-25.007	73.539
104909.944	-25.369	73.043	-4.409	-27.481	-24.806	73.143
106076.821	-25.260	72.839	-4.788	-31.623	-24.592	72.697
107256.677	-25.154	72.621	-5.212	-35.519	-24.368	72.170
108449.657	-25.051	72.389	-5.674	-39.150	-24.136	71.563
109655.906	-24.951	72.162	-6.166	-42.522	-23.896	70.866
110875.571	-24.854	71.951	-6.684	-45.653	-23.648	70.072
112108.802	-24.757	71.757	-7.224	-48.547	-23.389	69.170
113355.750	-24.657	71.583	-7.783	-51.213	-23.119	68.143
114616.567	-24.553	71.409	-8.361	-53.649	-22.836	66.965
115891.408	-24.445	71.220	-8.952	-55.872	-22.541	65.617
117180.429	-24.335	70.998	-9.557	-57.902	-22.229	64.066
118483.787	-24.226	70.747	-10.176	-59.758	-21.896	62.252
119801.642	-24.118	70.471	-10.810	-61.448	-21.544	60.081
121134.155	-24.013	70.167	-11.460	-62.976	-21.169	57.430
122481.489	-23.914	69.849	-12.127	-64.335	-20.774	54.127
123843.809	-23.821	69.547	-12.812	-65.544	-20.376	49.964
125221.281	-23.730	69.280	-13.516	-66.610	-20.010	44.691
126614.075	-23.637	69.050	-14.245	-67.536	-19.735	38.051
128022.360	-23.538	68.834	-15.004	-68.308	-19.661	29.936
129446.309	-23.431	68.600	-15.796	-68.904	-19.921	20.618
130886.096	-23.319	68.314	-16.626	-69.311	-20.624	10.830
132341.898	-23.207	67.959	-17.495	-69.516	-21.823	1.674
133813.892	-23.097	67.511	-18.419	-69.487	-23.509	-5.652
135302.258	-23.002	66.968	-19.412	-69.184	-25.625	-9.860
136807.179	-22.932	66.403	-20.485	-68.509	-28.015	-9.429
138328.838	-22.887	65.940	-21.647	-67.348	-30.355	-3.269

Frequency [Hz]	$\lvert H_1H_2\rvert$ [dB]	$\angle H_1H_2$ [degrees]	$\lvert X_1X_2\rvert$ [dB]	$\angle X_1X_2$ [degrees]	$\lvert H_1X_2\rvert$ [dB]	$\angle H_1X_2$ [degrees]
139867.423	-22.853	65.668	-22.913	-65.568	-32.220	8.221
141423.121	-22.810	65.587	-24.301	-63.011	-33.269	22.912
142996.122	-22.743	65.612	-25.873	-59.345	-33.415	37.745
144586.619	-22.651	65.616	-27.697	-53.264	-32.846	50.038
146194.807	-22.545	65.518	-29.609	-42.748	-31.919	58.529
147820.882	-22.438	65.328	-31.170	-27.053	-30.972	63.659
149465.043	-22.335	65.086	-31.938	-7.798	-30.156	66.725
151127.492	-22.238	64.815	-31.730	11.871	-29.479	68.733
152808.431	-22.146	64.533	-30.689	28.770	-28.906	70.179
154508.068	-22.060	64.268	-29.198	41.121	-28.411	71.276
156226.608	-21.978	64.047	-27.671	49.190	-27.972	72.142
157964.264	-21.892	63.876	-26.316	54.612	-27.572	72.837
159721.246	-21.798	63.730	-25.107	58.660	-27.198	73.376
161497.771	-21.695	63.569	-23.991	61.659	-26.844	73.782
163294.056	-21.586	63.365	-22.976	63.772	-26.510	74.069
165110.320	-21.476	63.109	-22.059	65.250	-26.199	74.253
166946.786	-21.369	62.819	-21.225	66.270	-25.907	74.351
168803.678	-21.266	62.517	-20.463	66.968	-25.633	74.377
170681.224	-21.164	62.218	-19.764	67.431	-25.375	74.351
172579.653	-21.063	61.919	-19.122	67.719	-25.130	74.286
174499.198	-20.961	61.619	-18.533	67.873	-24.896	74.199
176440.093	-20.858	61.310	-17.989	67.927	-24.671	74.097
178402.576	-20.754	60.982	-17.483	67.903	-24.455	73.965
180386.887	-20.650	60.632	-17.004	67.801	-24.247	73.809
182393.269	-20.547	60.266	-16.554	67.642	-24.046	73.634
184421.967	-20.448	59.899	-16.129	67.436	-23.853	73.439
186473.230	-20.349	59.510	-15.726	67.195	-23.666	73.226
188547.308	-20.249	59.100	-15.342	66.919	-23.486	73.005
190644.456	-20.149	58.684	-14.976	66.611	-23.312	72.774
192764.929	-20.050	58.276	-14.626	66.281	-23.143	72.545
194908.988	-19.953	57.890	-14.290	65.932	-22.979	72.328
197076.894	-19.857	57.515	-13.967	65.564	-22.817	72.108
199268.913	-19.763	57.162	-13.655	65.183	-22.656	71.889
201485.313	-19.667	56.794	-13.355	64.779	-22.497	71.653
203726.366	-19.568	56.400	-13.065	64.346	-22.339	71.407
205992.345	-19.470	56.003	-12.785	63.895	-22.184	71.139
208283.527	-19.374	55.595	-12.514	63.440	-22.032	70.878
210600.194	-19.278	55.175	-12.251	62.978	-21.882	70.613
212942.628	-19.183	54.754	-11.996	62.506	-21.734	70.336
215311.117	-19.088	54.315	-11.747	62.024	-21.588	70.057

Frequency [Hz]	$\lvert H_1H_2\rvert$ [dB]	$\angle H_1H_2$ [degrees]	$\lvert X_1X_2\rvert$ [dB]	$\angle X_1X_2$ [degrees]	$\lvert H_1X_2\rvert$ [dB]	$\angle H_1X_2$ [degrees]
217705.949	-18.993	53.875	-11.504	61.527	-21.445	69.787
220127.418	-18.898	53.420	-11.267	61.013	-21.302	69.502
222575.820	-18.804	52.965	-11.035	60.495	-21.160	69.211
225051.455	-18.711	52.506	-10.810	59.967	-21.020	68.921
227554.626	-18.619	52.032	-10.589	59.425	-20.881	68.627
230085.638	-18.526	51.554	-10.373	58.878	-20.741	68.310
232644.803	-18.435	51.069	-10.161	58.315	-20.607	67.989
235232.432	-18.343	50.570	-9.953	57.734	-20.471	67.669
237848.842	-18.252	50.080	-9.749	57.152	-20.332	67.335
240494.353	-18.162	49.586	-9.548	56.551	-20.189	66.986
243169.290	-18.073	49.085	-9.351	55.946	-20.047	66.642
245873.979	-17.984	48.568	-9.158	55.321	-19.908	66.314
248608.752	-17.896	48.042	-8.968	54.682	-19.772	65.976
251373.942	-17.808	47.502	-8.782	54.034	-19.641	65.636
254169.889	-17.721	46.951	-8.599	53.373	-19.513	65.293
256996.934	-17.634	46.388	-8.420	52.714	-19.381	64.935
259855.423	-17.548	45.822	-8.244	52.050	-19.251	64.566
262745.707	-17.464	45.251	-8.070	51.378	-19.120	64.191
265668.138	-17.379	44.671	-7.898	50.711	-18.990	63.825
268623.074	-17.296	44.089	-7.726	50.030	-18.859	63.447
271610.877	-17.214	43.495	-7.555	49.346	-18.729	63.066
274631.912	-17.133	42.880	-7.385	48.645	-18.598	62.675
277686.549	-17.053	42.260	-7.216	47.921	-18.467	62.281
280775.162	-16.974	41.635	-7.047	47.187	-18.336	61.876
283898.129	-16.898	41.007	-6.880	46.433	-18.204	61.457
287055.831	-16.822	40.365	-6.713	45.659	-18.073	61.023
290248.655	-16.749	39.698	-6.547	44.858	-17.942	60.595
293476.992	-16.677	39.027	-6.381	44.030	-17.811	60.154
296741.237	-16.607	38.333	-6.215	43.172	-17.679	59.705
300041.788	-16.541	37.631	-6.051	42.286	-17.547	59.234
303379.051	-16.478	36.918	-5.887	41.374	-17.414	58.761
306753.433	-16.420	36.193	-5.724	40.435	-17.281	58.258
310165.347	-16.367	35.456	-5.561	39.448	-17.148	57.741
313615.210	-16.320	34.723	-5.399	38.420	-17.014	57.213
317103.445	-16.280	33.989	-5.238	37.350	-16.879	56.661
320630.479	-16.250	33.271	-5.077	36.226	-16.746	56.075
324196.743	-16.233	32.577	-4.918	35.041	-16.613	55.456
327802.673	-16.228	31.967	-4.760	33.790	-16.484	54.795
331448.710	-16.233	31.509	-4.606	32.464	-16.360	54.104
335135.301	-16.234	31.261	-4.456	31.061	-16.244	53.381

Frequency [Hz]	$\lvert H_1H_2\rvert$ [dB]	$\angle H_1H_2$ [degrees]	$\lvert X_1X_2\rvert$ [dB]	$\angle X_1X_2$ [degrees]	$\lvert H_1X_2\rvert$ [dB]	$\angle H_1X_2$ [degrees]
338862.897	-16.211	31.217	-4.311	29.586	-16.137	52.673
342631.953	-16.149	31.267	-4.170	28.031	-16.037	52.001
346442.932	-16.043	31.263	-4.032	26.371	-15.937	51.395
350296.299	-15.902	31.071	-3.897	24.574	-15.831	50.825
354192.525	-15.748	30.609	-3.767	22.594	-15.716	50.260
358132.088	-15.599	29.911	-3.650	20.377	-15.592	49.647
362115.469	-15.469	29.042	-3.556	17.880	-15.463	48.943
366143.156	-15.360	28.073	-3.500	15.056	-15.336	48.139
370215.642	-15.269	27.067	-3.505	11.882	-15.217	47.211
374333.424	-15.192	26.052	-3.600	8.368	-15.113	46.177
378497.007	-15.125	25.048	-3.830	4.618	-15.034	45.034
382706.901	-15.067	24.048	-4.245	0.921	-15.000	43.831
386963.619	-15.016	23.062	-4.883	-2.120	-15.026	42.764
391267.684	-14.970	22.084	-5.714	-3.627	-15.103	42.106
395619.621	-14.927	21.100	-6.617	-2.858	-15.187	42.054
400019.963	-14.887	20.110	-7.404	0.331	-15.223	42.581
404469.249	-14.851	19.109	-7.905	5.289	-15.169	43.413
408968.022	-14.820	18.081	-8.041	10.826	-15.020	44.205
413516.834	-14.796	17.027	-7.851	15.766	-14.803	44.651
418116.241	-14.781	15.950	-7.455	19.400	-14.559	44.686
422766.806	-14.774	14.864	-6.982	21.651	-14.317	44.386
427469.097	-14.775	13.770	-6.516	22.836	-14.089	43.876
432223.690	-14.784	12.670	-6.087	23.298	-13.872	43.234
437031.167	-14.802	11.559	-5.700	23.287	-13.666	42.519
441892.116	-14.831	10.436	-5.353	22.950	-13.468	41.741
446807.131	-14.870	9.291	-5.041	22.390	-13.278	40.925
451776.815	-14.921	8.135	-4.758	21.672	-13.092	40.073
456801.774	-14.986	6.964	-4.502	20.837	-12.910	39.184
461882.625	-15.068	5.788	-4.269	19.932	-12.730	38.250
467019.988	-15.167	4.596	-4.055	18.971	-12.551	37.284
472214.492	-15.289	3.394	-3.858	17.963	-12.373	36.287
477466.773	-15.436	2.189	-3.677	16.923	-12.194	35.254
482777.473	-15.612	0.986	-3.508	15.860	-12.015	34.179
488147.243	-15.824	-0.201	-3.351	14.777	-11.835	33.062
493576.738	-16.080	-1.348	-3.206	13.680	-11.652	31.894
499066.624	-16.388	-2.430	-3.070	12.574	-11.468	30.664
504617.572	-16.761	-3.392	-2.945	11.463	-11.282	29.366
510230.262	-17.215	-4.160	-2.830	10.358	-11.093	27.993
515905.379	-17.761	-4.607	-2.725	9.270	-10.902	26.534
521643.619	-18.426	-4.612	-2.628	8.214	-10.707	24.982

Frequency [Hz]	$\lvert H_1H_2\rvert$ [dB]	$\angle H_1H_2$ [degrees]	$\lvert X_1X_2\rvert$ [dB]	$\angle X_1X_2$ [degrees]	$\lvert H_1X_2\rvert$ [dB]	$\angle H_1X_2$ [degrees]
527445.683	-19.271	-4.014	-2.539	7.198	-10.507	23.320
533312.282	-20.413	-1.822	-2.456	6.233	-10.298	21.513
539244.133	-21.773	4.335	-2.376	5.320	-10.080	19.503
545241.961	-22.913	16.045	-2.300	4.458	-9.852	17.209
551306.502	-23.265	32.198	-2.230	3.662	-9.615	14.554
557438.496	-22.495	49.307	-2.174	3.018	-9.352	11.380
563638.695	-20.685	63.177	-2.116	2.738	-9.057	6.845
569907.856	-18.293	70.935	-1.995	2.818	-8.991	-0.085
576246.747	-15.908	72.314	-1.788	2.883	-9.534	-7.640
582656.143	-13.930	69.426	-1.516	2.746	-10.644	-12.414
589136.829	-12.397	64.714	-1.182	2.312	-11.903	-12.432
595689.597	-11.194	59.266	-0.787	1.401	-12.815	-8.207
602315.250	-10.248	53.472	-0.357	-0.226	-13.072	-2.278
609014.597	-9.520	47.593	0.066	-2.753	-12.712	2.115
615788.459	-8.976	41.829	0.411	-6.248	-12.117	2.908
622637.664	-8.588	36.366	0.584	-10.427	-11.750	0.779
629563.051	-8.324	31.353	0.533	-14.437	-11.746	-1.834
636565.466	-8.144	26.880	0.335	-17.394	-11.973	-3.579
643645.767	-8.010	22.907	0.125	-19.115	-12.311	-3.901
650804.820	-7.899	19.305	0.000	-19.949	-12.610	-2.588
658043.500	-7.804	15.959	0.002	-20.483	-12.727	-0.095
665362.694	-7.728	12.810	0.110	-21.226	-12.595	2.653
672763.296	-7.671	9.858	0.268	-22.401	-12.253	4.757
680246.213	-7.628	7.118	0.438	-23.940	-11.802	5.768
687812.360	-7.592	4.579	0.611	-25.728	-11.337	5.758
695462.663	-7.556	2.216	0.791	-27.749	-10.903	5.039
703198.057	-7.516	-0.009	0.980	-30.038	-10.510	3.859
711019.490	-7.471	-2.125	1.180	-32.694	-10.153	2.355
718927.917	-7.420	-4.155	1.382	-35.833	-9.830	0.594
726924.307	-7.363	-6.120	1.573	-39.629	-9.539	-1.383
735009.639	-7.297	-8.042	1.715	-44.288	-9.281	-3.544
743184.901	-7.222	-9.940	1.737	-50.042	-9.058	-5.858
751451.093	-7.138	-11.834	1.509	-56.837	-8.871	-8.304
759809.228	-7.043	-13.747	0.871	-63.904	-8.725	-10.851
768260.327	-6.936	-15.707	-0.247	-69.379	-8.629	-13.480
776805.425	-6.815	-17.747	-1.668	-71.119	-8.603	-16.184
785445.567	-6.666	-19.973	-2.997	-68.270	-8.714	-18.664
794181.810	-6.497	-22.730	-3.839	-61.994	-8.961	-19.694
803015.224	-6.397	-26.269	-4.009	-54.767	-9.078	-18.322
811946.889	-6.468	-30.048	-3.588	-49.179	-8.732	-15.765

Frequency [Hz]	$\lvert H_1H_2\rvert$ [dB]	$\angle H_1H_2$ [degrees]	$\lvert X_1X_2\rvert$ [dB]	$\angle X_1X_2$ [degrees]	$\lvert H_1X_2\rvert$ [dB]	$\angle H_1X_2$ [degrees]
820977.898	-6.686	-33.084	-2.862	-46.876	-7.848	-14.735
830109.355	-6.880	-35.008	-2.191	-47.936	-6.666	-17.665
839342.379	-6.889	-37.371	-1.811	-50.998	-5.671	-25.571
848678.098	-7.122	-42.096	-1.769	-54.476	-5.387	-36.359
858117.655	-8.010	-45.761	-1.992	-57.088	-5.868	-45.933
867662.206	-9.202	-44.268	-2.322	-58.089	-6.701	-51.858
877312.917	-10.014	-37.105	-2.572	-57.528	-7.464	-54.664
887070.970	-9.915	-27.125	-2.612	-56.318	-8.017	-55.878
896937.558	-8.818	-18.890	-2.462	-55.640	-8.352	-56.459
906913.889	-7.151	-16.124	-2.257	-56.023	-8.493	-57.170
917001.183	-5.622	-19.316	-2.118	-57.188	-8.511	-58.445
927200.675	-4.697	-25.027	-2.087	-58.478	-8.436	-60.242
937513.612	-4.118	-29.623	-2.125	-59.342	-8.242	-63.089
947941.257	-3.538	-33.752	-2.161	-59.621	-8.041	-67.727
958484.884	-2.984	-38.182	-2.131	-59.463	-7.987	-74.079
969145.785	-2.471	-42.737	-2.007	-59.219	-8.173	-81.720
979925.263	-1.950	-47.321	-1.802	-59.207	-8.684	-90.183
990824.638	-1.358	-52.154	-1.542	-59.565	-9.705	-98.844
1001845.243	-0.650	-57.840	-1.244	-60.366	-9.624	-98.668
1012988.427	0.158	-65.354	-0.931	-61.674	-11.544	-129.042
1024255.552	0.922	-75.790	-0.632	-63.459	-16.326	-146.536
1035647.997	1.359	-89.506	-0.361	-65.582	-21.610	-136.747
1047167.157	1.163	-105.474	-0.113	-67.946	-25.130	-103.041
1058814.441	0.163	-121.547	0.115	-70.559	-25.618	-58.666
1070591.273	-1.603	-135.253	0.321	-73.445	-23.135	-20.303
1082499.095	-3.940	-144.798	0.502	-76.609	-19.049	-1.996
1094539.364	-6.606	-148.980	0.653	-80.093	-15.655	-8.492
1106713.552	-9.288	-146.873	0.761	-83.979	-14.965	-27.649
1119023.150	-11.560	-138.497	0.793	-88.453	-14.323	-22.630
1131469.664	-13.007	-125.557	0.645	-93.474	-13.299	-24.632
1144054.615	-13.404	-111.127	0.221	-98.113	-12.403	-27.129
1156779.545	-12.845	-98.633	-0.424	-100.981	-11.606	-30.387
1169646.010	-11.694	-90.259	-1.071	-101.269	-10.963	-34.220
1182655.584	-10.366	-86.097	-1.464	-99.375	-10.484	-37.907
1195809.859	-9.075	-84.696	-1.438	-96.727	-10.043	-40.530
1209110.445	-7.757	-84.885	-1.004	-95.120	-9.283	-42.492
1222558.968	-6.267	-87.106	-0.336	-95.860	-8.051	-47.422
1236157.075	-4.644	-92.961	0.329	-99.166	-6.862	-58.996
1249906.429	-3.183	-103.547	0.836	-104.412	-6.658	-76.782
1263808.713	-2.285	-118.439	1.121	-110.917	-8.120	-94.781

Frequency [Hz]	$\lvert H_1H_2\rvert$ [dB]	$\angle H_1H_2$ [degrees]	$\lvert X_1X_2\rvert$ [dB]	$\angle X_1X_2$ [degrees]	$\lvert H_1X_2\rvert$ [dB]	$\angle H_1X_2$ [degrees]
1277865.627	-2.240	-118.838	1.157	-118.131	-10.991	-104.769
1292078.891	-3.081	-176.014	0.934	-125.604	-14.153	-102.162
1306450.244	-4.599	-214.397	0.452	-132.978	-16.335	-88.900
1320981.445	-6.473	-129.743	-0.323	-140.080	-16.879	-72.011
1335674.272	-8.440	-23.624	-1.512	-146.179	-16.097	-58.652
1350530.521	-10.402	40.889	-3.128	-149.012	-14.769	-51.262
1365552.012	-12.380	36.296	-4.817	-146.399	-13.483	-48.509
1380740.582	-14.405	-32.455	-6.020	-138.463	-12.415	-47.899
1396098.089	-16.368	-131.480	-6.311	-127.920	-11.465	-48.127
1411626.413	-17.950	-202.393	-5.628	-118.725	-10.556	-49.052
1427327.453	-18.766	-166.183	-4.301	-114.123	-9.665	-50.626
1443203.130	-18.574	-115.368	-2.866	-115.090	-8.774	-52.835
1459255.386	-17.402	-114.128	-1.743	-120.087	-7.866	-55.685
1475486.187	-15.524	-103.851	-1.026	-126.824	-6.922	-59.184
1491897.517	-13.246	-98.349	-0.613	-134.144	-5.910	-63.558
1508491.385	-10.705	-97.658	-0.442	-141.684	-4.785	-69.352
1525269.821	-8.061	-86.361	-0.485	-132.612	-3.582	-77.770
1542234.877	-5.735	-139.449	-0.712	-180.834	-2.524	-89.929
1559388.631	-4.259	-165.868	-1.076	-196.286	-1.992	-105.699
1576733.179	-3.970	-132.995	-1.501	-150.002	-2.307	-122.761
1594270.645	-4.787	-47.898	-2.027	-54.140	-3.413	-137.843
1612003.174	-6.316	42.395	-2.864	58.719	-4.977	-149.497
1629932.937	-8.119	174.384	-3.987	152.017	-6.839	-157.986
1648062.125	-9.841	245.929	-5.157	197.983	-8.942	-162.371
1666392.959	-11.147	146.939	-6.108	190.444	-10.985	-161.569
1684927.680	-11.813	5.567	-6.673	157.009	-12.545	-156.142
1703668.557	-11.824	-44.162	-6.853	169.939	-13.303	-148.334
1722617.882	-11.369	-37.874	-6.915	166.574	-13.177	-141.420
1741777.974	-10.752	32.450	-7.291	160.463	-12.422	-122.119
1761151.177	-10.207	175.002	-7.330	163.550	-12.208	-162.573
1780739.861	-10.142	170.865	-10.524	135.687	-9.939	-156.895
1800546.424	-9.756	167.102	-11.689	135.368	-10.881	-106.933
1820573.289	-9.227	162.630	-12.061	147.931	-13.399	-44.782
1840822.905	-8.710	156.694	-12.570	161.056	-16.161	4.599
1861297.751	-8.332	148.903	-13.790	165.103	-18.169	24.332
1882000.332	-8.189	139.280	-15.900	153.461	-18.814	6.644
1902933.181	-8.342	128.307	-18.639	122.938	-17.915	-46.039
1924098.858	-8.810	116.979	-21.249	74.169	-15.775	-119.911
1945499.954	-9.571	106.856	-22.426	12.062	-13.236	-188.521
1967139.088	-10.549	100.126	-20.261	-53.726	-11.735	-211.410

A.2 State-Space Model Matrices

A.2.1 Pole Matrix A

Matrix A is a diagonal matrix.

$$A_{40x40} = \begin{bmatrix} a_{1,1} & 0 & \cdots & 0 \\ 0 & \ddots & & \vdots \\ \vdots & & \ddots & 0 \\ 0 & \cdots & 0 & a_{40,40} \end{bmatrix} \tag{A.1}$$

Table A.2: Comparisons between different test methods.

i	$a_{i,i}$	i	$a_{i,i}$
1	-11.642 +0.000i	21	-11.642 +0.000i
2	-384.221 +0.000i	22	-384.221 +0.000i
3	-4249.868 +0.000i	23	-4249.868 +0.000i
4	-2277211.337 +0.000i	24	-2277211.337 +0.000i
5	-65.983 +1565.665i	25	-65.983 +1565.665i
6	-65.983 -1565.665i	26	-65.983 -1565.665i
7	-4045.677 +59259.978i	27	-4045.677 +59259.978i
8	-4045.677 -59259.978i	28	-4045.677 -59259.978i
9	-10966.710+247385.399i	29	-10966.710+247385.399i
10	-10966.710-247385.399i	30	-10966.710-247385.399i
11	-35779.599+627531.804i	31	-35779.599+627531.804i
12	-35779.599-627531.804i	32	-35779.599-627531.804i
13	-1341364.345+1794830.151i	33	-1341364.345+1794830.151i
14	-1341364.345-1794830.151i	34	-1341364.345-1794830.151i
15	-1221063.949+5413959.158i	35	-1221063.949+5413959.158i
16	-1221063.949-5413959.158i	36	-1221063.949-5413959.158i
17	-1021423.357+7581616.126i	37	-1021423.357+7581616.126i
18	-1021423.357-7581616.126i	38	-1021423.357-7581616.126i
19	-6324.528+11365932.147i	39	-6324.528+11365932.147i
20	-6324.528-11365932.147i	40	-6324.528-11365932.147i

A.2.2 Residue Matrix C

$$C_{2x40} = \begin{bmatrix} C_{11}^{1} & C_{11}^{2} & \cdots & C_{11}^{20} & C_{12}^{1} & C_{12}^{2} & \cdots & C_{12}^{20} \\ C_{21}^{1} & C_{21}^{2} & \cdots & C_{21}^{20} & C_{22}^{1} & C_{22}^{2} & \cdots & C_{22}^{20} \end{bmatrix} \tag{A.2}$$

(See next page.)

Table A.3: Elements of residue matrix C

C_{11}^{1}	0.031 +0.000i	C_{21}^{1}	1.230 +0.000i
C_{11}^{2}	0.004 +0.000i	C_{21}^{2}	0.921 +0.000i
C_{11}^{3}	0.005 +0.000i	C_{21}^{3}	1.456 +0.000i
C_{11}^{4}	-19736.461 +0.000i	C_{21}^{4}	8708.877 +0.000i
C_{11}^{5}	0.007 +0.001i	C_{21}^{5}	0.010 -0.005i
C_{11}^{6}	0.007 -0.001i	C_{21}^{6}	0.010 +0.005i
C_{11}^{7}	0.057 +0.149i	C_{21}^{7}	434.519 +39.055i
C_{11}^{8}	0.057 -0.149i	C_{21}^{8}	434.519 -39.055i
C_{11}^{9}	26.389 +0.888i	C_{21}^{9}	17.659 -2.548i
C_{11}^{10}	26.389 -0.888i	C_{21}^{10}	17.659 +2.548i
C_{11}^{11}	3.312 +17.254i	C_{21}^{11}	1185.733 +11.693i
C_{11}^{12}	3.312 -17.254i	C_{21}^{12}	1185.733 -11.693i
C_{11}^{13}	-3619.192 -1765.294i	C_{21}^{13}	-11643.082 +26693.317i
C_{11}^{14}	-3619.192 +1765.294i	C_{21}^{14}	-11643.082 -26693.317i
C_{11}^{15}	11875.473 -25808.406i	C_{21}^{15}	-20118.151 -39249.153i
C_{11}^{16}	11875.473 +25808.406i	C_{21}^{16}	-20118.151 +39249.153i
C_{11}^{17}	6819.896 +1468.434i	C_{21}^{17}	3004.104 -15015.634i
C_{11}^{18}	6819.896 -1468.434i	C_{21}^{18}	3004.104 +15015.634i
C_{11}^{19}	-46.036 +10.954i	C_{21}^{19}	-12.765 +183.955i
C_{11}^{20}	-46.036 -10.954i	C_{21}^{20}	-12.765 -183.955i
C_{12}^{1}	0.031 +0.000i	C_{22}^{1}	1.230 +0.000i
C_{12}^{2}	0.004 +0.000i	C_{22}^{2}	0.921 +0.000i
C_{12}^{3}	0.005 +0.000i	C_{22}^{3}	1.456 +0.000i
C_{12}^{4}	-19736.461 +0.000i	C_{22}^{4}	8708.877 +0.000i
C_{12}^{5}	0.007 +0.001i	C_{22}^{5}	0.010 -0.005i
C_{12}^{6}	0.007 -0.001i	C_{22}^{6}	0.010 +0.005i
C_{12}^{7}	0.057 +0.149i	C_{22}^{7}	434.519 +39.055i
C_{12}^{8}	0.057 -0.149i	C_{22}^{8}	434.519 -39.055i
C_{12}^{9}	26.389 +0.888i	C_{22}^{9}	17.659 -2.548i
C_{12}^{10}	26.389 -0.888i	C_{22}^{10}	17.659 +2.548i
C_{12}^{11}	3.312 +17.254i	C_{22}^{11}	1185.733 +11.693i
C_{12}^{12}	3.312 -17.254i	C_{22}^{12}	1185.733 -11.693i
C_{12}^{13}	-3619.192 -1765.294i	C_{22}^{13}	-11643.082 +26693.317i
C_{12}^{14}	-3619.192 +1765.294i	C_{22}^{14}	-11643.082 -26693.317i
C_{12}^{15}	11875.473 -25808.406i	C_{22}^{15}	-20118.151 -39249.153i
C_{12}^{16}	11875.473 +25808.406i	C_{22}^{16}	-20118.151 +39249.153i
C_{12}^{17}	6819.896 +1468.434i	C_{22}^{17}	3004.104 -15015.634i
C_{12}^{18}	6819.896 -1468.434i	C_{22}^{18}	3004.104 +15015.634i
C_{12}^{19}	-46.036 +10.954i	C_{22}^{19}	-12.765 +183.955i
C_{12}^{20}	-46.036 -10.954i	C_{22}^{20}	-12.765 -183.955i

A.2.3 B Matrix and Constant Matrices D and E

$$B_{2x40}^{T} = \begin{bmatrix} \underbrace{11\cdots1}_{20} & \underbrace{00\cdots0}_{20} \\ \underbrace{00\cdots0}_{20} & \underbrace{11\cdots1}_{20} \end{bmatrix} \tag{A.3}$$

$$D_{2x2} = \begin{bmatrix} -4.738155170604688e-04 & -0.001648712221808 \\ -0.001648712221808 & 0.005290792492251 \end{bmatrix}$$

$$E_{2x2} = \begin{bmatrix} 2.444506942044341e-10 & 5.900800067528392e-11 \\ 5.900800067528392e-11 & -2.445051413268630e-10 \end{bmatrix}$$

A.3 The Crossover Frequencies from Hamiltonian Matrix

(See next page.)

Table A.4: The eigenvalues of Hamiltonian matrix. When the real part of the eigenvalues is zero, the imaginary part is the crossover frequency ω.

$eig(M)$	$eig(M)$
-10655591.1232316 -0.0000000i	-248704.6278689-305268.2247983i
10655591.1232316 -0.0000000i	248704.6278689-305268.2247982i
0.0000000+12301677.3579358i	60911.6303040+256703.6010327i
0.0000000-12301677.3579358i	60911.6303040-256703.6010327i
-0.0000000+11556862.3421968i	-60911.6303040+256703.6010327i
0.0000000+11149229.9278811i	-60911.6303040-256703.6010327i
-0.0000000-11556862.3421968i	203601.8583899 -0.0000000i
0.0000000-11149229.9278812i	-203601.8583899 +0.0000000i
-656.6342543+11367233.6050659i	-14521.8525346+246686.0834245i
656.6342543+11367233.6050659i	14521.8525346+246686.0834245i
-656.6342543-11367233.6050659i	-14521.8525346-246686.0834245i
656.6342543-11367233.6050659i	14521.8525346-246686.0834245i
-0.0000000+8190924.0618777i	0.0000000+56169.7726696i
0.0000000-8190924.0618777i	0.0000000-56169.7726696i
-971522.5586750+7349039.3976497i	-0.0000000+35517.7655118i
971522.5586750+7349039.3976497i	-0.0000000-35517.7655118i
-971522.5586750-7349039.3976497i	30100.7595986 -0.0000000i
971522.5586750-7349039.3976497i	-30100.7595986 -0.0000000i
-0.0000000+6977719.5700143i	-0.0000000+14045.6541871i
-0.0000000-6977719.5700143i	0.0000000-14045.6541871i
-5137700.5558921 +0.0000000i	8702.4043480 +0.0000000i
-0.0000000+6130117.5606055i	-8702.4043480 +0.0000000i
5137700.5558921 -0.0000000i	0.0000000+6212.4388810i
-0.0000000-6130117.5606055i	-0.0000000-6212.4388810i
0.0000000-5450557.1392844i	1526.6780634 +0.0000000i
0.0000000+5450557.1392844i	-1526.6780634 +0.0000000i
990375.6894809+1643763.9931673i	300.4340542+1245.8145231i
-990375.6894809+1643763.9931673i	-300.4340542+1245.8145231i
990375.6894809-1643763.9931673i	-68.1806462+1573.4921353i
-990375.6894809-1643763.9931673i	68.1806462+1573.4921353i
177247.9807524+904445.5782856i	300.4340542-1245.8145231i
-177247.9807524+904445.5782856i	-300.4340542-1245.8145231i
177247.9807524-904445.5782856i	-68.1806462-1573.4921353i
-177247.9807524-904445.5782856i	68.1806462-1573.4921353i
36390.0687543+609209.2004207i	1286.7686065 -0.0000000i
-36390.0687543+609209.2004207i	-1286.7686065 -0.0000000i
36390.0687543-609209.2004207i	-169.4496563 +0.0000000i
-36390.0687543-609209.2004207i	169.4496563 -0.0000000i
-248704.6278689+305268.2247983i	-73.7391235 +0.0000000i
248704.6278689+305268.2247983i	73.7391235 -0.0000000i

A.4 Singularity test matrix (S-matrix and T-matrix)

Table A.5: The square root of eigenvalues of S-matrix. When the imaginary part of the square root of eigenvalues of S-matrix is zero, the real part is the crossover frequency ω.

$\sqrt{eig(S)}$	$\sqrt{eig(S)}$
0.0000000-10655591.1232316i	305268.2247982-248704.6278688i
12301677.3579357 +0.0000000i	0.0000000+203601.8583899i
11556862.3421968 -0.0000000i	256703.6010327+60911.6303039i
11149229.9278811 +0.0000000i	256703.6010326-60911.6303040i
11367233.6050659-656.6342543i	246686.0834245+14521.8525346i
11367233.6050659+656.6342543i	246686.0834245-14521.8525347i
0.0000000+5137700.5558921i	56169.7726695 -0.0000000i
8190924.0618777 +0.0000000i	35517.7655129 -0.0000005i
7349039.3976497+971522.5586750i	0.0000016+30100.7596007i
7349039.3976497-971522.5586750i	14045.6541871 +0.0000000i
6977719.5700143 +0.0000000i	0.0000010-8702.4043468i
6130117.5606055 +0.0000000i	6212.4388810 -0.0000000i
5450557.1392844 -0.0000000i	0.0000025-1526.6780645i
1643763.9931673+990375.6894809i	0.0000000+1286.7686065i
1643763.9931673-990375.6894810i	1245.8145091-300.4340587i
904445.5782856+177247.9807524i	1245.8145302+300.4340592i
904445.5782856-177247.9807524i	1573.4921354-68.1806462i
609209.2004207+36390.0687543i	1573.4921354+68.1806461i
609209.2004207-36390.0687543i	0.0000055+169.4496646i
305268.2247982+248704.6278688i	0.0000001+73.7391234i

Table A.6: The square root of eigenvalues of S-matrix. When the imaginary part of the square root of eigenvalues of T-matrix is zero, the real part is the crossover frequency ω.

$\sqrt{eig(T)}$	$\sqrt{eig(T)}$
0.0000000+10655591.1232316i	305268.2247982-248704.6278689i
12301677.3579357 +0.0000000i	0.0000000-203601.8583899i
11556862.3421968 -0.0000000i	256703.6010327+60911.6303040i
11149229.9278811 +0.0000000i	256703.6010327-60911.6303040i
11367233.6050659+656.6342543i	246686.0834245+14521.8525346i
11367233.6050659-656.6342543i	246686.0834245-14521.8525346i
0.0000000-5137700.5558921i	56169.7726695 +0.0000000i
8190924.0618777 -0.0000000i	35517.7655117 -0.0000003i
7349039.3976497+971522.5586750i	0.0000008+30100.7595980i
7349039.3976497-971522.5586750i	14045.6541871 +0.0000000i
6977719.5700143 -0.0000000i	0.0000000-8702.4043476i
6130117.5606055 -0.0000000i	6212.4388810 -0.0000000i
5450557.1392844 +0.0000000i	0.0000034-1526.6780606i
1643763.9931673+990375.6894809i	0.0000000+1286.7686065i
1643763.9931673-990375.6894809i	1245.8145182-300.4340510i
904445.5782856+177247.9807524i	1245.8145271+300.4340512i
904445.5782856-177247.9807524i	1573.4921353-68.1806462i
609209.2004207+36390.0687543i	1573.4921353+68.1806461i
609209.2004207-36390.0687543i	0.0000026-169.4496455i
305268.2247983+248704.6278688i	0.0000000-73.7391235i

A.5 Proposed Model Circuit Elements

Table A.7: Y_{11} Circuit Elements.

Branches	Y_{11}			
1	$R[\Omega]$			
	1.30388e+04			
2	$C\ [\mu F]$			
	1.5306e-04			
3	$R[\Omega]$		$L[mH]$	
	3.7466e+02		3.21815e+04	
4	$R[\Omega]$		$L[mH]$	
	1.18863e+05		3.09362e+05	
5	$R[\Omega]$		$L[mH]$	
	4.2874e+05		1.00884e+05	
6	$R[\Omega]$		$L[mH]$	
	-93.9262		-0.0412461	
7	$R[\Omega]$	$L[mH]$	$R[\Omega]$	$C\ [\mu F]$
	1.78164e+06	-1.05019e+06	-3.19208e+06	-1.71333e-04
8	$R[\Omega]$	$L[mH]$	$R[\Omega]$	$C\ [\mu F]$
	-1.12506e+06	-9.0615e+03	1.40051e+06	-6.151e-06
9	$R[\Omega]$	$L[mH]$	$R[\Omega]$	$C\ [\mu F]$
	-5.32566e+03	1.18382e+02	1.138008e+05	1.3130962e-04
10	$R[\Omega]$	$L[mH]$	$R[\Omega]$	$C\ [\mu F]$
	-6.92952e+03	-13.3850	1.878235e+04	-1.1933e-04
11	$R[\Omega]$	$L[mH]$	$R[\Omega]$	$C\ [\mu F]$
	-2.7047e+04	0.8635912	2.7174996e+04	1.08223e-06
12	$R[\Omega]$	$L[mH]$	$R[\Omega]$	$C\ [\mu F]$
	-8.4882	0.020455	2.2901e+02	0.00153
13	$R[\Omega]$	$L[mH]$	$R[\Omega]$	$C\ [\mu F]$
	2.7097e+03	0.14713	-3.23564e+03	1.88742e-05
14	$R[\Omega]$	$L[mH]$	$R[\Omega]$	$C\ [\mu F]$
	5.19379e+07	3.55519e+02	-5.22523e+07	1.31011e-10

Table A.8: Y_{12} Circuit Elements.

Branches	Y_{12}			
1	$R[\Omega]$			
	1.130887e+003			
2	$C\ [\mu F]$			
	-1.616804e-005			
3	$R[\Omega]$		$L[mH]$	
	-5.703882e+005		-4.899293e+007	
4	$R[\Omega]$		$L[mH]$	
	2.569958e+006		6.688758e+006	
5	$R[\Omega]$		$L[mH]$	
	-1.654375e+007		-3.892767e+006	
6	$R[\Omega]$		$L[mH]$	
	-1.643320e+002		-7.216369e-002	
7	$R[\Omega]$	$L[mH]$	$R[\Omega]$	$C\ [\mu F]$
	1.5763e+004	6.6744e+004	-1.5884e+006	6.0407e-003
8	$R[\Omega]$	$L[mH]$	$R[\Omega]$	$C\ [\mu F]$
	4.3088e+005	5.6714e+003	-7.2564e+005	2.03e-005
9	$R[\Omega]$	$L[mH]$	$R[\Omega]$	$C\ [\mu F]$
	-1.5526e+002	2.5507e+001	5.5974e+004	6.3757e-004
10	$R[\Omega]$	$L[mH]$	$R[\Omega]$	$C\ [\mu F]$
	2.8096e+004	3.9525e+001	-5.2523e+004	2.9782e-005
11	$R[\Omega]$	$L[mH]$	$R[\Omega]$	$C\ [\mu F]$
	-9.4502e+002	-2.5245e-001	2.1401e+003	-4.4057e-004
12	$R[\Omega]$	$L[mH]$	$R[\Omega]$	$C\ [\mu F]$
	-3.2908e+004	-5.3620e-001	3.3188e+004	-5.1129e-007
13	$R[\Omega]$	$L[mH]$	$R[\Omega]$	$C\ [\mu F]$
	-6.9736e+001	6.4810e-002	1.2858e+003	2.4934e-004
14	$R[\Omega]$	$L[mH]$	$R[\Omega]$	$C\ [\mu F]$
	-9.1899e+006	3.0203e+002	1.0471e+007	3.1372e-009

Table A.9: Y_{22} Circuit Elements.

Branches	Y_{22}			
1	$R[\Omega]$			
	3.156113e+002			
2	$C\ [\mu F]$			
	1.909180e-005			
3	$R[\Omega]$		$L[mH]$	
	9.134427e+000		7.845925e+002	
4	$R[\Omega]$		$L[mH]$	
	4.145413e+002		1.078915e+003	
5	$R[\Omega]$		$L[mH]$	
	1.308013e+004		3.077773e+003	
6	$R[\Omega]$		$L[mH]$	
	-4.338453e+002		-1.905160e-001	
7	$R[\Omega]$	$L[mH]$	$R[\Omega]$	$C\ [\mu F]$
	-6.4489e+005	1.9005e+005	7.7729e+005	3.6496e-004
8	$R[\Omega]$	$L[mH]$	$R[\Omega]$	$C\ [\mu F]$
	1.0418e+001	1.3118e+000	3.0884e+004	2.1612e-001
9	$R[\Omega]$	$L[mH]$	$R[\Omega]$	$C\ [\mu F]$
	-2.4870e+004	-1.1289e+002	5.9772e+004	-8.4344e-005
10	$R[\Omega]$	$L[mH]$	$R[\Omega]$	$C\ [\mu F]$
	6.5244e+000	5.6383e-001	3.7068e+003	4.4971e-003
11	$R[\Omega]$	$L[mH]$	$R[\Omega]$	$C\ [\mu F]$
	1.0676e+003	-2.1990e-001	-1.2141e+003	-1.0926e-004
12	$R[\Omega]$	$L[mH]$	$R[\Omega]$	$C\ [\mu F]$
	-4.0921e+005	1.5888e+000	4.0940e+005	9.3947e-009
13	$R[\Omega]$	$L[mH]$	$R[\Omega]$	$C\ [\mu F]$
	-2.5539e+007	3.4668e+001	2.5541e+007	5.3001e-011
14	$R[\Omega]$	$L[mH]$	$R[\Omega]$	$C\ [\mu F]$
	1.8421e+008	7.1719e+002	-1.8457e+008	2.1094e-011

A.6 Proposed Model PSCAD Lightning Simulation

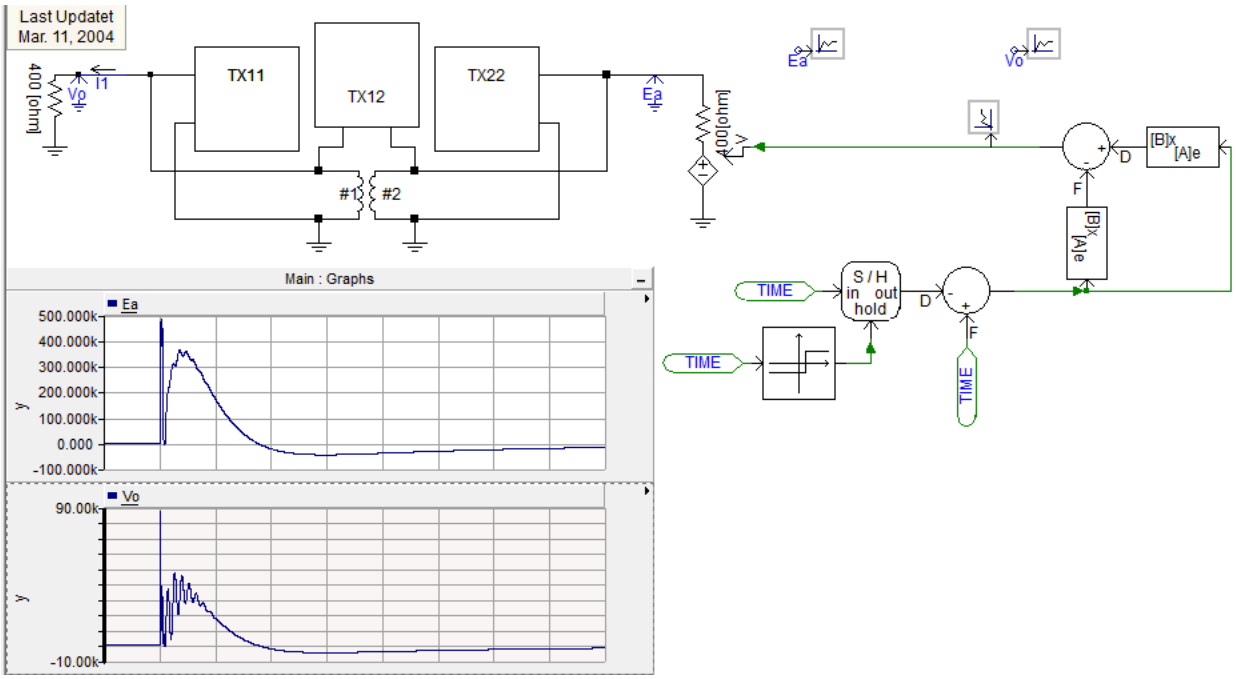

Figure A.1: Implemented circuit to study the effects of applying 1.2/50 μs lightning impulse to the proposed model.

References

[1] F. de Len, P. Gmez, J. A. Martinez-Velasco, and M. Rioual, *Power System Transients Parameter Determination*. CRC Press, 2010, ch. 4, pp. 177–249.

[2] D. W. Durbak, A. M. Gole, E. H. Camm, M. Marz, R. C. Degeneff, R. P. O'Leary, R. Natarajan, J. Martinez-Velasco, K.-C. Lee, A. Morched, R. Shanahan, E. R. Pratico, G. C. Thomann, B. Shperling, A. J. F. Keri, D. A. Woodford, L. Rugeles, V. Rashkes, and A. Sarshar, "Modeling guidelines for switching transients," in *Modeling and Analysis of System Transients Using Digital Programs*, A. J. F. Keri, A. M. Gole, and J. Martinez-Velasco, Eds. IEEE Power Engineering Society, 1998, ch. 4, pp. 4–1 to 4–24.

[3] P. Vaessen, "Transformer model for high frequencies," *Power Delivery, IEEE Transactions on*, vol. 3, no. 4, pp. 1761–1768, 1988.

[4] R. J. Bachega and M. L. B. Martinez, "Transformer modeling for transferred voltages," in *Transmission and Distribution Conference and Exposition: Latin America, 2004 IEEE/PES*, 2004, pp. 355–359.

[5] S. Okabe, M. Koto, G. Ueta, T. Saida, and S. Yamada, "Development of high frequency circuit model for oil-immersed power transformers and its application for lightning surge analysis," *Dielectrics and Electrical Insulation, IEEE Transactions on*, vol. 18, no. 2, pp. 541–552, 2011.

[6] E. Rahimpour and M. Bigdeli, "Simplified transient model of transformer based on geometrical dimensions used in power network analysis and fault detection studies," in *Power Engineering, Energy and Electrical Drives, 2009. POWERENG '09. International Conference on*, 2009, pp. 375–380.

[7] J. A. S. B. Jayasinghe, Z. Wang, P. Jarman, and A. W. Darwin, "Winding movement in power transformers: a comparison of fra measurement connection methods," *IEEE Transactions on Dielectrics and Electrical Insulation*, vol. 13, no. 6, pp. 1342–1349, 2006.

[8] N. Abeywickrama, Y. Serdyuk, and S. Gubanski, "High-frequency modeling of power transformers for use in frequency response analysis (fra)," *IEEE Transactions on Power Delivery*, vol. 23, no. 4, pp. 2042–2049, 2008.

[9] Z. Wang, J. Li, and D. Sofian, "Iinterpretation of transformer fra responses part i: Influence of winding structure," *IEEE Transactions on Power Delivery*, vol. 24, no. 2, pp. 703–710, 2009.

[10] P.C.Sen, *Principles of Electric Machines and Power Electronic Applications*. John Wiley &Sons, 1997.

[11] D. Sofian, Z. Wang, and P. Jarman, "Interpretation of transformer fra measurement results using winding equivalent circuit modelling technique," in *Annual Report Conference on Electrical Insulation and Dielectric Phenomena, CEIDP*, 2005, pp. 613–616.

[12] M. Wang, A. Vandermaar, and K. Srivastava, "Improved detection of power transformer winding movement by extending the fra high frequency range," *IEEE Transactions on Power Delivery*, vol. 20, no. 3, pp. 1930–1938, 2005.

[13] A. Shintemirov, W. H. Tang, and Q. Wu, "Transformer core parameter identification using frequency response analysis," *IEEE Transactions on Magnetics*, vol. 46, no. 1, pp. 141–149, 2010.

[14] H. Firoozi, M. Kharezi, A. Farshidnia, and A. Azirani, "Investigations on the transformer high frequency transfer function to interpretation of fra measurements," in *Electrical Insulation Conference, 2009. IEEE*, pp. 119–123.

[15] D. Sofian, Z. Wang, and J. Li, "Interpretation of transformer fra responses part ii: Influence of transformer structure," *IEEE Transactions on Power Delivery*, vol. 25, no. 4, pp. 2582–2589, 2010.

[16] Suwarno and F. Donald, "Frequency response analysis (fra) for diagnosis of power transformers," in *2010 International Conference on, Electrical Engineering/Electronics Computer Telecommunications and Information Technology (ECTICON)*, 2010, pp. 112–116.

[17] E. S. Kuh and R. A. Rohrer, *Theory of linear active networks.* Holden-Day, 1967.

[18] E. Li, *Electrical Modeling and Design for 3D System Integration:3D Integrated Circuits and Packaging, Signal Integrity, Power Integrity and EMC.* Wiley-IEEE Press, 2012.

[19] S. Grivet-Talocia, "On passivity characterization of symmetric rational macromodels," *IEEE Transactions on Microwave Theory and Techniques*, vol. 58, no. 5, pp. 1238–1247, 2010.

[20] A. Semlyen and B. Gustavsen, "A half-size singularity test matrix for fast and reliable passivity assessment of rational models," *IEEE Transactions on Power Delivery*, vol. 24, no. 1, pp. 345–351, 2009.

[21] C. Saunders and M. Steer, "Passivity enforcement for admittance models of distributed networks using an inverse eigenvalue method," *IEEE Transactions on Microwave Theory and Techniques*, vol. 60, no. 1, pp. 8–20, 2012.

[22] B. Gustavsen and A. Semlyen, "Enforcing passivity for admittance matrices approximated by rational functions," *IEEE Transactions on Power Systems*, vol. 16, no. 1, pp. 97–104, 2001.

[23] S. Grivet-Talocia, "Passivity enforcement via perturbation of hamiltonian matrices," *IEEE Transactions on Circuits and Systems I: Regular Papers*, vol. 51, no. 9, pp. 1755–1769, 2004.

[24] B. Gustavsen, "Fast passivity enforcement for pole-residue models by perturbation of residue matrix eigenvalues," *IEEE Transactions on Power Delivery*, vol. 23, no. 4, pp. 2278–2285, 2008.

[25] B. Gustavsen and A. Semlyen, "Rational approximation of frequency domain responses by vector fitting," *IEEE Transactions on Power Delivery*, vol. 14, no. 3, pp. 1052–1061, 1999.

[26] B. Gustavsen, "Wide band modeling of power transformers," *IEEE Transactions on Power Delivery*, vol. 19, no. 1, pp. 414–422, 2004.

[27] ——, "Computer code for rational approximation of frequency dependent admittance matrices," *IEEE Transactions on Power Delivery*, vol. 17, no. 4, pp. 1093–1098, 2002.

[28] I. Pordanjani, C. Chung, H. Mazin, and W. Xu, "A method to construct equivalent circuit model from frequency responses with guaranteed passivity," *IEEE Transactions on Power Delivery*, vol. 26, no. 1, pp. 400–409, 2011.

[29] B. Gustavsen and C. Heitz, "Modal vector fitting: A tool for generating rational models of high accuracy with arbitrary terminal conditions," *IEEE Transactions on Advanced Packaging*, vol. 31, no. 4, pp. 664–672, 2008.

[30] B. Gustavsen, "Improving the pole relocating properties of vector fitting," *IEEE Transactions on Power Delivery*, vol. 21, no. 3, pp. 1587–1592, 2006.

[31] D. Saraswat, R. Achar, and M. Nakhla, "A fast algorithm and practical considerations for passive macromodeling of measured/simulated data," *IEEE Transactions on Advanced Packaging*, vol. 27, no. 1, pp. 57–70, 2004.

[32] S. Grivet-Talocia, F. Canavero, I. Stievano, and I. Maio, "Circuit extraction via time-domain vector fitting," in *International Symposium on Electromagnetic Compatibility*, vol. 3, 2004, pp. 1005–1010 vol.3.

[33] A. Budak, *Passive and Active Network Analysis and Synthesis*. Houghton Mifflin Company, 1974.

[34] E.-P. Li, E.-X. Liu, L.-W. Li, and M.-S. Leong, "A coupled efficient and systematic full-wave time-domain macromodeling and circuit simulation method for signal integrity analysis of high-speed interconnects," *IEEE Transactions on Advanced Packaging*, vol. 27, no. 1, pp. 213–223, 2004.

[35] Z. Zhongyuan, L. Fangcheng, and L. Guishu, "A high-frequency circuit model of a potential transformer for the very fast transient simulation in gis," *IEEE Transactions on Power Delivery*, vol. 23, no. 4, pp. 1995–1999, 2008.

[36] G. Antonini, "Spice equivalent circuits of frequency-domain responses," *IEEE Transactions on Electromagnetic Compatibility*, vol. 45, no. 3, pp. 502–512, 2003.

[37] W. Ren, "A new circuit modeling methodology for rfid antennas with vector fitting technique," in *6th International Conference on Wireless Communications Networking and Mobile Computing (WiCOM)*, 2010, pp. 1–4.

[38] J. Martinez and B. Mork, "Transformer modeling for low- and mid-frequency transients - a review," *IEEE Transactions on Power Delivery*, vol. 20, no. 2, pp. 1625–1632, 2005.

[39] Z. Zhongyuan, L. Fangcheng, and C. Yutong, "A high frequency circuit model for current transformer based on the scattering parameter," in *IEEE Asia Pacific Conference on Circuits and Systems, APCCAS*, 2006, pp. 860–863.

[40] B. Gustavsen and C. Heitz, "Rational modeling of multiport systems by modal vector fitting," in *IEEE Workshop on Signal Propagation on Interconnects, SPI*, 2007, pp. 49–52.

[41] G. DeJean and M. Tentzeris, "The application of lumped element equivalent circuits approach to the design of single-port microstrip antennas," *IEEE Transactions on Antennas and Propagation*, vol. 55, no. 9, pp. 2468–2472, 2007.

[42] B. Badrzadeh and B. Gustavsen, "High-frequency modeling and simulation of wind turbine transformer with doubly fed asynchronous generator," *IEEE Transactions on Power Delivery*, vol. 27, no. 2, pp. 746–756, 2012.

[43] A. Ramirez, "Vector fitting-based calculation of frequency-dependent network equivalents by frequency partitioning and model-order reduction," *IEEE Transactions on Power Delivery*, vol. 24, no. 1, pp. 410–415, 2009.

[44] T. Sano and K. Miyagi, "Influence of measurement parameters on fra characteristics of power transformers," in *International Conference on Condition Monitoring and Diagnosis, CMD*, 2008, pp. 968–973.

[45] W. S. Z. John Kuffel, E. Kuffel, *High Voltage Engineering Fundamentals*. Newnes, 2000.